2012

The Effect of Exercise on Endothelin and Endothelin Receptor Levels in SHR and WKY Male and Female Rats

Lacey Stiller
Minnesota State University, Mankato

THE EFFECT OF EXERCISE ON ENDOTHELIN AND ENDOTHELIN RECEPTOR LEVELS IN SHR AND WKY MALE AND FEMALE RATS

By

LACEY A. STILLER

A THESIS SUBMITTED

IN PARTIAL FULFILLMENT

OF THE REQUIREMENTS FOR THE DEGREE

MASTER OF SCIENCE

IN

BIOLOGY

MINNESOTA STATE UNIVERSITY, MANKATO

MANKATO, MN

JUNE 2012

"The Effect of Exercise on Endothelin and Endothelin Receptors in SHR and WKY Male and Female Rats"

Lacey A. Stiller, Master of Science Degree Candidate

Department of Biological Sciences

Minnesota State University, Mankato

This thesis paper has been examined and is approved by the examining committee.

Dr. Marilyn Hart, Committee Chairperson Date

Dr. Penny Knoblich, Committee Member Date

Dr. Michael Bentley, Committee Member Date

ABSTRACT

The role of exercise as a means to modulate renal function in hypertension is unclear. However, prior studies in the laboratory of Dr. Penny Knoblich indicate that exercised female spontaneously hypertensive rats (SHR) and Wistar Kyoto (WKY) rats excrete significantly more sodium in response to a rise in blood pressure relative to exercised male and sedentary female SHR and WKY rats. The purpose of this study was to evaluate the effects of exercise on endothelin and endothelin receptor levels in the urine and kidneys of male and female SHR and WKY rats, to elucidate potential mechanisms to explain an increase in urinary sodium excretion in exercised female SHR and WKY rats as previously described by Dr. Penny Knoblich. Eighty male and female SHR and WKY rats were randomly assigned to an exercise or a sedentary control group. Each rat assigned to the exercise group ran voluntarily on a wire wheel for ten to twelve weeks. After ten to twelve weeks, the urine and kidneys of each exercised and sedentary rat was collected. The urine from each group of rats was pooled and analyzed using an ELISA assay to determine the concentration of endothelin-1 (ET-1). The excised kidneys from each rat was examined using Western blot analysis and immunofluorescence microscopy to determine the amount and location of ET-1, endothelin-A (ET-A) receptors, and endothelin-B (ET-B) receptors within the tissue. The amount of urinary ET-1 excretion was elevated in female rats relative to male rats of the same strain and activity level, with exercised female SHR rats being the only exception. Male and female WKY rats were found to excrete more ET-1 than male and female SHR rats. Exercise had a variable effect on urinary ET-1 excretion levels. ET-A receptor levels were increased in kidney lysate of SHR rats when compared to WKY rats and in male rats relative to female rats of the same strain and activity level, with exercised male SHR rats being the only exception. Exercise had a variable effect on renal ET-A receptor expression. ET-B receptors were detectable in the kidney lysate of exercised female SHR rats, but not observed in any other group of rats. Immunofluorescence microscopy revealed that ET-A and ET-B receptor staining was very broad and localized in most components of the nephron. However, while ET-A receptor staining was observed in each group of rats, ET-B receptors were only detected in renal tissue extracted from exercised female SHR rats. ET-1 receptors were undetectable in the kidney tissue of each group of rats using Western blot analysis and immunofluorescence microscopy. An upregulation of ET-B receptors in the kidney tissue of exercised female SHR rats may explain previous reports that these rats excrete more sodium in response to a rise in blood pressure relative to other experimental groups of rats. An increase in ET-B receptor expression was not observed in the renal tissue of exercised female WKY rats. However, exercised female WKY rats excreted the greatest amount of ET-1 in their urine, which may be responsible for their previously reported increase in urinary sodium excretion in response to a rise in blood pressure.

TABLE OF CONTENTS

TABLE OF CONTENTS

FIGURE INDEX

FIGURE INDEX

TABLE INDEX

ABBREVIATIONS USED

ACE:	Angiotensin Converting Enzyme
Ach:	Acetlycholine
ANP:	Atrial natriuretic Peptide
BCIP:	5-Bromo-4-Chloro-3-Indoyl Phosphate Disodium Salt
BigET-1:	Big Endothelin-1
cAMP:	Cyclic Adenosine Monophosphate
cGMP:	Cyclic Guanosine Monophosphate
DG:	Diacylglycerol
DAPI:	4’,6-Diamidino-2-Phenylindole
DOCA:	Deoxycorticosterone Acetate
ECE-1:	Endothelin-Converting Enzyme-1
ELISA:	Enzyme-Linked Immunosorbent Assay
eNOS:	Endothelial Nitric Oxide Synthase
ET-1:	Endothelin-1
ET-2:	Endothelin-2
ET-3:	Endothelin-3
ET-A:	Endothelin-A
ET-B:	Endothelin-B
FCS:	Fetal Calf Serum
F-SHR-E:	Female SHR Exercised
F-SHR-S:	Female SHR Sedentary
F-WKY-E:	Female WKY Exercised
F-WKY-S:	Female WKY Sedentary
IMCD:	Inner Medullar Collecting Duct
IP_3:	Inositol-1,4,5-Triphosphate
MBF:	Medullary Blood Flow
M-SHR-E:	Male SHR Exercised
M-SHR-S:	Male SHR Sedentary
M-WKY-E:	Male WKY Exercised
M-WKY-S:	Male WKY Sedentary
NBT:	Nitro Blue Tetrazoliumchloride
NO:	Nitric Oxide
PBS:	Phosphate Buffered Saline
PGE_2:	Prostaglandin E
PGI_2:	Prostacyclin
PKB:	Protein Kinase B
PKC:	Protein Kinase C

ABBREVIATIONS USED

PLA_2:	Phospholipase A_2
PLC:	Phospholipase C
PMS:	Phenazine Methosulfate
PreproET-1:	Preproendothelin-1
RAAS:	Renin-Angiotensin-Aldosterone System
RIHP:	Renal Interstitial Hydrostatic Pressure
ROC:	Receptor-Operated Calcium Channel
RPP:	Renal Perfusion Pressure
SDS-PAGE:	Sodium Dodecyl Sulfate Polyacrylamide Gel Elecrophoresis
SHR:	Spontaneously Hypertensive Rat
TXA_2:	Thrombaxane
TTBS:	Tween Tris-Buffered Saline
VDC:	Voltage-Dependent Calcium Channel
WKY:	Wistar-Kyoto

INTRODUCTION

Cardiovascular Physiology and Hypertension

Hypertension, a medical condition in which the blood exerts an excessive amount of hydrostatic pressure against the walls of blood vessels, is an emerging epidemic which affects approximately one in three adults in the United States, more than 1 billion people worldwide (1). The complications associated with high blood pressure often lead to potentially fatal conditions of the brain and heart, including stroke, heart attack, and congestive heart failure (2). The blood pressure of a healthy adult should be equal to or less than 120 mm Hg systolic and 80 mm Hg diastolic. With every 20/10 mm Hg increase in blood pressure as low as 115/75 mm Hg, the rate of mortality from cardiovascular disease doubles (1). Hypertension is reported to be the underlying cause of 39% of heart failure cases in men and 59% of cases in women (3). Given this information, it is evident that blood pressure strongly affects the cardiovascular system and therefore plays a large role in shaping an individual's overall health.

Cardiovascular Regulation of Mean Arterial Pressure

The pressure of blood flow through the body, also known as mean arterial pressure, is regulated by a very complex process (Figure 1). However, the determinants of blood pressure can be simplified and approximated by Ohm's law modified for fluid dynamics (pressure = flow x resistance) (4). Mean arterial blood pressure is defined as

the average arterial blood pressure during a single cardiac cycle and is determined by the cardiac output and total peripheral resistance of the cardiovascular system (5).

Cardiac output, which is defined as the amount of blood pumped from the ventricle per minute, depends on the number of heart beats per minute (heart rate) and the volume of blood ejected from the heart per beat (stroke volume) (4; 6). The human heart beating rate, normally ranging from 60 to 100 beats per minute, is determined by the speed at which pacemaker cells located in the sinoatrial node of the heart spontaneously depolarize to threshold level (4; 6; 7). An intrinsic heart rate can be increased by activating the sympathetic autonomic nervous system and decreased by activating the parasympathetic autonomic nervous system. Stroke volume, the difference between the ventricular end diastolic blood volume and the end systolic blood volume, is influenced by venous return of blood to the heart from the respiratory and skeletal systems (4; 6; 7). According to the Frank-Starling principle, a larger venous return increases the end diastolic blood volume, which stretches the muscle fibers of the heart, strengthens the force of ventricular contraction, and results in more blood being ejected and an increase in stroke volume (4). An increase in heart rate or stroke volume will result in an increase in cardiac output, and therefore an increase in mean arterial blood pressure (4).

The total peripheral vascular resistance refers to the resistance of blood vessels, specifically arterioles, to the flow of blood. Arterioles are smaller in diameter, have thicker muscular walls, and are less elastic than other vessels in the cardiovascular

system (4; 6; 7). The muscular walls of arterioles allow for the diameter of the vessels to actively change and therefore, regulate peripheral blood flow through the body. The radius of arteriolar walls is regulated extrinsically by the endocrine system and the autonomic sympathetic nervous system and intrinsically via metabolic control (4; 8). Epinephrine, a component of the endocrine system, is released by the adrenal medulla gland in response to stress and binds to arteriolar α receptors (8). The sympathetic nervous system regulates arterioles by norepinephrine binding to receptors on the smooth muscles of arterioles (8). An increase in circulating levels of epinephrine and norepinephrine in the body leads to vasoconstriction, while a decrease leads to vasodilation of arteriolar walls (4; 8). The presence of metabolites, such as carbon dioxide and potassium, and signaling molecules such as nitric oxide (NO), in the body also affects arteriolar blood flow (4). An increase in these chemicals stimulates the vasodilation of local arterioles and the resulting increase in blood flow gradually lowers the level of these molecules in the tissue, which triggers arterioles to return to their original diameter (4). Overall, a decrease of blood flow caused by the constriction of arterioles generally leads to an increase in mean arterial pressure, whereas an increase of blood flow caused by dilation of arterioles is accompanied by a decrease in mean arterial pressure (4; 6; 7).

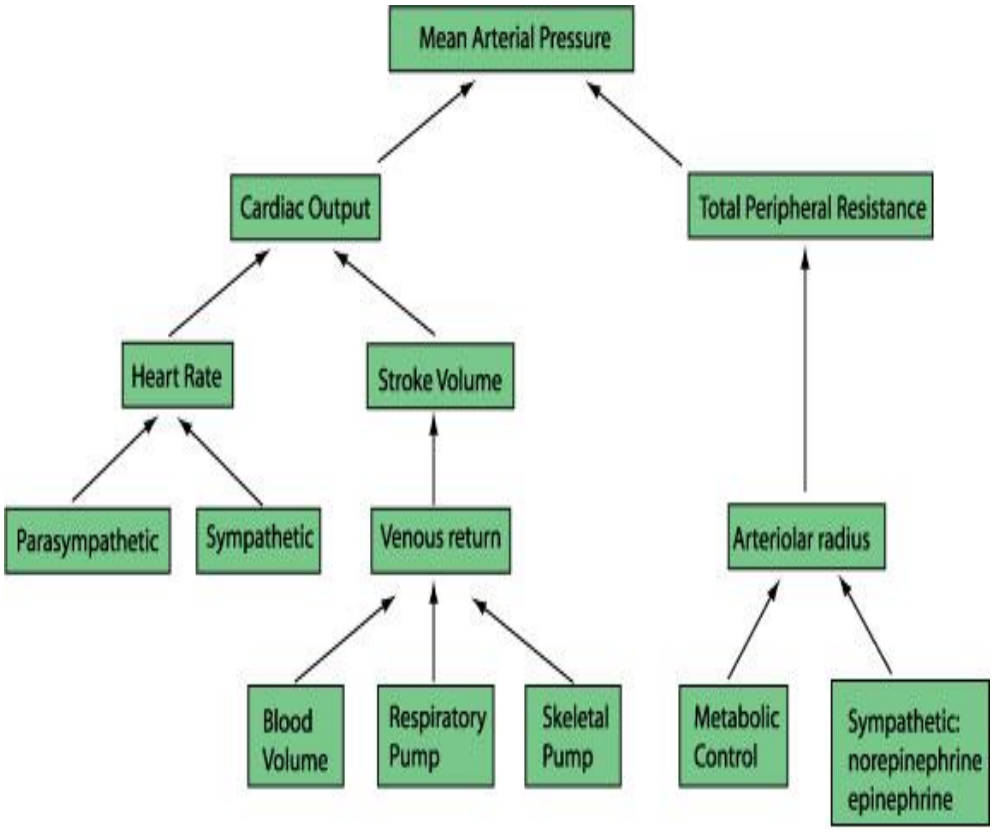

Figure 1. Determinants of Mean Arterial Blood Pressure. A summary of the factors that affect mean arterial pressure (9).

The Effect of Hypertension on the Cardiovascular System

Untreated and prolonged elevation of blood pressure leads to changes in the myocardial structure, vasculature, and conduction system of the heart (4). These modifications of the cardiovascular system may lead to several heart diseases, including left ventricular hypertrophy, coronary artery disease, cardiac arrhythmias, and congestive heart failure (4).

Left ventricular hypertrophy, the enlargement of the muscle tissue in the wall of the left ventricle, is observed in 15-20% of patients with hypertension (10). Left

ventricular hypertrophy usually develops in response to increased blood pressure, which increases the work of the left ventricle, and eventually leads to the development of myocardial dysfunction (10).

Patients with untreated hypertension are susceptible to artery damage because elevated blood pressure places additional force against arterial walls, leading to the narrowing and plaque buildup associated with atherosclerosis (4). Atherosclerotic arterial damage prevents blood flow and oxygen delivery throughout the body, and may cause coronary artery disease, the leading cause of death in the United States for men and women (4).

Several cardiac arrhythmias, including premature ventricular contractions and ventricular tachycardia, an abnormally rapid heart rhythm that originates in the ventricles of the heart, are commonly noted in patients with high blood pressure (11). However, atrial fibrillation, the irregular and chaotic beating of the atria of the heart, is the most frequently observed arrhythmia seen in hypertensive patients. In fact, elevated blood pressure is the most common cause of atrial fibrillation in the Western hemisphere (11). Although the connection between hypertension and atrial fibrillation is unclear, structural and functional defects of the left atrium may be contributing factors (11).

Congestive heart failure, the inability of the heart to pump an adequate amount of blood to the body, is also a common complication seen in patients with chronically elevated blood pressure (12). The development of congestive heart failure in

hypertensive individuals can be attributed to several factors, including coexistent coronary artery disease and left ventricular hypertrophy (12). According to the Framingham Study, hypertension accounts for about 25 percent of all heart failure cases and as much as 68 percent in elderly patients (13). Hypertensive women and men have a two-fold and three fold increased risk, respectively, of developing congestive heart failure (12).

Renal Physiology and Hypertension

The kidneys play a key role in the regulation of blood pressure by indirectly controlling the amount of blood in the body. The kidneys regulate electrolytes, such as sodium and potassium, and maintain fluid levels in the body (6; 7) . The kidneys also directly control blood pressure by regulating hormones secreted from both the hypothalamus and adrenal gland (6; 7). In addition to having detrimental effects on the cardiovascular system, high blood pressure is also one of the leading causes of kidney damage and may lead to kidney failure. In fact, it has been reported that hypertension causes more than 25,000 new cases of kidney failure in the United States every year (1). In order to understand the effect of hypertension on the kidneys, it is important to consider the structure and function of the renal system.

The human renal system consists of two bean-shaped kidneys located on the posterior wall of the abdominal cavity, with one on each side of the vertebral column, as well as two ureters, a urinary bladder, and the urethra (14; 15) (Figure 2). The kidneys filter blood and produce urine, which is then transported by the ureter to the urinary

bladder, where it is stored until it is excreted from the body via the urethra (14; 15). Kidney tissue is divided into two distinct regions, the inner renal medulla and the outer renal cortex, which in humans, contains more than one million nephrons (14; 15). A nephron, the functional unit of the kidney, is divided into two parts, the renal corpuscle and the renal tubule (14; 15). The renal corpuscle is responsible for filtering blood plasma and has two parts, the glomerulus, a network of capillaries, and the Bowman's capsule, an epithelial cup within which the glomerulus is contained (14; 15). The glomerular capillaries are located between the afferent arteriole, which brings blood to the glomerulus, and the efferent arteriole, which branches into peritubular capillaries that wrap around the nephron and drain blood away from the glomerulus (14; 15). Blood from the afferent arteriole is forced into the glomerulus and either filtered into the Bowman's capsule or travels out of the kidney via the efferent arteriole (14; 15). The renal tubule, which consists of the proximal tubule, loop of Henle, distal tubule, and collecting duct, is responsible for adjusting the water and ion composition of the glomerular filtrate (14; 15).

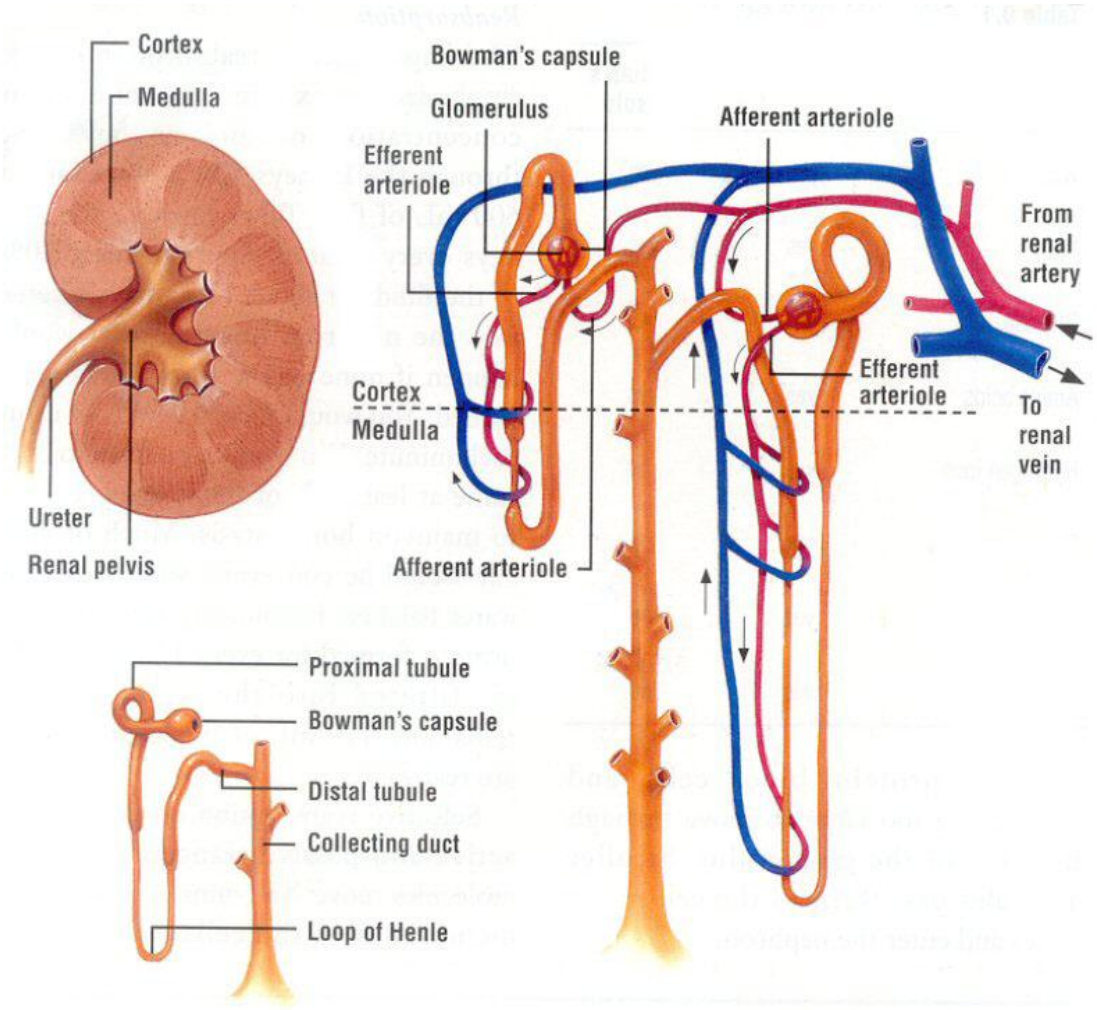

Figure 2. Renal Physiology. Structure of the kidney and nephron (14).

Renal Regulation of Blood Volume

The formation of urine and regulation of the composition and volume of blood by the renal system involves three physiological processes known as glomerular filtration, tubular reabsorption, and tubular secretion (14; 15) (Figure 3). Urine formation begins with the process of glomerular filtration, which is driven by pressure

generated by the beating heart (14; 15). Glomerular filtration takes place in the renal corpuscle of the nephron and involves the nonselective movement of water, waste products, ions, and solutes from the blood into the Bowman's capsule (14; 15). The substance that exits the blood, collectively known as glomerular filtrate, consists primarily of water, salts, glucose, and urea (14; 15). After the glomerular filtrate has been formed, it passes from the Bowman's capsule to the renal tubule, where tubular reabsorption takes place (14; 15). The process of tubular reabsorption returns approximately 99% of the glomerular filtrate to the blood via diffusion and active transport of ions and solutes, and osmosis of water from the renal tubules into the peritubular capillaries.

(14; 15). The proximal tubule is responsible for reabsorbing approximately 80% of the glomerular filtrate, while the remaining water, salts, and urea are reabsorbed in the loop of Henle and the distal tubule (14; 15). The final step of urine formation, tubular secretion, actively transports excess amounts of hydrogen ions, potassium ions, urea, and other solutes that are potentially harmful to the body back into the filtrate contained in the renal tubules so that they may be excreted in the urine (14; 15).

The concentration of solutes in the urine relies on the different permeability properties of the two limbs of the loop of Henle (14; 15). The descending loop of Henle is permeable to water but not permeable to salt (14; 15). Therefore, water gradually moves from the descending limb into the interstitial fluid surrounding the nephron, which results in more concentrated filtrate (14; 15). The ascending loop of Henle is

permeable to salt but impermeable to water (14; 15). As sodium and chloride ions are transported out of the ascending limb, a concentration gradient is formed, with the saltiest interstitial fluid located in the deepest part of the renal medulla (14; 15). The transport of salt into the interstitial fluid also causes the filtrate to become less concentrated than normal body fluid (14; 15). The distal tubule then delivers the filtrate to the collecting duct, which passes deep into the renal medulla (14; 15). The collecting duct is highly permeable to urea and therefore, the filtrate loses urea to the surrounding interstitial fluid, allowing additional concentration (14; 15). As urine then passes through the collecting duct, water is reabsorbed into the salty interstitial fluid by osmosis, which in turn increases the concentration of solutes and waste excreted in the urine (14; 15). In general, dilute urine results in less water in the blood due to osmosis, a lower blood volume, and therefore a decrease in mean arterial blood pressure (14; 15).

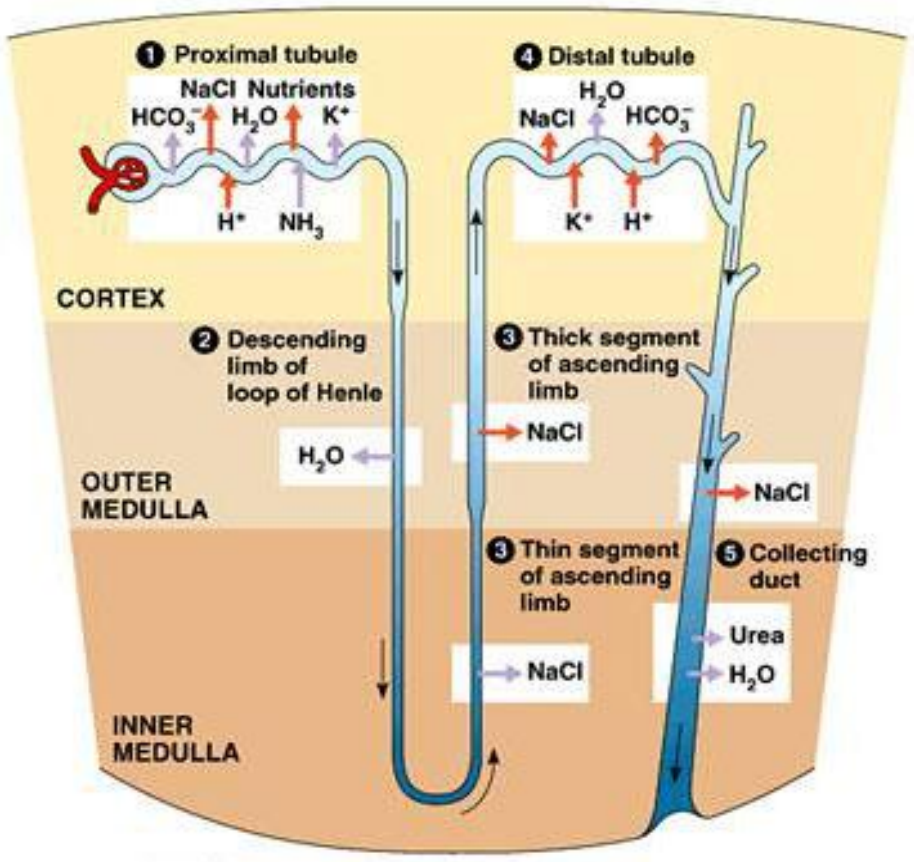

Figure 3. Nephron Regulation of Urine Concentration. The physiological process responsible for the regulation of urine formation and concentration (14).

Pressure Natriuresis Relationship and Regulation

The long term control of mean arterial blood pressure is linked to the kidney's intrinsic ability to maintain normal sodium levels, extracellular fluid volume, and blood volume (16). Pressure natriuresis and diuresis, which respectively increase sodium excretion and urine volume in response to increased renal perfusion pressure (RPP), play an important role in the feedback system that regulates arterial pressure (16). The intrarenal mechanisms behind pressure natriuresis and diuresis appear to be related to

increased hemodynamic factors such as medullary blood flow (MBF), renal interstitial hydrostatic pressure (RIHP), and renal chemical transmitters such as NO (17).

The impact of MBF on long-term blood pressure control is believed to be mediated by its impact on renal sodium and water handling. The role of MBF in the regulation of salt and water excretion was elucidated by studies completed by Cowley and colleagues (18). These experiments demonstrated that reduced MBF increased sodium reabsorption and lead to the development of hypertension and that enhanced MBF has the opposite effect on renal sodium handling and attenuates hypertension in SHR rats (18).

Scientists have also proposed that an elevation in MBF, due to an increase in RPP, is transmitted into the renal medullary interstitium and leads to a rise in medullary interstitial hydrostatic pressure (16; 19). Due to renal encapsulation, an increase in interstitial hydrostatic pressure in the medulla leads to higher interstitial hydrostatic pressure throughout the entire kidney (16). The resulting increase in RIHP is believed to inhibit renal sodium reabsorption (20). Therefore, a direct causal link is postulated to exist between increases in RPP, MBF, RIHP, and the amount of sodium excreted in the urine. Studies by Roman and associates have confirmed that increased renal papillary blood flow resulting from elevated RPP is correlated with equivalent increases in medullary capillary pressure, RIHP, and natriuresis (21).

There are two possible mechanisms that may explain the process by which an increase in RIHP impairs tubular sodium retention (18; 22). The first mechanism states

that an increase in interstitial pressure reduces the movement of sodium and water from the tubular fluid to the capillaries, thereby elevating the amount of sodium excreted in the urine (18; 22). The second mechanism suggests that an increase in RIHP drives water into the descending loop of Henle, which lowers water retention and sodium reabsorption and produces a dilute filtrate (18; 22). The decrease in sodium reabsorption is thought to be facilitated by increased levels of nitric oxide in the endothelium (23).

Nitric oxide, known for its potent vasodilation properties, is believed to play an important role in the regulation of urinary sodium excretion through mechanisms involving effects on renal blood flow, glomerular filtration rate, and direct tubular actions (16; 24). Several investigators have demonstrated that the acute or chronic inhibition of NO synthesis via oral administration of nitric oxide synthase inhibitors results in arterial hypertension and a markedly suppressed pressure natriuresis and diuresis response in animals (23; 25; 26). Studies have also reported that increased intrarenal NO levels and urinary excretion of NO metabolites correlates with an increase in RPP in dogs (25). The production of NO, caused by an increase in arterial shear stress due to elevated mean arterial pressure and renal blood flow, increases natriuresis by directly inhibiting tubular sodium reabsorption and transport in the kidney (23; 27). A recent study by Nakano and colleagues has shown that increased sodium and water excretion associated with elevated levels of NO is linked to an upregulation of renal endothelin and endothelin-B receptor levels (28).

Hormonal Control of Mean Arterial Pressure

In addition to regulating blood pressure and urine concentration with intrinsic mechanisms of the nephron, sodium and water handling in the renal tubules is controlled by hormones excreted from the adrenal gland and the hypothalamus. Aldosterone, a steroid hormone produced by the adrenal cortex of the adrenal gland, causes tubular sodium retention, which leads to an increase in blood pressure (29; 30). The release of aldosterone is controlled via the renin-angiotensin-aldosterone system (RAAS), which can be triggered by a decrease in blood volume or a lack of sodium delivery to the distal tubules of the kidney (29; 30) (Figure 4). Activation of the RAAS is initiated by the regulated secretion of renin from the juxtaglomerular cells in the kidneys. Angiotensinogen, a protein secreted by the liver into the blood, is converted into angiotensin I by renin (29; 30). Another enzyme, angiotensin converting enzyme (ACE), subsequently converts angiotensin I into angiotensin II, which causes blood vessels to contract and stimulates the release of aldosterone from the adrenal gland and vasopressin from the pituitary gland (29; 30). Aldosterone increases the activity of sodium-potassium pumps, which causes the distal tubule and collecting duct to increase the reabsorption of sodium (29; 30). Due to osmosis, the reabsorption of water into the renal tubules also increases, which increases the volume of blood and therefore the mean arterial blood pressure (29; 30). Vasopressin controls the reabsorption of water molecules in the renal tubules of the kidneys by increasing the permeability of the distal tubules and collecting ducts to water (29; 30). As a result, more water diffuses out of

the filtrate and is absorbed by blood in the peritubular capillaries, which decreases the amount of water excreted in the urine and increases the mean arterial blood pressure (29; 30).

In contrast to aldosterone and vasopressin, atrial natriuretic peptide (ANP) is a hormone that increases urinary sodium excretion (8). ANP is released by muscle cells in the atria of the heart in response to stretch of the atrial walls due to a high blood volume (8). Once released from the atria, ANP directly inhibits aldosterone by preventing its secretion from the adrenal cortex and indirectly inhibits the RAAS by impeding renin secretion from the kidneys, which leads to a decrease in mean arterial blood pressure (8).

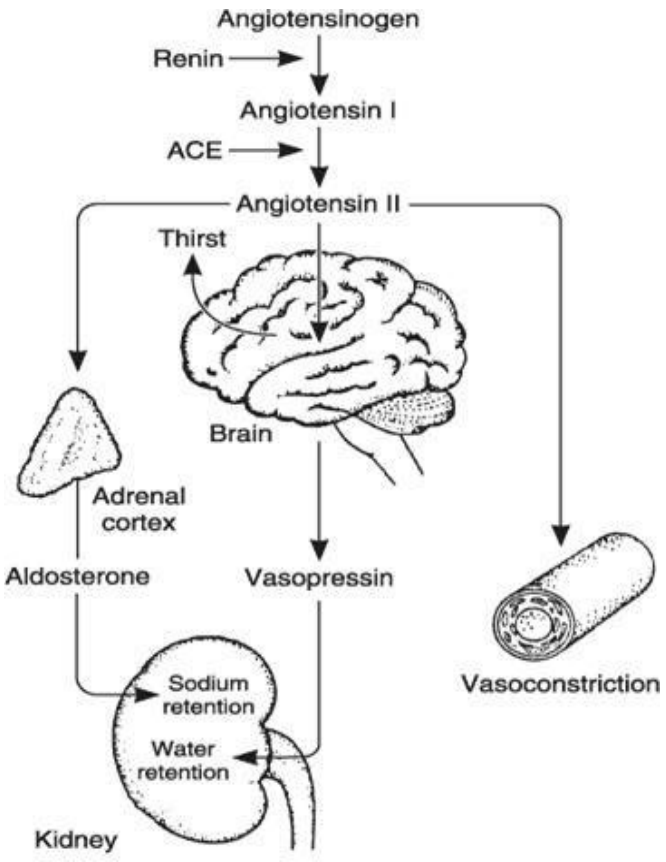

Figure 4. RAAS System. The mechanism and effect of the RAAS system on renal function (30).

The Effect of Hypertension on the Renal System

Chronic high blood pressure, if left untreated, may damage the blood vessels of the renal system. In fact, hypertension is the number two cause of chronic kidney disease (1). If the blood vessels of the kidneys are impaired, the process of removing waste and excess fluid from the body may cease. Persistant impairment may lead to the development of kidney damage, such as kidney scarring, kidney artery aneurysm, or kidney failure (4; 15).

Types of Hypertension

Hypertension may be classified as primary or secondary depending upon the etiology of the increase in blood pressure (31). Primary hypertension, which accounts for approximately 95% of all cases, has no identifiable cause, but tends to gradually develop with age and appears to be the result of an interaction of environmental and genetic factors (31). Some factors that are believed to play a role in the development of primary hypertension are obesity or sedentary lifestyle, insulin resistance, genetic predisposition, high alcohol and sodium consumption, high levels of stress, and low potassium and calcium intake (31). Approximately 5% of hypertension cases are classified as secondary hypertension, in which an increase in blood pressure results from an underlying, identifiable, and often correctable cause (32). Several different factors, including chronic renal disease, hyper- or hypothyroidism, aortic coarctation, primary hyperaldosteronism, and certain pharmaceutical drugs, may lead to the development of secondary hypertension (32).

Mechanisms of Hypertension

Hypertension is the most common treatable risk factor for several potentially fatal diseases, including stroke, congestive heart failure, and renal disease. Despite the harmful effects of elevated mean arterial blood pressure and the wide availability of effective treatments, hypertension is only sufficiently controlled in 34% of patients (33). Doctors are often unable to effectively lower blood pressure in patients due to the fact that so little is known about the mechanisms and molecular pathogenesis of

hypertension (33). Thoroughly understanding the pathophysiology of hypertension involves the consideration of several factors that influence blood pressure homeostasis, including sodium intake, and renal structure and function.

Sodium Consumption and Hypertension

High sodium intake is considered one of the major factors in primary blood pressure elevation (34). In fact, primary hypertension is not present in populations where sodium chloride intake is less than 50 mmol per day. Studies in Finland have shown that a progressive decrease in salt intake plays an important role in decreasing the occurrence of cardiovascular disease and the average blood pressure of the population (35). During the past 30 years, the salt intake in Finland has decreased by one-third, which has resulted in a 10 mm Hg fall in the average systolic and diastolic blood pressure of the population, and a 75% decrease in stroke and coronary heart disease mortality rates (35). According to the Dietary Approaches to Stop Hypertension trial, reducing sodium intake from 150 mmol per day to 100 mmol per day may reduce systolic blood pressure by 2.1 mm Hg and reducing sodium intake from 100 mmol per day to 50 mmol per day may reduce systolic blood pressure by an additional 4.6 mm Hg (34).

Kidney Structure and Function and Hypertension

The importance of the kidney in hypertension is supported by kidney cross-transplantation studies in strains of hypertensive rats. These studies have reported that transplanting a kidney from a hypertensive rat leads to elevated blood pressure in a

previously healthy rat and, vice versa, that a kidney transplanted from a normotensive rat normalizes the blood pressure in a previously hypertensive rat (36). Hypertension is believed to be caused by several factors, including abnormalities in kidney structure, renal vascular remodeling, a shift in the blood pressure natriuresis relationship, inappropriate activation of the RAAS, and over activity of the sympathetic nervous system (37).

Abnormalities in the kidney structure, particularly a reduction in the number of glomeruli or in the filtration surface area per glomerulus, limits the ability of the kidney to excrete sodium and may result in elevated blood pressure (38). This hypothesis was tested by comparing the number and volume of glomeruli in patients with high blood pressure relative to healthy control patients (38). The researchers reported that the number of glomeruli was significantly lower, and in an attempt to compensate, the volume of each glomeruli was significantly higher in hypertensive individuals (38).

The remodeling of large and small resistance arteries, an adaptive response to long-term changes in hemodynamic conditions, has been reported to contribute to the development and complications of hypertension (39). Patients with mild essential hypertension tend to undergo inward eutrophic arterial remodeling, which reduces the outer and lumen diameters, does not affect the cross-sectional area of the media, and increases the media/lumen ratio (39; 40). Hypertrophic vascular remodeling, common in cases of more severe hypertension, is characterized by excessive media growth that encroaches the arterial lumen, thereby increasing the vascular media/lumen

ratio (39; 40). Cell growth, apoptosis, inflammation, and fibrosis are some of the factors that are believed to contribute to hypertensive vascular remodeling (39).

Chronic elevated mean arterial blood pressure causes an abnormal pressure natriuresis relationship, in which urinary sodium excretion is consistent with normotension despite the elevation in pressure (41; 42) (Figure 5). The resetting of the pressure natriuresis mechanism to higher pressures is essential for the development and sustainment of hypertension because if unaltered, sodium excretion levels would be increased until arterial pressure returned to its original set point (41; 42). The alteration in renal function responsible for the resetting of the pressure natriuresis curve is believed to be caused by several factors, including increased sympathetic nervous system and RAAS activity (41; 42).

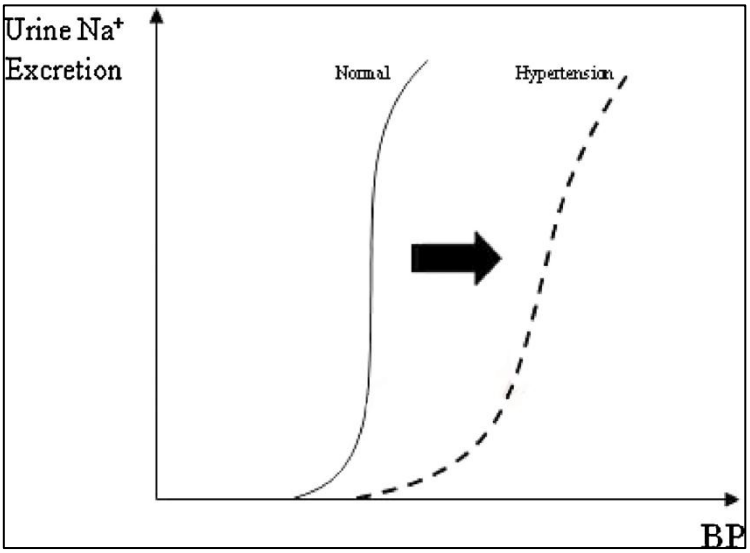

Figure 5. The Effect of Hypertension on the Pressure Natriuresis Curve. Urinary sodium excretion of patients with hypertension relative to normotensive patients (43).

The RAAS is believed to play a primary role in the pathogenesis of hypertension in that angiotensin II affects various physiologic components that regulate mean arterial blood pressure (44). The release of angiotensin II causes aldosterone secretion, vascular hypertrophy, vasoconstriction, and a decrease in the vasodilatory effects of nitric oxide. Therefore, an overactive RAAS could lead to the development of hypertension (44). Recent studies have postulated that an increase in proximal tubule angiotensin II receptors, which leads to an increase in sodium retention, may be responsible for the development of hypertension (45). In addition, high renin levels observed in patients with elevated blood pressure are caused by the defective feedback regulation of RAAS within the kidneys and adrenal glands (45).

Increased sympathetic nervous system activity, which results in elevated circulating plasma levels of norepinephrine and epinephrine, has been detected in patients with hypertension as well as in experimental hypertensive animal models (46). An increase in these neurotransmitter levels is thought to raise mean arterial blood pressure by impairing the ability of the kidneys to effectively excrete sodium and water from the body (46). Overactive sympathetic activity results in several effects that may lead to the development of hypertension, such as increased tubular sodium reabsorption, vasoconstriction, renal vascular resistance, and angiotensin II production (46).

Endothelin System and Hypertension

The human endothelin proteins, a gene family that consists of endothelin-1 (ET-1), endothelin-2 (ET-2), and endothelin-3 (ET-3), play an important role in regulating vascular tone and renal homeostasis through antagonistic vasoactive effects (47; 48). ET-1, the most prevalent member of the endothelin family, is synthesized in endothelial cells and inner medullary collecting ducts in response to growth factors such as thrombin, transforming growth factor β, and insulin, and to vasoactive substances such as angiotensin II, norepinephrine, and ADH (48). The release of ET-1 is also stimulated in response to low levels of shear stress. In fact, high shear stress is a potent inhibitor of ET-1 secretion (49).

Endothelin-1 Synthesis

The biologically active form of ET-1 is produced by a sequence of cleavage steps (Figure 6). Preproendothelin-1 (preproET-1), the 212-amino acid ET-1 precursor, is cleaved by a paired basic amino acid cleaving enzyme (50; 51). This enzymatic step is believed to be relatively nonspecific and results in the formation of a 38-amino acid intermediate peptide known as big endothelin-1 (BigET-1)(50; 51). BigEt-1 is cleaved at Trp21-Val22 and converted into mature ET-1, a 21-amino acid peptide, by endothelin-converting enzyme-1 (ECE-1), which is specific for endothelin (51). ECE-1, an essential component of ET-1 processing, has been localized predominantly to human blood vessel endothelial cells, which is also the primary source of ET-1 secretion (51). The expression of ECE-1 is mediated by protein kinase C (PKC), ET-B receptors, and cytokines (51).

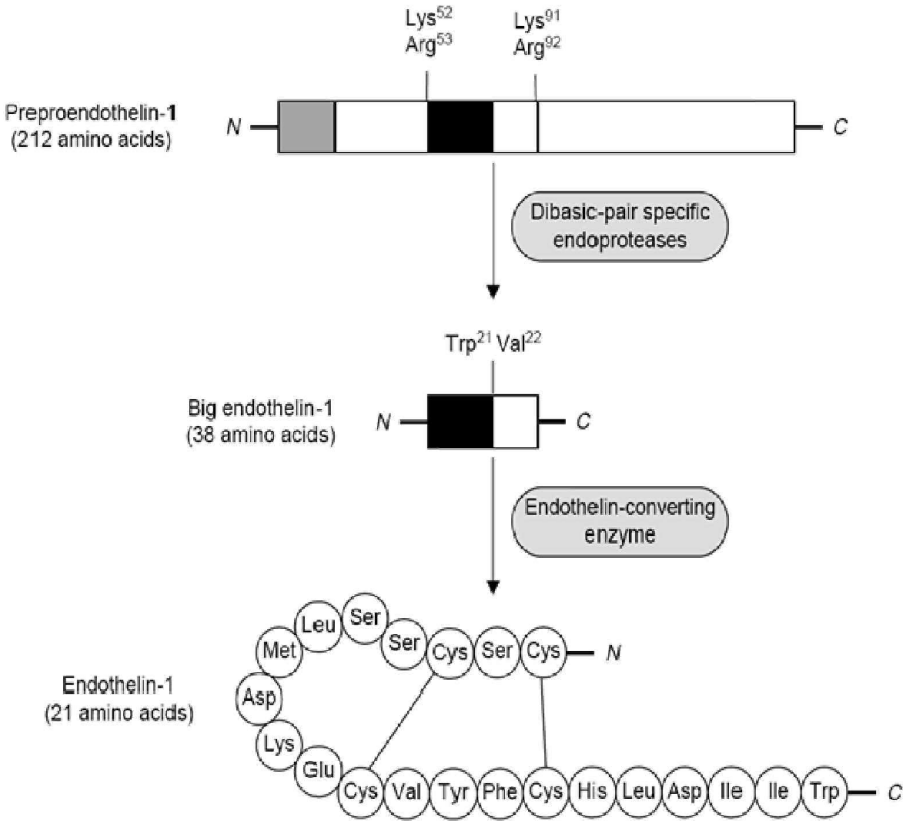

Figure 6. Biosynthesis of Endothelin-1. The pathway of vascular endothelin-1 synthesis (52).

Endothelin-1 and the Regulation of Mean Arterial Pressure

The presence of a vasoconstrictor peptide secreted by endothelial cells was discovered in 1985, but ET-1 was not isolated and cloned until 1988 (53). The vasoconstricting ability of ET-1 has never been disputed; in fact, it remains the most potent vasoconstrictor found to date. However, ET-1 has also been determined to have other effects on the vasculature, including vasodilation.

The biological effects of ET-1 are regulated by two plasma-membrane-bound receptors, endothelin-A (ET-A) receptor and endothelin-B (ET-B) receptor, both of which bind to ET-1 with equal affinity (51; 54). The ET-A and ET-B receptors exhibit sequence similarity, sharing about 63% of amino acid identity and have a high degree of sequence conservation, about 90%, across mammalian species (51; 54). Both endothelin receptor subtypes belong to the rhodopsin superfamily, are characterized by the presence of seven trans-membrane segments, and are G-protein coupled (55).

Endothelin receptors are found in many locations in the body, which explains why ET-1 is capable of producing several different physiological responses (Figure 7). ET-A receptors are found primarily in the heart and on vascular smooth muscle cells and are regarded as mediating vasoconstriction, cell proliferation, apoptosis, and fibrosis (56). Low densities of ET-B receptors, which function similar to ET-A receptors, are also present on smooth muscle cells (56). However, ET-B receptors are predominately expressed on endothelial cells throughout the human vasculature, especially in the human kidney, where they represent approximately 70% of the receptors present in the cortex and medulla (56). Upon activation by ET-1, the ET-B receptors located on endothelial cells mediate dilation by releasing endothelium-derived vasodilators, such as nitric oxide, in a feedback mechanism that limits ET-A induced vasoconstriction (56). ET-B receptors also function as a clearing receptor and remove ET-1 from circulation, explaining the relatively short ET-1 plasma half-life (56). Within the renal tubular system, ET-A receptors are located in distal tubules and cortical collecting ducts and

ET-B receptors are found in epithelial cells of proximal tubules and inner medullary collecting ducts (57). ET-1 derived from endothelial cells of the renal system usually binds to ET-A receptors and provokes vasoconstriction, while ET-1 produced in the medulla causes vasodilation and sodium excretion via ET-B receptors (58).

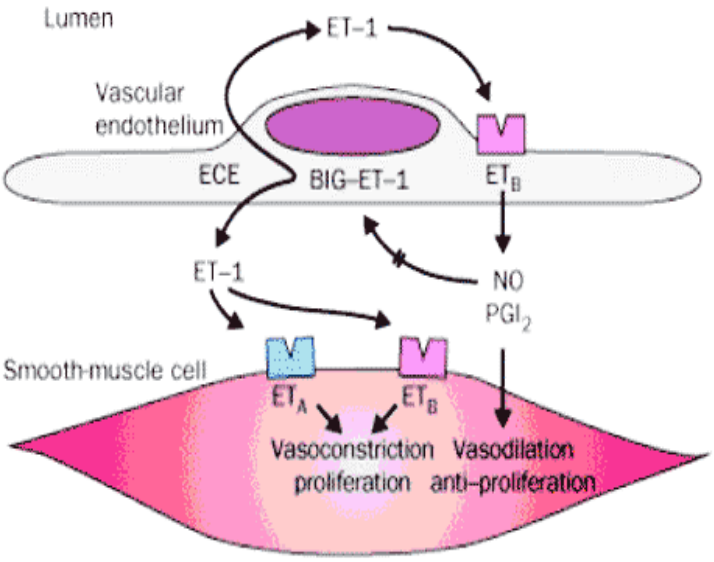

Figure 7. The Endothelin System. Interactions of Endothelin-1 with Endothelin-A and Endothlelin-B receptors in vascular endothelium and smooth muscle cells (59).

The Physiological Effects of Endothelin-A Receptor Binding

When ET-1 binds to the ET-A receptor, which is coupled to the G(q)-G11 protein, phospholiphase C (PLC) is activated (47; 54) (Figure 8). This leads to the breakdown of phosphatidylinositol 4,5-bisphosphate and the generation of inositol 1,4,5-triphosphate (IP_3) and diacylglycerol (DG) (47; 54). The formation of IP_3 stimulates the release of calcium from intracellular storage sites and facilitates the influx of extracellular calcium through voltage-dependent calcium channels (VDC) and receptor-operated calcium channels (ROC) (47; 54). The increase in the total intracellular free calcium level regulates various processes, including the activation of cellular contractile machinery (47; 54). The release of DAG stimulates prolonged activation of PKC activity, which, by causing phosphorylation of different proteins, could result in either activation or inactivation of proteins and the regulation of gene expression (47; 54).

ET-1 induced activation of ET-A receptors stimulates phospholipase A_2 (PLA_2), which produces prostacyclin (PGL_2), prostaglandin E (PGE_2), and thromboxane (TXA_2) to help mediate the contractile response (54). The binding of ET-1 to ET-A also causes an increase in intracellular pH via stimulation of the sarcolemmal Na^+H^+ antiporter, which enhances the sensitivity of myofilaments to calcium and may cause cellular contraction without an increase in calcium concentration (47; 54).

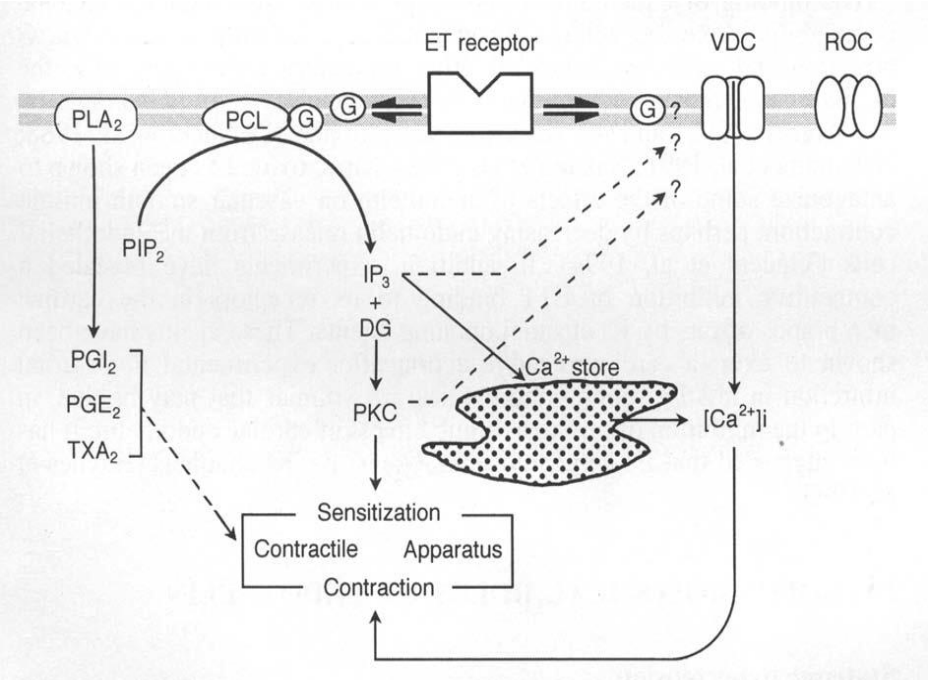

Figure 8. Endothelin-A Receptor Binding. The intracellular signal transduction pathways activated by ET-1 binding to ET-A receptors (54).

The Physiological Effects of Endothelin-B Receptor Binding

Similar to ET-A, the binding of ET-1 to ET-B receptors located in vascular smooth muscle cells stimulates vasoconstriction (56). However, the activation of ET-B receptors found in endothelial cells triggers signaling pathways that promote the release of vasodilator substances such as NO, PGI_2, and endothelium-derived hyperpolarizing factors (47). The signaling of NO production through ET-B receptors is coupled to the $G_{\beta\gamma}$ protein, which has been linked to protein kinase B (PKB) phosphorylation of endothelial nitric oxide synthase and the upregulation of NO production (47). NO

diffuses into vascular smooth muscle, where it stimulates guanylate cyclase and increases the levels of cyclic guanosine monophosphate (cGMP) (47). The increased concentration of cGMP causes vascular smooth muscle relaxation by decreasing intracellular calcium concentrations and myofilament sensitivity to calcium (47). The decrease in endothelial calcium stimulates prostacyclin production. Prostacyclin, a potent vasodilator, causes the activation of adenylate cyclase and increases cyclic adenosine monophosphate (cAMP), which affects the vascular smooth muscle in the same way as cGMP (47). The activation of ET-B receptors also triggers the release of endothelium-derived hyperpolarizing factors, which activate potassium channels and cause hyperpolarization, inhibition of calcium influx, and dilation of the vascular smooth muscle (47).

The Pathophysiology of the Endothelin System

Endothelin appears to be contributory to the development of several diseases, including systemic hypertension. Intravenous injections of endothelin causes a brief decrease in blood pressure, due to activation of ET-B receptors, followed by a lengthy increase in blood pressure caused by the stimulation of ET-A receptors (51; 54). It has been reported that treatment with an ET-A/ET-B receptor antagonist lowers blood pressure in patients with essential hypertension, suggesting that ET-1 may contribute to the development and maintenance of hypertension in these subjects (51).

A significant relationship between the concentration of ET-1 in vascular tissue and mean arterial blood pressure has been established in rats with

deoxycorticosterone acetate (DOCA)-salt-induced hypertension and in rats with hyperinsulinemic hypertension (51; 54). Studies have shown that elevated blood pressure in rats with DOCA-salt-induced hypertension is significantly reduced by ET-A receptor antagonists and by an ECE-1 inhibitor (51; 54). Hyperinsulinemic hypertensive rats, which have increased mesenteric ET-1 levels due to high levels of plasma insulin, experience a decrease in systemic blood pressure when treated with an ET-A/ET-B receptor antagonist without affecting the insulin concentration in the plasma or the ET-1 concentration in the mesentery (51; 54).

Adult mice lacking ET-B receptors have significantly elevated systemic blood pressure, which is shown to be salt sensitive and resistant to ET-A receptor antagonists, suggesting that ET-B receptors play a natriuretic role in the kidneys (51). Studies of the isolated perfused mouse kidney have shown that ET-1 increases sodium excretion and leads to a decrease in mean arterial blood pressure (51).

Exercise and Hypertension

Patients with elevated mean arterial blood pressure are commonly prescribed a treatment plan that includes lifestyle modifications and pharmacological interventions. However, in studies where only pharmacological management is prescribed only 25% to 62% of patients achieved normal blood pressure values (60). Because management of blood pressure is difficult with pharmacology, many doctors also recommend lifestyle adjustments, such as initiating a regular exercise regime (60). Regular physical activity, such as walking, jogging, cycling, or swimming, has been shown to decrease peripheral

arterial and vascular resistance, increase venous capacity, and improve arterial compliance and vascular endothelial function thus significantly lowering blood pressure in both hypertensive and normotensive patients (61). Frequent aerobic exercise of moderate intensity improves endothelial function in patients with primary hypertension. This leads to a decrease in systolic blood pressure by 6 to 10 mm Hg and diastolic pressure by 4 to 8 mm Hg and lowers the risk of cardiovascular mortality and morbidity (61; 62). The Joint National Committee of High Blood Pressure recommends that patients with mild to moderate primary hypertension exercise at an intensity of approximately 50% of maximum oxygen consumption for 30 minutes, 5 to 7 times per week, for at least 10 weeks to see the beneficial effects of physical activity on high blood pressure (61).

Physiological Effects of Exercise

The mechanism by which exercise improves endothelial function is not entirely clear, but is believed to be associated with an increase in nitric oxide production due to up regulation of endothelial nitric oxide synthase (eNOS) gene expression, a decrease in NO inactivation, and vascular endothelial growth factor induced angiogenesis (62). Acetylcholine (Ach), an endothelium-dependent vasodilator, is also found in higher concentrations after physical training in hypertensive patients as well as healthy individuals (62). One possible mechanism by which regular aerobic activity raises the level of vascular NO and Ach is via an increase in vascular shear stress resulting from

increased blood flow (62). The acute or chronic increase in shear stress is known to stimulate the release of NO in isolated vessels and cultured cells.

A recent study has reported that an increase in shear stress in epicardial coronary arteries of dogs after 10 days of treadmill exercise increased the expression of the eNOS gene, which caused the Ach stimulated NO release (63). The effect of exercise is also believed to cause a 20% decrease in plasma renin activity, a 29% decrease in the concentration of a potent vasoconstrictor, norepinephrine, and a 7.1% decrease in vascular resistance after endurance training for at least four weeks (61).

Exercise and the Endothelin System

The effect of chronic exercise training on the function of vascular endothelial cells has been documented in humans and rats. According to recent studies, regular aerobic exercise reduces plasma ET-1 levels in human subjects and this reduction may prevent vasoconstriction and the progression of hypertension (64). On the contrary, exercise has been documented to have an opposite effect on the renal endothelin system in rats (65) . It has been reported that exercise causes an increase in kidney ET-1 and a decrease in kidney NO production, both of which contribute to an exercise-induced decrease in renal blood flow (65). The same study also noted that the magnitude of decrease in renal blood flow during exercise was significantly lessened by the administration of an ET-A receptor antagonist (65).

Limited information is available on the effect of exercise on endothelin receptor expression in rats. However, an experiment recently conducted on swine has reported

that exercise lowers systemic ET-A receptor levels, thereby contributing to metabolic vasodilation, and has no effect on ET-B expression (66).

Spontaneously Hypertensive Rats

The Spontaneously Hypertensive Rat (SHR) is commonly used in genetic hypertension studies because it develops essential hypertension similar to humans (67). The SHR strain originated in the 1960s by selective breeding of Wistar-Kyoto (WKY) rats with high blood pressure (68). Relative to WKY rats, SHRs have a reduced kidney and body mass, which may be caused by a metabolic irregularity (67). Unlike WKY rats, SHRs begin to develop hypertension around 5 weeks of age and may reach systolic pressures as high as 180 to 200 mmHg (68). SHRs are known to undergo an alteration in their pressure natriuresis relationship, which requires an increased RPP to excrete a normal volume of sodium and water (68) and they also exhibit lower renal nitric oxide synthase activity and protein expression relative to normotensive control rats (69).

The Effects of Exercise on Spontaneously Hypertensive Rats

Studies have shown that moderate exercise wheel activity and forced treadmill exercise significantly lower the resting mean arterial pressure of young rats of the SHR strain (70). According to research by Overton and associates, SHRs that ran 3-7 kilometers per day for 12 weeks reduced their resting blood pressure by approximately 20 mmHg (70). These findings were confirmed by Edwards, who reported that systolic blood pressures in SHRs were significantly decreased in exercise-trained animals relative to non-exercised SHR control animals (71). It is believed that the exercise-induced blood

pressure reduction in SHRs may be caused by an increase in endothelial nitric oxide formation (72).

Rats of the SHR strain tend to engage in less physical activity than WKY rats when given access to an exercise wheel. One possible mechanism explaining this decrease in physical activity is that unlike WKY rats, SHRs are unable to increase their aortic elasticity or compliance during exercise (73). SHRs are also reported to have a reduction in endothelial function and nitric oxide synthesis, which leads to a decrease in blood flow rate and vessel diameter during exercise, relative to WKY rats (74).

The Endothelin System of Spontaneously Hypertensive Rats

Several studies have provided evidence that the endothelin system is involved in the pathogenesis and maintenance of hypertension in SHRs. One such study has documented that, because of a reduced capacity of the kidney to synthesize ET-1, the mean daily urinary excretion of ET-1 in SHRs is significantly lower than that measured in WKY rats (75). The same study also reported that the outer and inner medulla derived from SHRs released less ET-1 relative to WKY rats of the same age (75). This study revealed a decrease in ET-1 excretion and medulla levels in 8-9 week old rats, which is the age of high blood pressure development, but not in 3-4 week old rats (75).

SHR rats tend to have an increased amount of vascular shear stress, which has been reported to have a strong effect on the synthesis and expression of endothelin in humans (49). A recent study exposed cultures of human umbilical vein endothelial cells to laminar shear stress and found that long-term application of shear stress lead to a

down regulation of preproET-1 mRNA, ECE-1 mRNA, and ET-1 protein expression levels (49). This study also reported an upregulation of ET-B receptor protein levels in response to long-term arterial shear stress (49).

The expression of endothelin receptor subtypes in the kidneys of SHRs has also been examined. ET-A receptors are upregulated in the glomeruli and smooth muscle cells of SHRs relative to age-matched WKY rats due to an increase in ET-A receptor expression, as shown by an increase in mRNA formation (55). Similarly, ET-B receptors are also upregulated in the glomeruli of SHRs compared to age-matched WKY rats (55). However, this increase in receptor density is not caused by an upregulation of ET-B mRNA but results from a decrease in ET-B receptor degradation or to inactivation of enzymes involved in ET-B receptor degradation (55). Studies have also shown that blocking endothelin receptors in SHR rats with either an ET-A receptor antagonist or an ET-A/ET-B receptor antagonist results in a similar decrease in mean arterial blood pressure (58). This suggests that the overexpression of vascular ET-A receptors is essential in renal blood flow regulation and contributes to the development of high blood pressure in SHRs (58).

Purpose of Current Study

Prior studies in the laboratory of Dr. Penny Knoblich have reported a significant increase in sodium excretion in exercised female spontaneously hypertensive rats (SHR) and Wistar Kyoto (WKY) rats in response to a rise in blood pressure induced by either

vessel ligation or angiotensin II infusion. However, this effect was not observed in exercised male and sedentary SHR and WKY rats (76).

The blood pressure lowering effect of exercise has been established; however it is unknown how exercise affects the endothelin system. The purpose of this study was to evaluate the effect of exercise on the endothelin system of female SHR and WKY rats. The study also included male SHR and WKY rats to confirm that any alterations in the measured parameters explained the sex difference previously observed in Dr. Penny Knoblich's laboratory. Exercised induced changes in endothelin and or endothelin receptor levels were analyzed to elucidate potential mechanisms to explain an increase in sodium excretion in exercised female SHR and WKY rats as previously described in the laboratory of Dr. Penny Knoblich.

Our experiments were based on three hypotheses. The first hypothesis states that since ET-A receptors function in vasoconstriction, levels of ET-A receptors would be down regulated in the kidneys of exercised female SHR and WKY rats relative to sedentary female SHR and WKY rats. It was also hypothesized that there would be no change in the expression of ET-A receptors in exercised male SHR and WKY rats relative to their sedentary counterpart. Western blot analysis and immunofluorescence microscopy were utilized to evaluate the level of ET-A receptors in the kidneys of each group of rats. Our hypothesis would be supported if ET-A receptor levels were lowest in the kidneys of exercised female SHR and WKY rats.

ET-B receptors play an important role in vasodilation and the facilitation of sodium excretion from the body, therefore the second hypothesis states that ET-B receptor levels would be up regulated in the kidneys of exercised female SHR and WKY rats relative to sedentary female SHR and WKY rats. It was also hypothesized that there would be no change in the expression of ET-B receptors in exercised male SHR and WKY rats relative to their sedentary counterpart. The expression of ET-B receptors in the kidney tissue of each group of rats were evaluated using western blot analysis and immunofluorescence microscopy. If our hypothesis was supported, ET-B receptor levels would be highest in kidney tissue extracted from exercised female SHR and WKY rats.

The third hypothesis states that since ET-1 is required to activate both ET-A and ET-B receptors, there would be no significant difference in ET-1 concentration in the kidneys of exercised and sedentary female and male rats of either strain. ET-1 levels in the kidneys of each group of rats were assessed using western blot analysis, enzyme-linked immunosorbent assay, and immunofluorescence microscopy. If ET-1 expression levels were similar in the kidney tissue extracted from each group of rats, then our hypothesis would be supported.

MATERIALS AND METHODS

Animal Husbandry and Exercise Regime

Twenty male SHR rats, twenty male WKY rats, twenty female SHR rats, and twenty female WKY rats, maintained in the animal care facility at Minnesota State University, Mankato, were given *ad libitum* access to tap water and standard rat chow (Purina LabDiet, Brentwood, MO). The temperature of the colony was kept at a constant 21 $\pm$ 2^{o} Celsius with a 12:12 night/day light cycle. At four weeks of age, ten rats from each group were randomly assigned to an exercise group and ten rats from each group were randomly assigned to a control group. The rats assigned to the exercise group ran voluntarily on wire exercise wheels that measured 28 cm in diameter for ten to twelve weeks. A magnet and magnetic counter recorded the number of exercise wheel revolutions, and a bicycle odometer was used to record the total distance and duration of wheel activity. Data was recorded two times per week, and the total weekly distance and duration of activity was calculated for each rat. The control group was not exercised and therefore not provided a wire exercise wheel.

Surgical Procedure

After ten to twelve weeks post exercise, the exercised and control rats were prepared for surgery as follows: Each rat was placed in a 22.9 cm x 12.7 cm x 10.2 cm plastic anesthetic chamber until its bladder was voided. After urination, the rat was removed and the urine was collected using a 1cc sterile syringe and stored at -20^{o} Celsius for future analysis. The rat was returned to the chamber and euthanized using

carbon dioxide inhalation for approximately two minutes or until breathing ceased. The body mass to the nearest tenth of a gram was recorded. An incision was made on the ventral midline, from the pubic bone extending to the thorax. The kidneys were located and cut free from surrounding fat tissue. Nylon surgical thread (Coats & Clark, Greenville, SC) was then tied around the renal arteries to reduce blood flow to the kidneys preceding their excision. After removal, the kidneys were rinsed in phosphate buffered saline (PBS) [(137mM NaCl, 2.7mM KCl, 10mM Na_2HPO_4, 2mM KH_2PO_4 (pH 7.4)] and mass and overall morphology noted. The kidneys were flash frozen in liquid nitrogen and stored at -20^{o} Celsius for future analysis.

Enzyme-Linked Immunosorbent Assay

Reagent Preparation

A commercially available Endothelin-1 enzyme-linked immunosorbent assay (ELISA) kit (Assay Designs, Ann Arbor, MI) was used. Wash buffer was prepared by diluting 50 ml of the supplied wash buffer concentrate with 950 ml of deionized water and stored at room temperature. Endothelin-1 standards were prepared by serial dilutions of the supplied 1,000 pg/ml endothelin-1 standard stock solution (Figure 9). The endothelin-1 antibody was prepared by diluting 40 µl of the supplied antibody concentrate with 4 ml of antibody diluent. An equal amount of urine from each rat in each experimental group, totaling 20 µl per group, was pooled and centrifuged at 4,000 x gravity for 5 minutes.

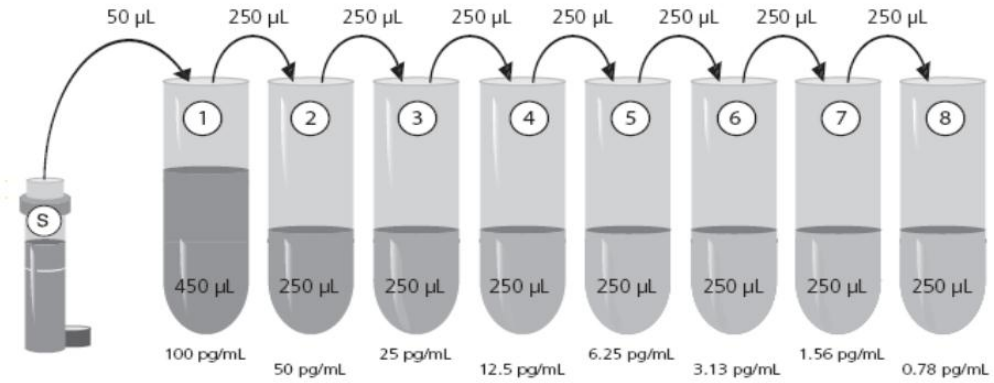

Figure 9. Preparation of Endothelin-1 standards. The serial dilution scheme used to prepare the eight standards needed for the ELISA analysis. Cartoon adapted and modified from the manufacturer supplied literature (Assay Designs, Ann Arbor, MI)

Assay Procedure

100 µl of the assay buffer was added to the 0 pg/ml standard wells, followed by adding 100 µl of standards #1 through #8 and 100 µl of each urine sample from the 8 groups to the bottom of their respective wells. The plate was sealed and incubated overnight at room temperature. Following incubation, the wells were washed with 400 µl of wash buffer five times for five minutes each. After the final wash, the wells were emptied and the plate firmly tapped against a paper towel to ensure all remaining buffer was removed. 100 µl of the diluted antibody was added to each well with the exception of the blanks, and the plate was sealed and incubated at room temperature for one hour. Following incubation, the wells were emptied and washed with 400 microliters of wash buffer five times for five minutes each. 100 µl of the substrate solution was added to each well and the plate was incubated at room temperature for

30 minutes before adding 100 µl of stop solution into each well. The Multiscan Microplate Spectrophotometer (Thermo-Fisher Scientific, Rockford, IL) and ScanIt 2.4.4 Software (Thermo-Fisher Scientific, Rockford, IL) were utilized to measure the optical density of each standard and sample at 450 nm. A standard curve of optical density was generated using Microsoft Excel 2007. A line of best fit was generated and the corresponding equation was used to calculate the amount of endothelin-1 protein in each urine sample based upon its optical density.

Western Blot Analysis

Solubilization of the Kidneys

Six kidneys randomly chosen from six rats in each group, female SHR exercised (F-SHR-E), female SHR sedentary (F-SHR-S), female WKY exercised (F-WKY-E), female WKY sedentary (F-WKY-S), male SHR exercised (M-SHR-E), male SHR sedentary (M-SHR-S), male WKY exercised (M-WKY-E), and male WKY sedentary (M-WKY-S) were pulverized between two pieces of one inch thick sheet metal by direct force using a hammer. The pulverized tissue was resuspended in 1X SDS Sample Buffer [(50mM Tris/HCL (pH 6.8), 2% SDS (w/v), 0.1% (w/v) bromophenol blue, 10% glycerol (v/v), 100mM Dithiothreitol] to a concentration of 0.1mg/ml. The tissue was solubilized using a dounce homogenizer and boiled for approximately five minutes before centrifugation at 2,000 x gravity for five minutes. The solubilized kidney tissue was partitioned into 1.5 microcentrifuge tubes and stored at -20^{o} Celsius for future sodium dodecyl sulfate polyacrylamide gel electrophoresis (SDS-PAGE).

SDS-PAGE and Transfer to Nitrocellulose Membrane

The BioRad Model 422 electrophoresis chamber system (BioRad, Hercules, CA) was utilized in this experiment. The glass gel casting plates were washed and rinsed with ethanol before being clipped into the casting plate holder. Once the plates were in place, approximately ten ml of the lower resolving gel [(0.375M Tris/HCL (pH 8.8), 0.1% SDS (w/v), 9.9% acrylamide (w/v), 0.05% TEMED, 0.08% ammonium persulfate (w/v) (pH 8.8))] was poured into each cast. While waiting for the lower gel to solidify, the upper stacking gel, [(0.125M Tris/HCL (pH 7.0), 0.1% SDS (w/v), 4.8% acrylamide (w/v), 0.1% TEMED, 0.1% ammonium persulfate (w/v) (pH 7.0))], was mixed. After the lower resolving gel had solidified, the casting plates were filled with approximately 5 ml of the upper stacking gel and 1.5 mm well combs were submerged into the gel. Once the upper stacking gel had solidified, the combs were removed and the wells were washed with 1x SDS running buffer [(0.25M Tris/HCL, 1.92M Glycine, 1% SDS)] before the protein standard (Sigma High Molecular Weight Marker, Sigma-Aldrich, St. Louis, MO) and samples were added to their respective wells. The gels were then inserted into separate electrical chambers filled with 1x SDS running buffer and connected to an electrical source. The gels were resolved at 80 volts until the protein bands migrated below the stacking gel and then increased to approximately 120 volts for the next 90 minutes. The gels were removed from their chamber, the upper stacking gel taken off, and the lower resolving gel immersed in Coomassie Brilliant Blue protein stain [(0.25%

Coomassie brilliant blue R-250 (w/v), 45% methanol (v/v), 10% glacial acetic acid (v/v)] for 24 hours. The Coomassie dye was removed and replaced with Coomassie destaining solution [(5% methanol (v/v), 7.5% glacial acetic acid (v/v)] until enough dye had been removed to visualize the bands of protein in the gel. Each gel was scanned and analyzed using ImageJ software (National Institute of Health). Based upon the results, the protein load was adjusted and SDS-PAGE was repeated to ensure an equal amount of protein in each kidney sample.

After the optimal protein load was determined, proteins were resolved by SDS-PAGE as previously described and transferred to nitrocellulose membrane (Whatman, Piscataway, NJ). The BioRad Mini-Trans Blot electrophoretic transfer cell system (BioRad, Hercules, CA) was used to transfer the proteins. Immediately after electrophoresis, the gel was removed from the electrical chamber and layered between two sheets of filter paper and one nitrocellulose membrane. The gel was then squeezed inside in the cassette holder and placed inside the electrical chamber, which was filled with transfer buffer [(25mM Tris/HCL, 191.8 mM Glycine, 20% methanol (v/v))], before being connected to an electrical source. The gels were transferred at 30 volts for four hours. After transfer was complete, the membrane was removed and stored at -20^{o} Celsius.

Western Blotting

The nitrocellulose membrane was submerged in Ponceau staining solution [(5% Ponceau S (w/v), 0.05mM Trichloroacetic acid)] for approximately two minutes before being immersed in 1% glacial acetic acid solution two times for 15 seconds or until enough dye had been removed to visualize the bands of protein on the nitrocellulose. The protein standard was removed from the membrane using a razor blade and stored. Nonspecific binding sites were blocked by submerging the membrane in 10 milliliters of a commercially available Superblock solution (Thermo-Fisher Scientific, Rockford, IL) for 15 minutes at room temperature. The Superblock was removed and replaced with 5-10 ml of a block solution that consisted of 50 ml 1x TweenTris-buffered saline (TTBS) [(136.89mM NaCl, 24.76mM Tris/HCL, 2.68mM KCL, 0.823mM Triton X-100)], 5% bovine serum albumin (Calbiochem-Novabiochem International, La Jolla, CA) and 1% inactivated fetal calf serum (FCS) for 30 minutes at room temperature. The block was removed after 30 minutes and replaced with approximately two milliliters of the appropriate primary antibody diluted in block solution. The primary antibodies used were: 1:250 dilution of ET-1 goat polyclonal IgG antibody (Santa Cruz Biotechnology, Santa Cruz, CA), 1:300 dilution of ET-A receptor mouse monoclonal IgG_1 antibody (Santa Cruz Biotechnology, Santa Cruz, CA), and 1:100 dilution of ET-B rabbit polyclonal IgG antibody (Santa Cruz Biotechnology, Santa Cruz, CA). The nitrocellulose membrane was incubated overnight at 4^{o} Celsius. The membrane was removed from the solution and washed with 1x TTBS, three times for ten minutes each. This was followed by

incubation with 3-5 ml of an appropriate enzyme conjugated secondary antibody diluted in block and applied to the nitrocellulose membrane for 2-4 hours at room temperature. The secondary antibodies used in this experiment were: 1:3500 dilution of alkaline phosphatase conjugated anti-goat IgG antibody produced in rabbit (Sigma-Aldrich, St. Louis, MO), 1:5000 dilution of alkaline phosphatase conjugated anti-mouse IgG antibody produced in goat (Sigma-Aldrich, St. Louis, MO), and 1:3000 dilution of alkaline phosphatase conjugated anti-rabbit IgG antibody produced in goat (Sigma-Aldrich, St. Louis, MO). The membrane was removed from the solution and washed with 1x TTBS three times for ten minutes each. The membrane was briefly washed in substrate buffer [(0.1mM Tris/HCL, 25mM diethanolamine, 0.1M NaCl, 2mM $MgCl_2$, 1 µM $ZnCl_2$ (pH 9.55))]. Antibodies bound to the nitrocellulose membrane were detected via the addition of substrate buffer with 0.4 µM of Nitro Blue Tetrazolium Chloride (NBT) (Tokyo Chemical Industry Corporation, Tokyo, Japan), 1.57 µM of 5-Bromo-4-Chloro-3-Indoyl Phosphate Disodium Salt (BCIP) (USB Corporation, Cleveland, OH), and 4.37 µM of Phenazine Methosulfate (PMS) for three to five minutes at room temperature. The developer was removed after purple bands developed on the nitrocellulose membrane. The membrane was washed in deionized water and stored at 4^{o} Celsius.

Image Analysis

The image of the gel or nitrocellulose membrane was analyzed using Image J software. The protein band or lane of interest was selected and a profile was generated

to determine the relative amount of protein in each lane and the relative reactivity of the immunoblot in the kidney samples from each experimental subset of rats.

Immunohistochemistry

Cryosectioning

5-7 µm sections of frozen kidneys from each experimental group were prepared using a Leica CM 1850 UV cryostat (Leica Microsystems, Buffalo Grove, IL). Each section was transferred to a VistaVision HistoBond microscope slide (VWR International, Radnor, PA) and stored at -20^{o} Celsius.

Immunostaining

Prior to staining, each tissue section was outlined using liquid blocking pap pen (Daido Sangyo Corporation, Tokyo, Japan) and rinsed for approximately two minutes in PBS. The tissue was fixed with 0.1% paraformaldehyde in PBS at room temperature for 15 minutes. After removing the fixative, each slide was overlaid with 10 mM ethanolamine in PBS for 10 minutes to quench the excess paraformaldehyde followed by a methanol shock at -20^{o} Celsius for 5 minutes to permeabilize the kidney tissue. The tissue was rehydrated in PBS for approximately 5 minutes before a blocking solution (1x PBS, 5% BSA, 1% inactivated FCS) was added to each section. After approximately one hour, the blocking solution was removed and replaced with the appropriate antibody diluted in the blocking solution. A 1:100 dilution of a monoclonal anti-actin antibody conjugated with Cy3 (Sigma-Aldrich, St. Louis, MO) was used as a positive control. The primary antibodies used were: 1:50 dilution of ET-1 goat polyclonal IgG

antibody (Santa Cruz Biotechnology, Santa Cruz, CA), 1:100 dilution of ET-A receptor mouse monoclonal IgG_1 antibody (Santa Cruz Biotechnology, Santa Cruz, CA), and 1:50 dilution of ET-B rabbit polyclonal IgG antibody (Santa Cruz Biotechnology, Santa Cruz, CA). Following overnight incubation at 4^{o} Celsius, each slide was washed 3 times, for 15 minutes in PBS. Kidney tissue that was previously exposed to ET-1 primary antibody was incubated with a 1:100 dilution of Alexa Fluor 488 rabbit anti-goat IgG antibody (Invitrogen Molecular Probes, Carlsbad, CA). Kidney tissue that was previously treated with ET-A primary antibody was incubated with a 1:1500 dilution of Alexa Fluor 555 goat anti-mouse IgG antibody (Invitrogen Technologies, Carlsbad, CA). Kidney tissue that was previously exposed to ET-B primary antibody was incubated with a 1:25 dilution of goat anti-rabbit IgG-PerCP-Cy5.5 antibody (Santa Cruz Biotechnology, Santa Cruz, CA). After 2-4 hours of incubation at room temperature, each slide was washed 3 times, 15 minutes each time, in PBS. Number 1 coverslips (VWR International, Radnor, PA) were applied to each slide using ProLong Gold antifade reagent with DAPI media (Invitrogen Technologies, Carlsbad, CA) and sealed using a commercially available clear nail polish. The slides were stored at 4^{o} Celsius.

Immunofluorescence and Image Capturing Software

The mercury lamp was powered on before turning on the Olympus BX40 trinocular fluorescence microscope (Olympus, Center Valley, PA) and the Hamamatsu C8484 digital camera (Hamamatsu Photonics, Hamamatusu City, Japan). The prepared slide was placed on the stage and secured with the stage clips. Once the specimen was

centered and focused, the bright field light was turned off and replaced with the fluorescent light and the appropriate wavelength excitation filter. The DAPI stain on each slide was visualized using the WU excitation filter (excitation: 359 nm; emission: 461 nm). Slides that were stained with ET-1 were viewed using the FITC excitation filter (excitation: 490 nm; emission: 525 nm) and slides that were stained with either ET-A or ET-B were viewed using the TRITC excitation filter (excitation: 557 nm; emission: 576 nm). If more than one antibody was being viewed at once, the multi-excitation filter was utilized. Once a suitable image was found, the view of the microscope was switched to the camera setting so it could be captured using the digital camera attachment. Digitized images were acquired using Simple PCI imaging software (Hamamatsu Photonics, Hamamatsu City, Japan).

RESULTS

To evaluate the effect of exercise on endothelin and endothelin receptors, male and female hypertensive and normotensive rats were either restricted from exercise (sedentary groups) or provided an exercise wheel (exercised groups) for eleven weeks. Subsequently, the total exercise distance and kidney and body mass of each rat was determined, the relative amount of ET-1 and ET-A and ET-B receptors in the kidney lysate was evaluated, and level of ET-1 excreted in the urine was measured. Immunofluorescence studies also characterized the localization of ET-1 and ET-A and ET-B receptors within the renal tissue and cells.

Exercise Distance

A total of 4 groups were exercised including male hypertensive (M-SHR-E), female hypertensive (F-SHR-E), male normotensive (M-WKY-E) and female normotensive (F-WKY-E). The total distance ran over the duration of the experiment was compared for each group (Table 1; Figure 10). Overall, the level of exercise activity was diminished at the onset and at the end of the study (week 1 and week 11, respectively), with the highest level of activity during weeks 2 through 10. Female SHR rats ran a significantly greater distance overall with increased levels during weeks 2, 3, 4, and 6 relative to male SHR rats (Figure 11). Although female WKY rats exercised more than male WKY rats, the difference in running distances was not statistically significant (Figure 12). In addition, WKY rats exercised more overall than SHR rats, regardless of sex.

Kidney and Body Mass

As an initial means of characterization of the differences between exercised and sedentary hypertensive and normotensive rats, the total kidney, body, and kidney (mg): body (g) mass was determined after eleven weeks. The mean kidney and body mass of female rats was significantly less than the mean kidney and body mass of male rats of the same strain and activity level (Table 2; Figure 13; Table 3; Figure 14). The mean kidney mass was significantly greater in exercised female WKY and female SHR rats relative to sedentary female WKY and female SHR rats. In addition, exercised female WKY and male WKY rats had a larger body mass than their sedentary counterpart. In general, WKY rats had an increased mean kidney and body mass relative to SHR rats.

The mean kidney: mean body mass ratio was slightly, but not significantly greater in exercised female SHR, female WKY, and male SHR rats relative to their sedentary counterparts (Table 4; Figure 15). Exercised male WKY rats had a significantly increased kidney: body ratio relative to sedentary male WKY rats. There was no difference in the ratio between female and male rats of the same strain and activity level.

The amount of total work, as determined by multiplying the mean body weight by the mean weekly running distance of each group of exercised rats, was greater in male and female WKY rats relative to male and female SHR rats (Table 5; Figure 16).

Levels of Endothelin in Urine

To determine if increased exercise activity led to an increase in endothelin excretion, the amount of ET-1 in urine pooled from each group of rats was analyzed using an ET-1 ELISA. The absorbance value of ET-1 standards were used to construct a linear curve (slope intercept form y = 0.0099x + 0.0064, coefficient of determination = 0.9964) (Table 6; Figure 17). The level of ET-1 in each urine sample was extrapolated from the standard curve.

The ELISA results demonstrated: 1) the amount of ET-1 was greater in the pooled urine of female SHR sedentary, female WKY exercised, and female WKY sedentary rats, but not female SHR exercised rats, relative to males of the same strain and activity level; 2) male and female WKY rats excreted more ET-1 than SHR rats; 3) the effect of exercise on ET-1 levels was inconsistent between WKY and SHR rats. The urine of exercised WKY rats contained more ET-1 than WKY sedentary rats and on the contrary, the urine of exercised SHR rats contained less ET-1 than SHR sedentary rats (Table 7; Figure 18).

Endothelin and Endothelin Receptor Levels in Solubilized Kidney Tissue

To evaluate the effect of exercise on ET-1 and ET-A and ET-B receptors, homogenized renal lysates from each group were resolved by SDS-PAGE, probed using Western blot analysis, and quantitated using Image J software (Figure 19; Figure 20; Figure 21; Figure 22). In the case of ET-A, 1) the amount of receptors was greater in the kidney homogenate of SHR rats relative to WKY rats; 2) receptor levels were greater in the kidney tissue of males relative to females of the same strain and activity level, with

male SHR exercised rats being the only exception; 3) Exercise had various effects on the level of ET-A in the kidney tissue of each group of rats. Male SHR sedentary rats had an increased level of ET-A relative to male SHR exercised rats; conversely, female SHR sedentary rats had a decreased level of ET-A relative to female SHR exercised rats; 4) the effect of exercise had an opposite impact on WKY rats, with a decrease in ET-A levels in male WKY sedentary rats relative to male WKY exercised rats and an increase in ET-A levels in female WKY sedentary rats relative to female WKY exercised rats (Table 8;Table 9; Figure 23). In the case of ET-B, receptors were detectable in the kidney homogenate of female SHR exercised rats but were not observed in any of the other group of rats (Figure 24). ET-1 levels were undetectable in all kidney homogenates.

Endothelin and Endothelin Receptor Localization within Kidney Tissue

The effect of exercise on the localization patterns of ET-1 and ET-A and ET-B receptors within the renal tissue and cells of each group of rats was determined using immunofluorescence microscopy on cryosections. Renal tissue from each group of rats was probed with an anti-actin antibody as a positive control. Broad actin staining localized around the proximal and distal tubules, perimeter of cells, and small blood vessels was found throughout each sample (Figure 25).

A common pattern of ET-A receptor staining was seen throughout each experimental group of rats (Figure 26; Figure 27; Figure 28; Figure 29; Figure 30; Figure 31; Figure 32; Figure 33; Figure 34; Figure 35; Figure 36; Figure 37; Figure 38; Figure 39; Figure 40; Figure 41). Broad ET-A receptor staining was consistently localized around

the perimeter of both proximal and distal convoluted tubules, with the most intense staining coinciding with the extracellular membrane. Intracellular cytoplasmic staining was noted within the structures of the nephron. ET-A receptors were also evenly distributed throughout epithelial wall of the Bowman's capsule and the glomerular matrix of the renal corpuscle. Kidney tissue extracted from sedentary male SHR rats had the most intense ET-A receptor staining. In comparison with sections of lower intensity, the staining of the face of the tubular extracellular membrane was greatly increased in sedentary male SHR rats.

Similar to ET-A receptors, ET-B receptor staining was very broad and evenly distributed throughout the majority of the components of the nephron (Figure 42; Figure 43; Figure 44; Figure 45). However, ET-B receptor staining was much less intense than renal sections stained with ET-A receptor primary antibody. Unlike ET-A receptor staining, intense ET-B receptor staining was only observed in kidney tissue extracted from exercised female SHR rats.

4',6-diamidino-2-phenylindole (DAPI) is a fluorescent stain that binds strongly to nucleic acids. There was a general overlap of DAPI and ET-A receptor and ET-B receptor staining; however, DAPI was more centrally localized within the cells that surround the perimeter of several renal structures, including blood vessels, proximal convoluted tubules, and distal convoluted tubules. DAPI staining was also well punctated throughout the renal corpuscle and glomerulus of the nephron.

Renal sections stained with the appropriate secondary antibody independent of the ET-A receptor and ET-B receptor primary antibodies served as a negative control. Nonspecific interstitial renal secondary antibody staining varied among the groups of experimental rats; however, it was generally very minimal.

Unlike ET-A receptor and ET-B receptor staining, kidney tissue stained with ET-1 primary antibody was indiscernible from kidney tissue stained only with secondary antibody (Figure 46).

	Week 1	Week 2	Week 3	Week 4	Week 5	Week 6	Week 7	Week 8	Week 9	Week 10	Week 11	Total	Mean Weekly Distance
Male SHR	22.38	23.6	23.15	42.59	38.58	33.93	46.94	38.38	49.37	48.49	27.88	395.28	35.93
Male WKY	12.13	27.51	47.93	51.5	50.54	56.76	54.54	58.68	45.21	47.07	25.32	477.19	43.38
Female SHR†	39.79	60.99*	62.27*	79.56*	69.49	65.41*	63.99	64.91	56.36	43.51	35.86	576.73	52.43
Female WKY	20.68	48.98	69.34	62.81	81.2	63.34	71.63	68.55	64.46	69.03	43.74	663.76	60.34

Table 1. Mean Weekly Exercise Distance. The mean exercise distance (km) of each experimental group of rats. Values are reported as mean ± standard error.
***** $p \leq 0.05$ when compared to weekly exercise distance of males of the same strain.
† $p \leq 0.05$ when compared to overall exercise distance of males of the same strain.

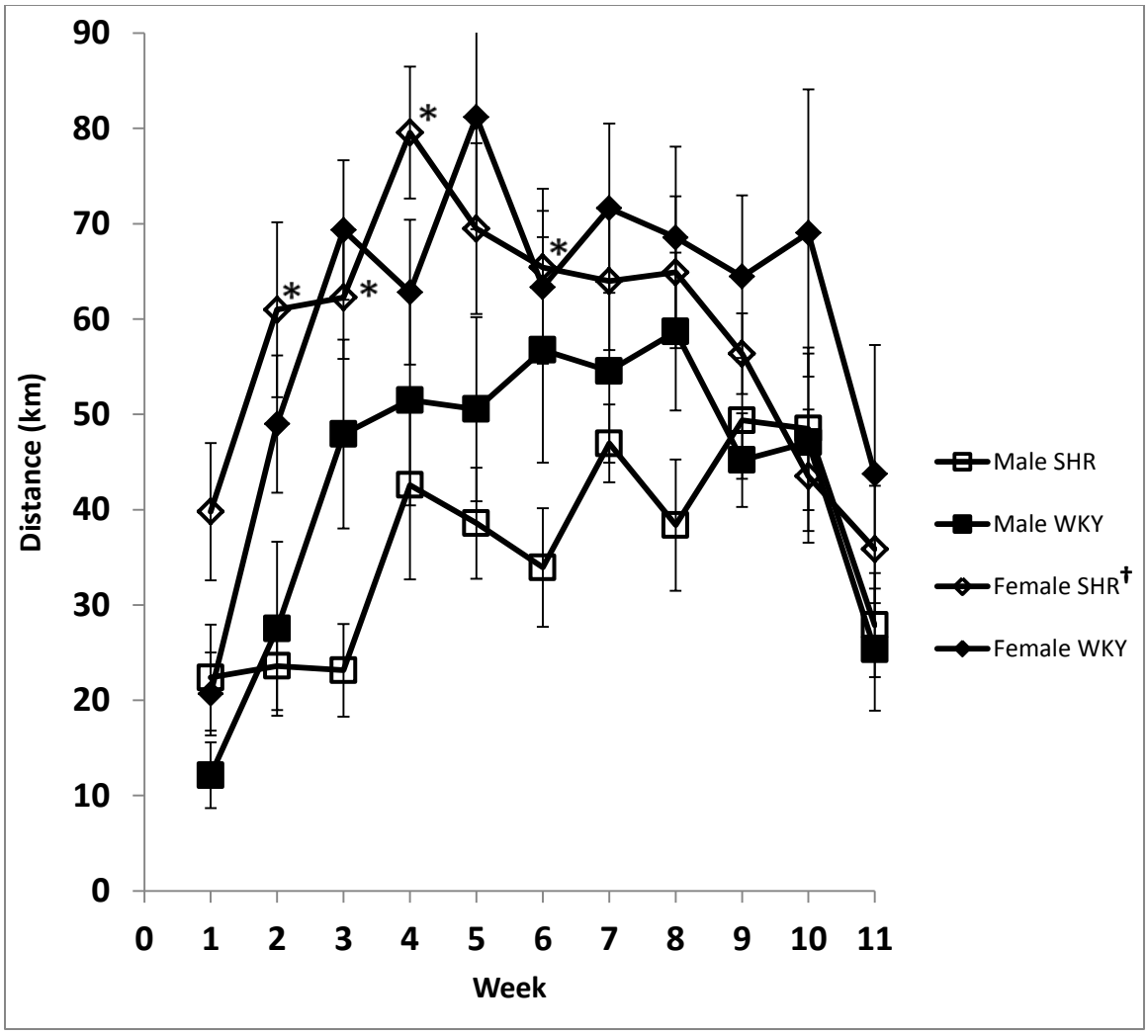

Figure 10. Mean Weekly Exercise Distance. The mean weekly exercise distance (km) of each experimental group of rats. Values are reported as mean ± standard error.

***** $p < 0.05$ when compared to weekly distance of males of the same strain.

† $p < 0.05$ when compared to overall distance of males of the same strain.

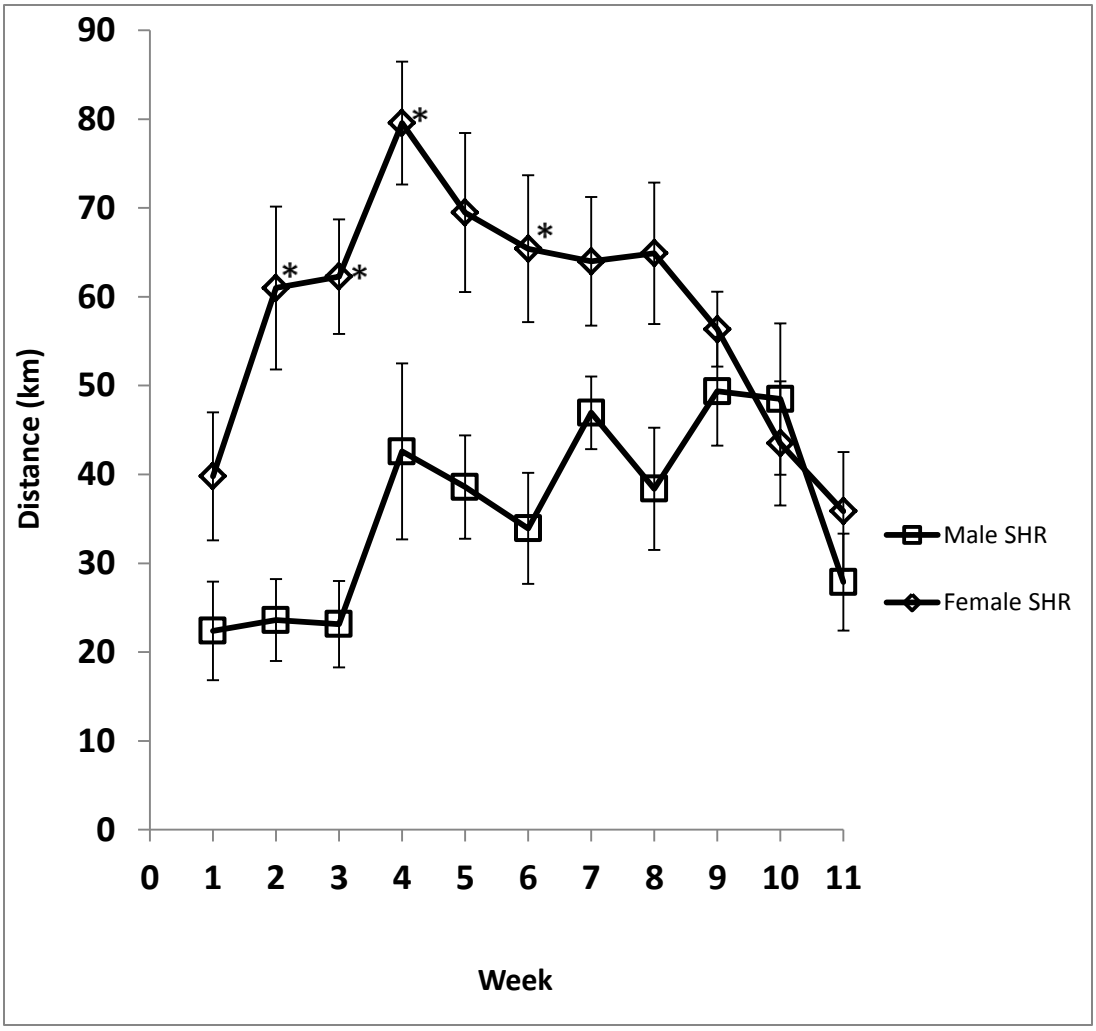

Figure 11. Mean Weekly SHR Exercise Distance. The mean weekly exercise distance of SHR male and female rats. Values are reported as mean ± standard error.

*****$p < 0.05$ when compared to weekly exercise distance of males.

† $p < 0.05$ when compared to overall exercise distance of males.

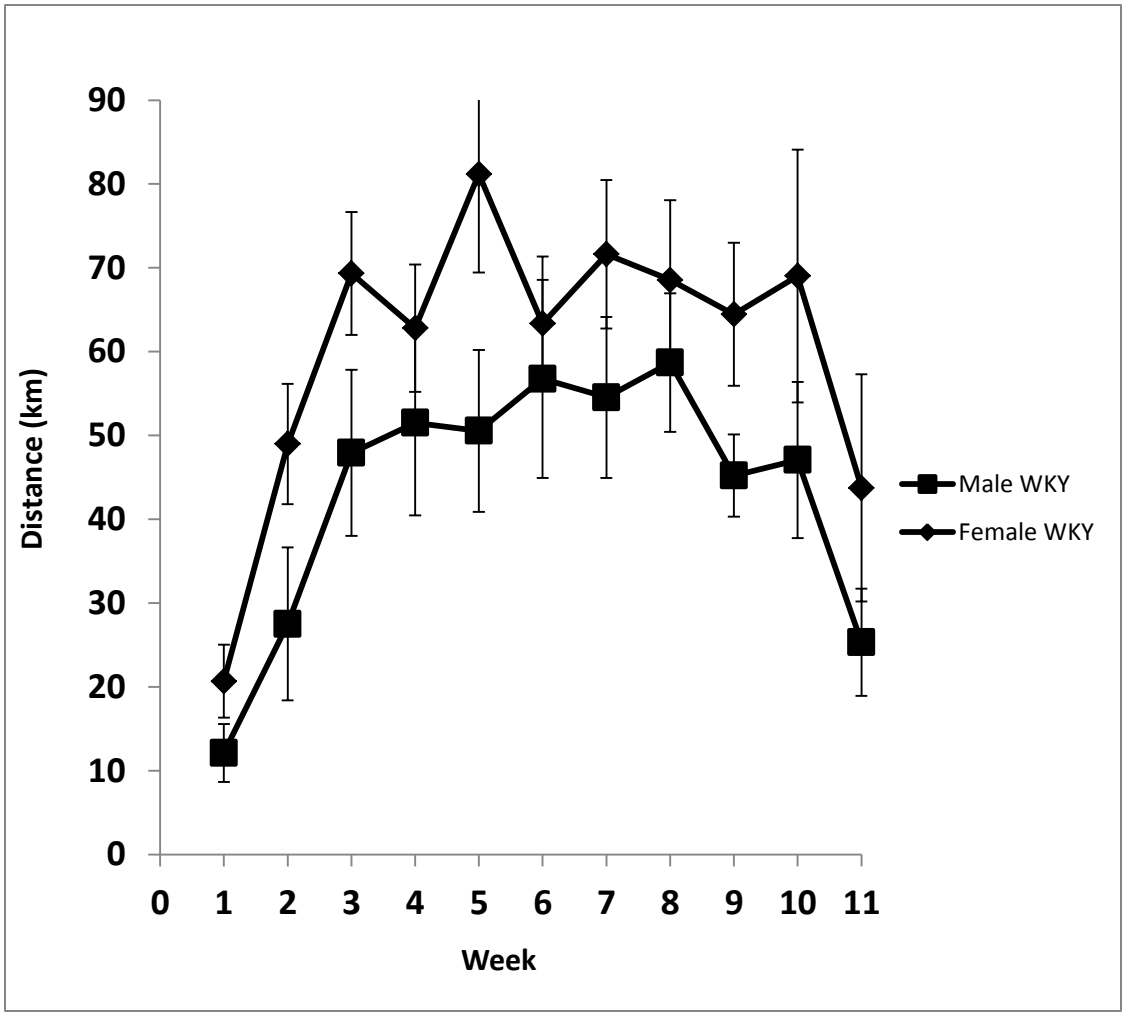

Figure 12. Mean Weekly WKY Exercise Distance. The mean weekly exercise distance of WKY male and female rats. Values are reported as mean ± standard error.

Rat Subset	Mean Kidney Mass (g)	± SEM
F-SHR-E	1.04	0.014
F-SHR-S	0.96	0.018
F-WKY-E	1.69	0.049
F-WKY-S	1.42	0.053
M-SHR-E	1.65	0.036
M-SHR-S	1.61	0.035
M-WKY-E	2.26	0.083
M-WKY-S	2.29	0.061

Table 2. Mean Kidney Mass. The mean kidney mass (g) of each experimental group of rats. Values are reported as mean ± standard error.

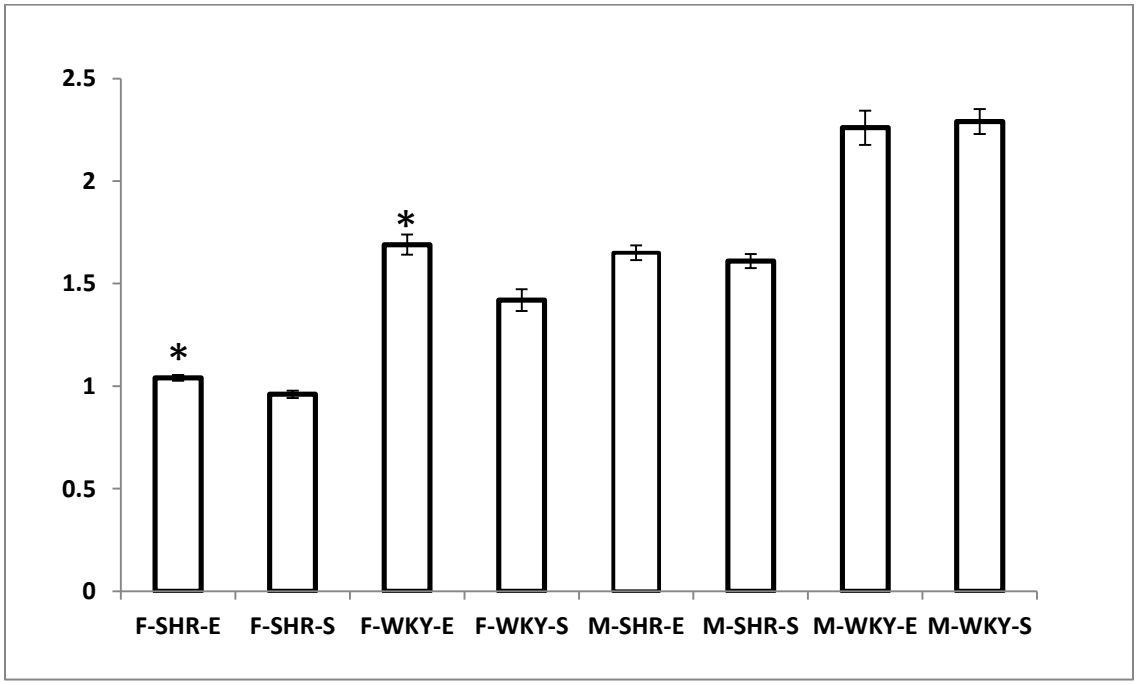

Figure 13. Mean Kidney Mass. The mean kidney mass (g) of each experimental group of rats. Values are reported as mean ± standard error.

* $p < 0.05$ when compared to mean kidney mass of sedentary rats of the same sex and strain.

Rat Subset	Mean Body Mass (g)	± SEM
F-SHR-E	220.6	5.36
F-SHR-S	215.9	7.98
F-WKY-E	314	7.47
F-WKY-S	282	9.87
M-SHR-E	343.2	9.98
M-SHR-S	349	9.01
M-WKY-E	440.5	19.1
M-WKY-S	484.8	17.37

Table 3. **Mean Body Mass.** The mean body mass (g) of each experimental group of rats prior to surgical removal of their kidneys. Values are reported as mean ± standard error.

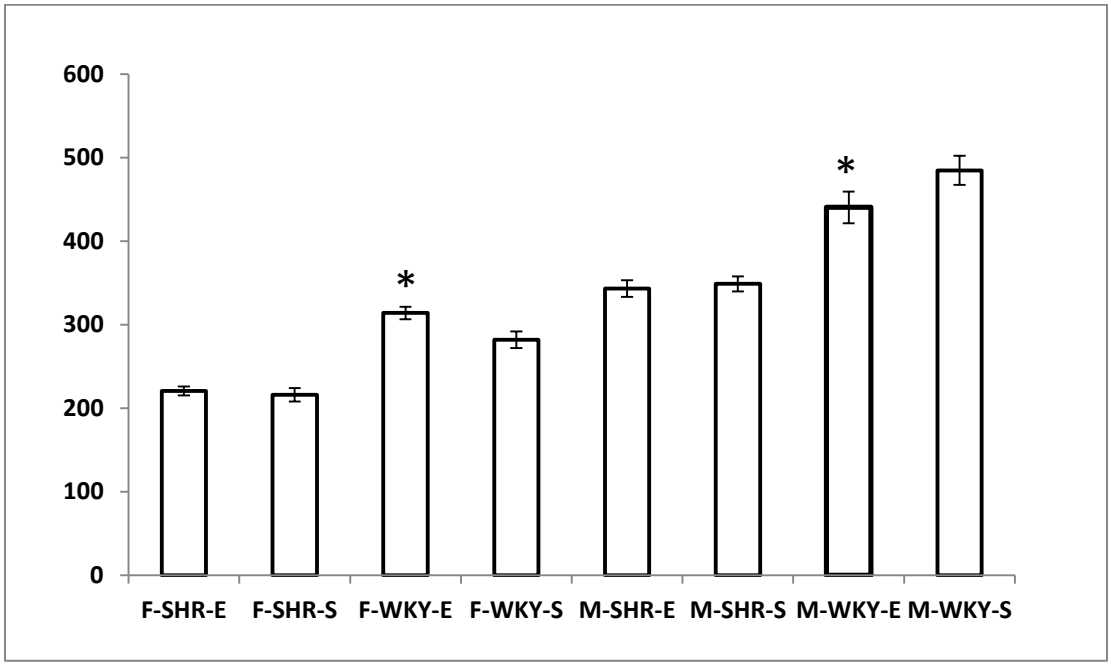

Figure 14. Mean Body Mass. The mean body mass (g) of each experimental group of rats prior to surgical removal of their kidneys. Values are reported as mean ± standard error.

* $p < 0.05$ when compared to mean body mass of sedentary rats of the same sex and strain.

Rat Subset	Mean Kidney Mass (g): Mean Body Mass (mg)	± SEM
F-SHR-E	4.79	0.15
F-SHR-S	4.51	0.11
F-WKY-E	5.40	0.23
F-WKY-S	5.10	0.17
M-SHR-E	4.82	0.13
M-SHR-S	4.64	0.09
M-WKY-E	5.16	0.15
M-WKY-S	4.76	0.09

Table 4. Mean Kidney to Body Mass Ratio. The ratio of mean kidney mass (g) to mean body mass (mg) of each experimental group of rats. Values are reported as mean ± standard error.

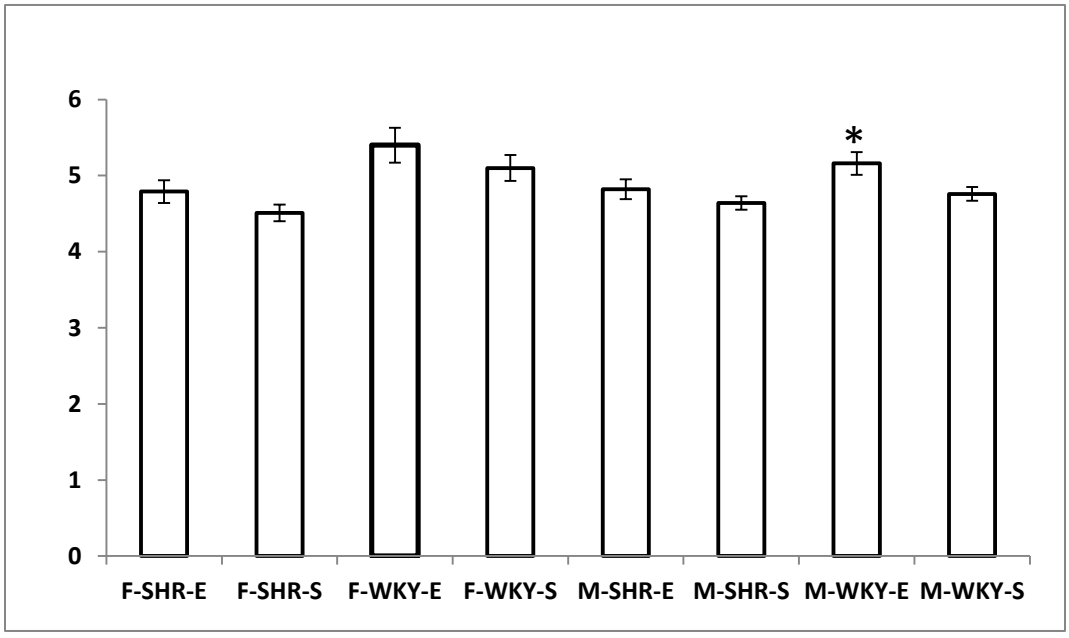

Figure 15. Mean Kidney to Body Mass Ratio. The ratio of mean kidney mass (g) to mean body mass (mg) of each experimental group of rats. Values are reported as mean ± standard error.
* $p < 0.05$ when compared to the ratio of mean kidney mass to mean body mass of sedentary rats of the same sex and strain.

Rat Subset	Total Work
F-SHR-E	11566.06
F-WKY-E	18946.76
M-SHR-E	12331.18
M-WKY-E	19108.89

Table 5. Total Work. The total work of each exercised group of rats determined by multiplying mean body mass (g) by mean weekly running distance.

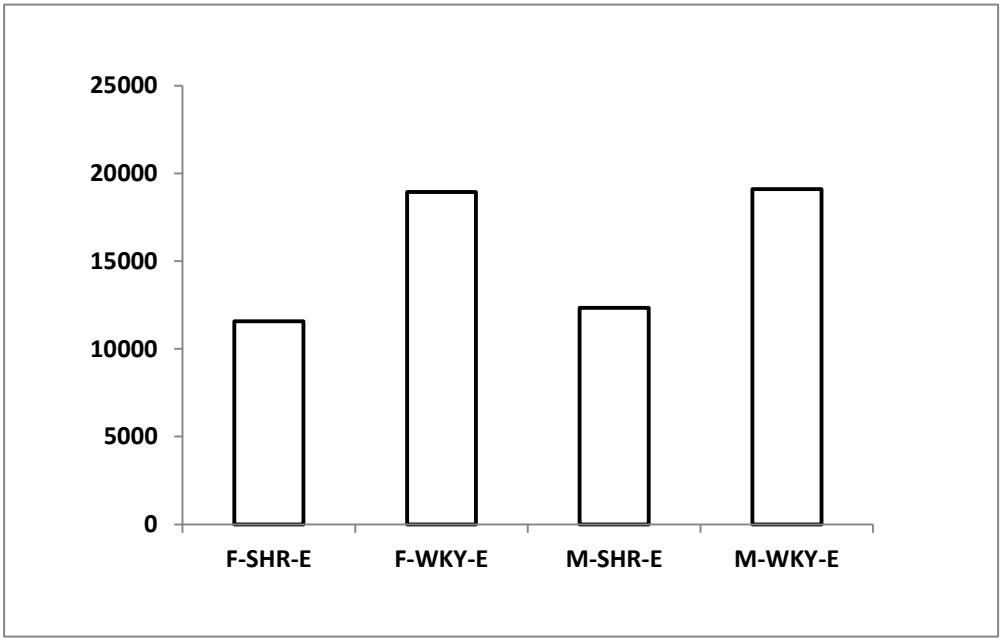

Figure 16. Total Work. The total work of each exercised group of rats determined by multiplying mean body mass (g) by mean weekly running distance.

Standard	ET-1 Concentration (pg/mL)	Absorbance
1	0	0.0012
2	0.78	0.0007
3	1.56	0.0096
4	3.13	0.0323
5	6.25	0.0701
6	12.5	0.161
7	25	0.2817
8	50	0.469
9	100	0.9983

Table 6. Absorbance of ELISA Standards. The absorbance of each Endothelin-1 standard solution derived from ELISA analysis.

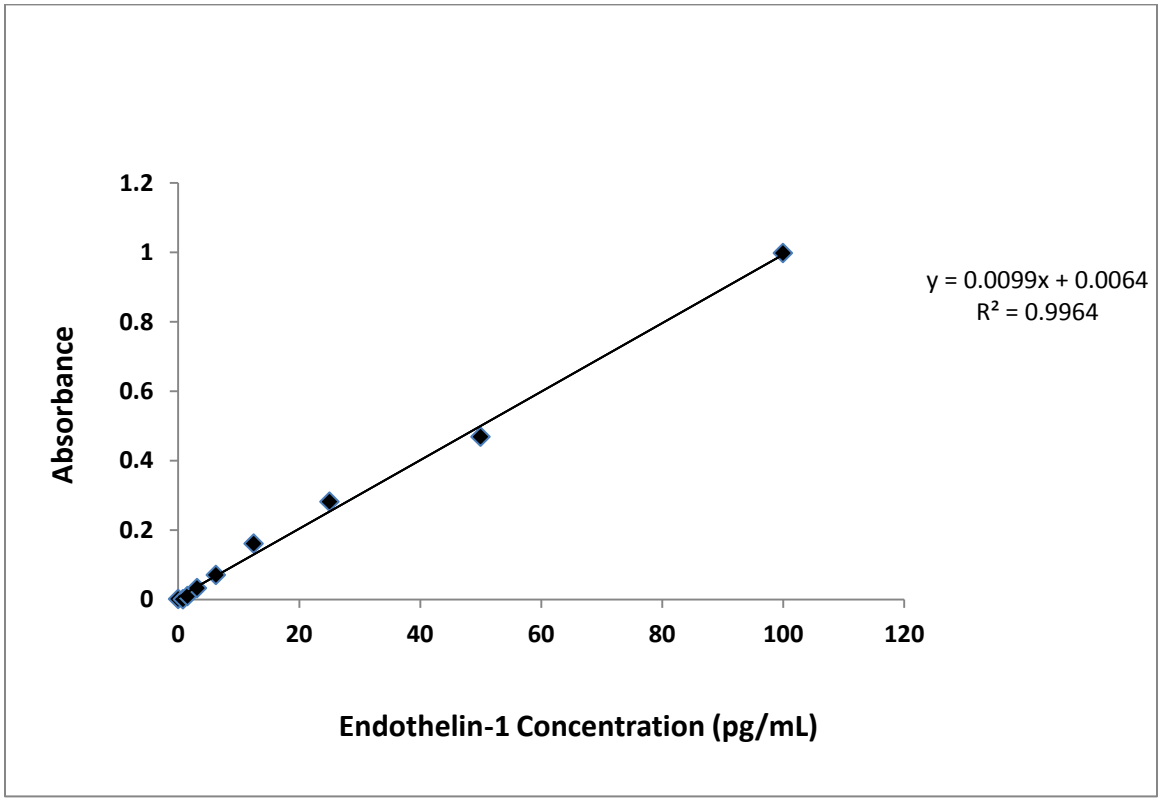

Figure 17. ELISA Standard Curve. The standard curve of Endothelin-1 concentration (pg/ml) vs. absorbance derived from Table 5. Y=0.0099x + 0.0064; R^2=0.9964.

Rat Subset	ET-1 Concentration (pg/ml)
F-SHR-E	0.1606
F-SHR-S	2.6667
F-WKY-E	9.5556
F-WKY-S	5.404
M-SHR-E	0.2929
M-SHR-S	1.6768
M-WKY-E	4.808
M-WKY-S	3.303

Table 7. Urinary Endothelin-1 Levels. The concentration (pg/ml) of endothelin-1 in pooled urine from each experimental subset of rats as determined by ELISA analysis.

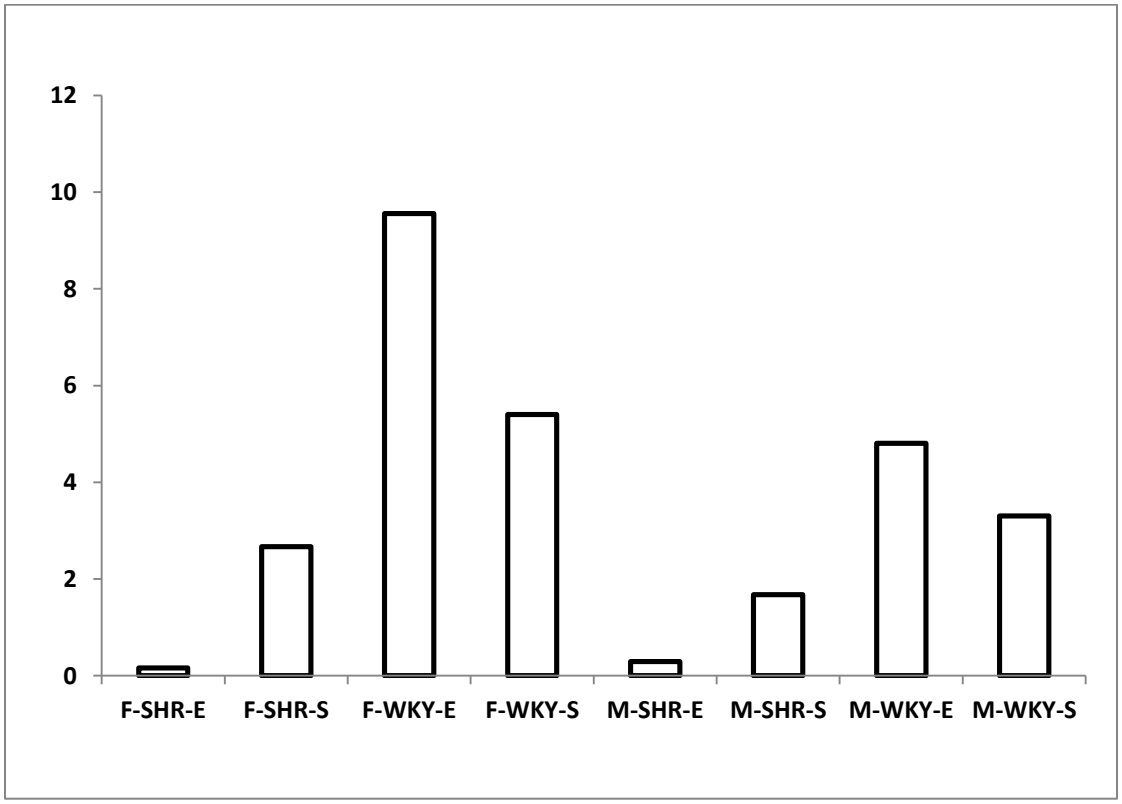

Figure 18. Urinary Endothelin-1 Levels. The amount of endothelin-1 (pg/ml) in pooled urine from each experimental subset of rats as determined by ELISA analysis.

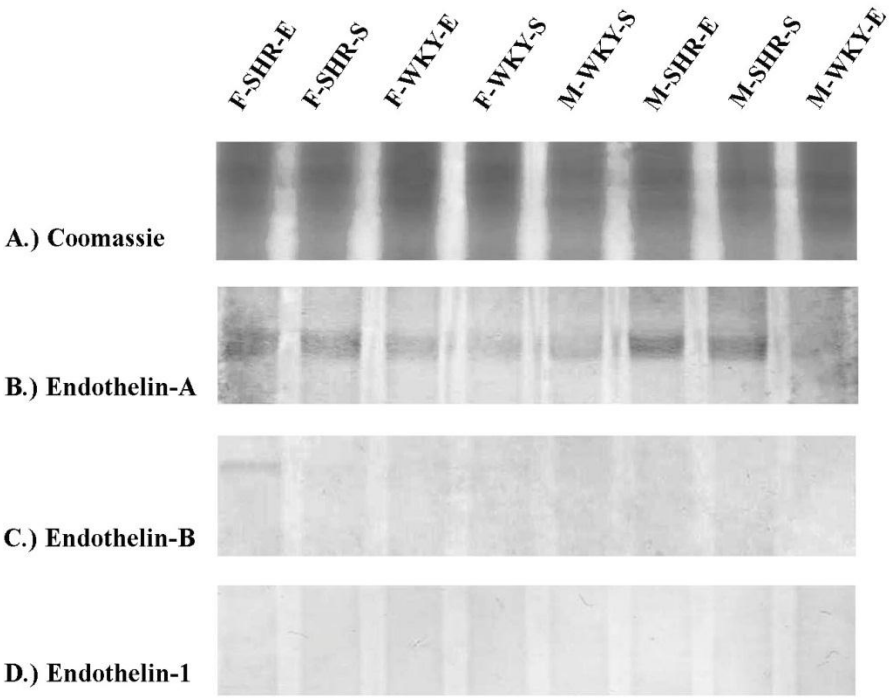

Figure 19. SDS-PAGE and Western Blot Composite. SDS-PAGE and Western Blot analysis of total protein and Endothelin expression in the kidney tissue extracted from each experimental group of rats. A.) Coomassie gel depicting the total kidney protein load. B.) Western Blot probed with Endothelin-A antibody. C.) Western Blot probed with Endothelin-B antibody. D.) Western Blot probed with Endothelin-1 antibody.

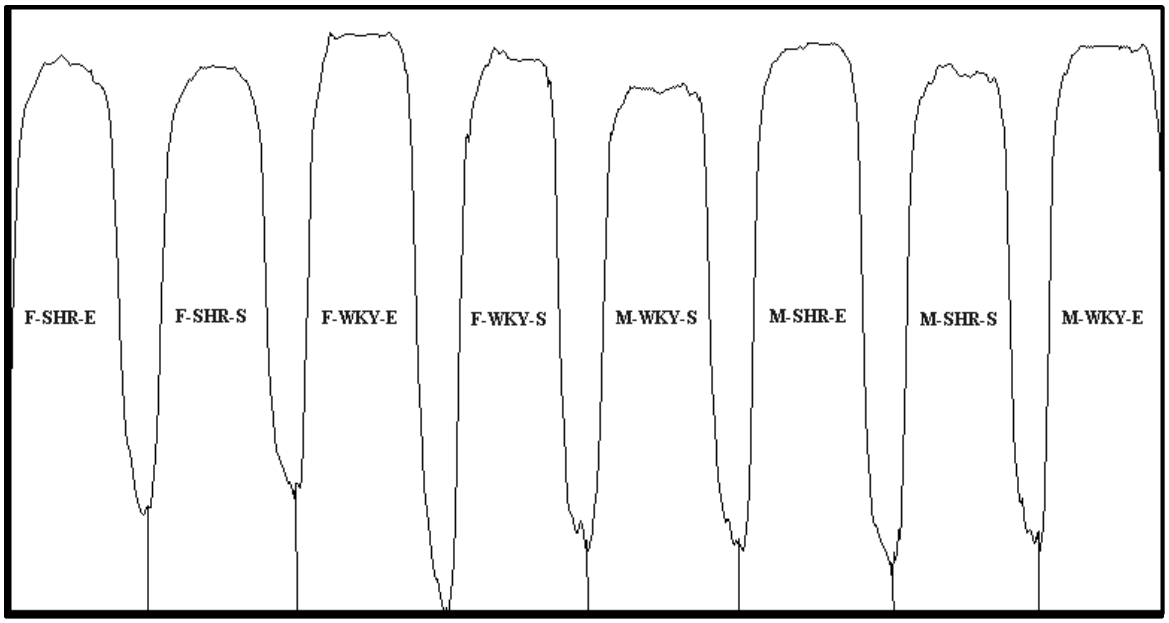

Figure 20. Total Protein Densitometry. Densitometry of total protein load in each lane of Coomassie gel as determined by Image J Software.

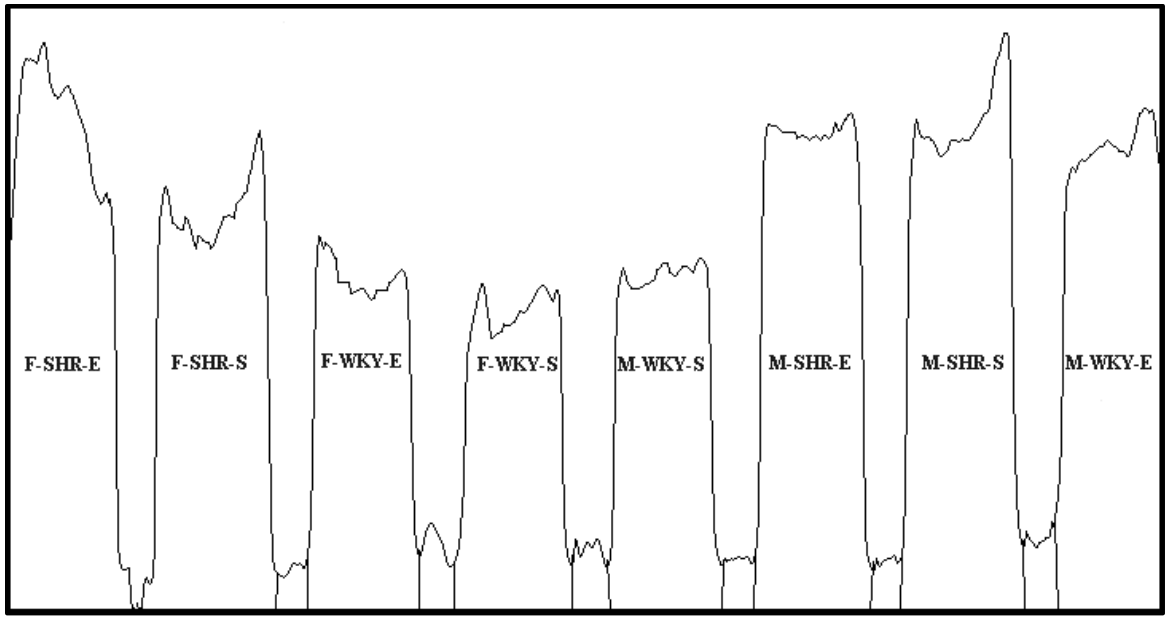

Figure 21. Endothelin-A Densitometry. Densitometry of Endothelin-A in Western Blot analysis as determined by Image J Software.

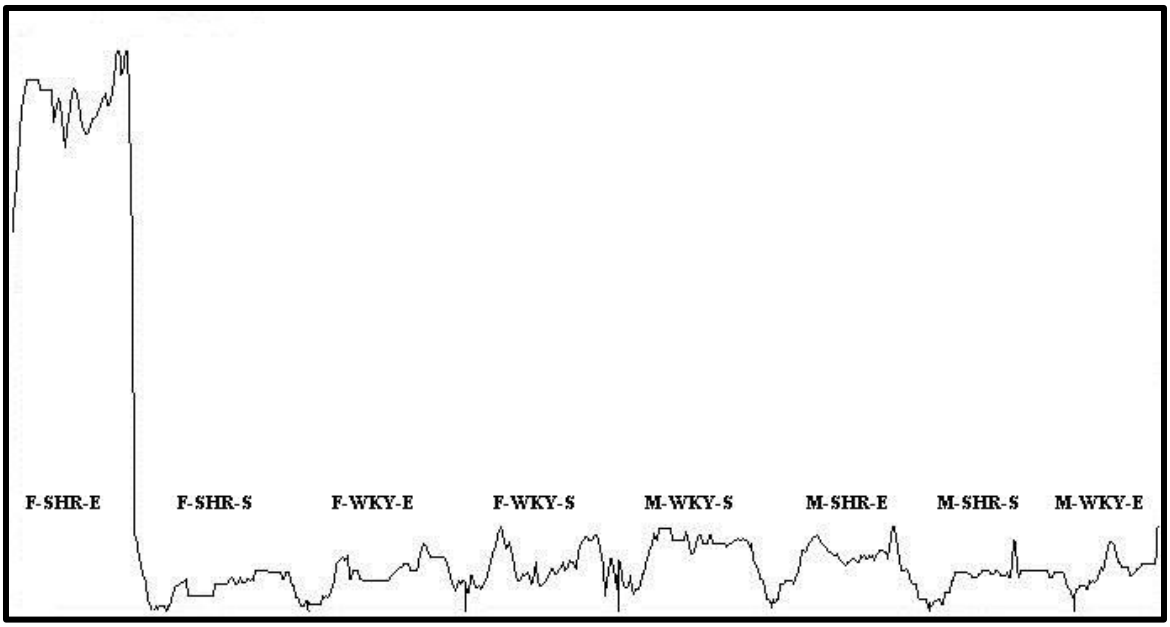

Figure 22. Endothelin-B Densitometry. Densitometry of Endothelin-B in Western Blot analysis as determined by Image J Software.

	Coomassie	ET-A	ET-B
F-SHR-E	26622	20644	22270
F-SHR-S	27192	17934	1452
F-WKY-E	28671	13144	2210
F-WKY-S	25220	11969	2636
M-SHR-E	28404	19407	2796
M-SHR-S	25932	20830	1894
M-WKY-E	27864	17980	1409
M-WKY-S	26370	13145	3301

Table 8. Total Protein and Endothelin Receptor Levels. The total protein load and the levels of Endothelin-A and Endothelin-B in the kidney homogenate of each experimental group of rats as determined by Image J analysis of Coomassie gel and Western Blots.

	ET-A	ET-B
F-SHR-E	0.7754	0.8365
F-SHR-S	0.6595	0.0534
F-WKY-E	0.4584	0.0771
F-WKY-S	0.4746	0.1045
M-SHR-E	0.6832	0.0984
M-SHR-S	0.8033	0.0730
M-WKY-E	0.6453	0.0506
M-WKY-S	0.4985	0.1252

Table 9. Endothelin Receptor Levels Relative to Total Protein. The levels of Endothelin-A and Endothelin-B in the kidney homogenate of each experimental group of rats relative to the total protein load in the Coomassie gel.

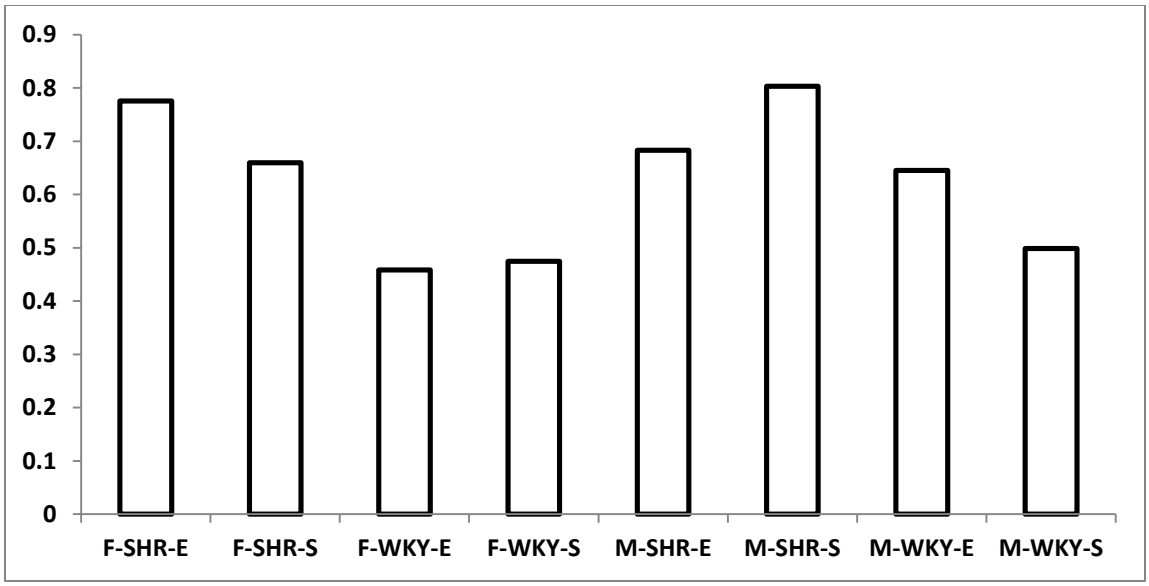

Figure 23. Endothelin-A Receptor Levels. The amount of endothelin-A receptors in the kidney homogenate of each experimental group of rats relative to total protein levels in the Coomassie gel as determined by Image J analysis of Western Blots.

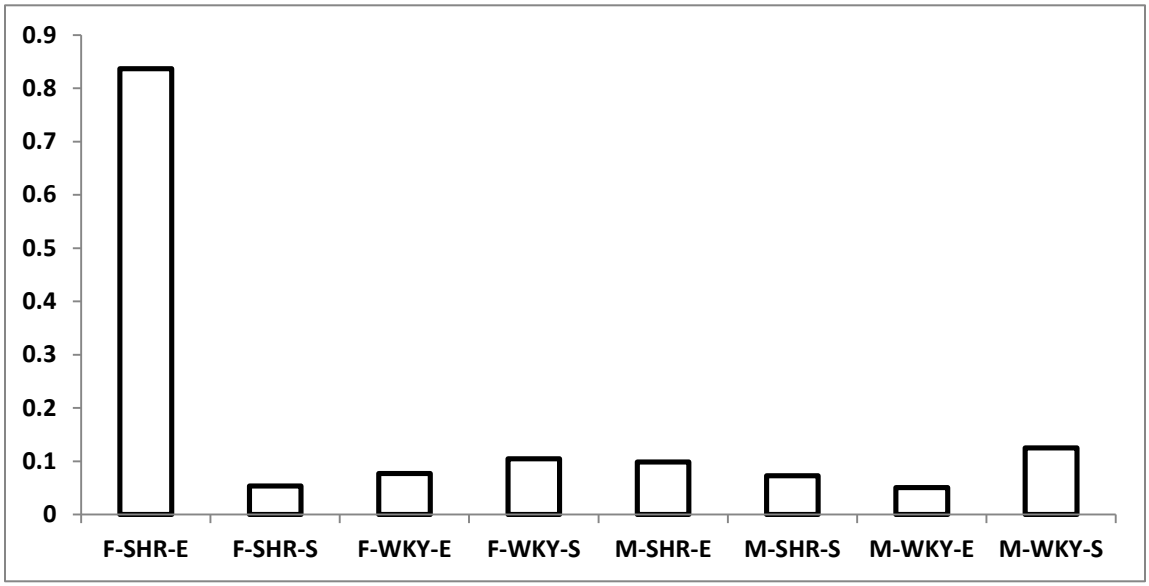

Figure 24. Endothelin-B Receptor Levels. The amount of endothelin-B receptors in the kidney homogenate of each experimental group of rats relative to total protein levels in the Coomassie Gel as determined by Image J analysis of Western Blots.

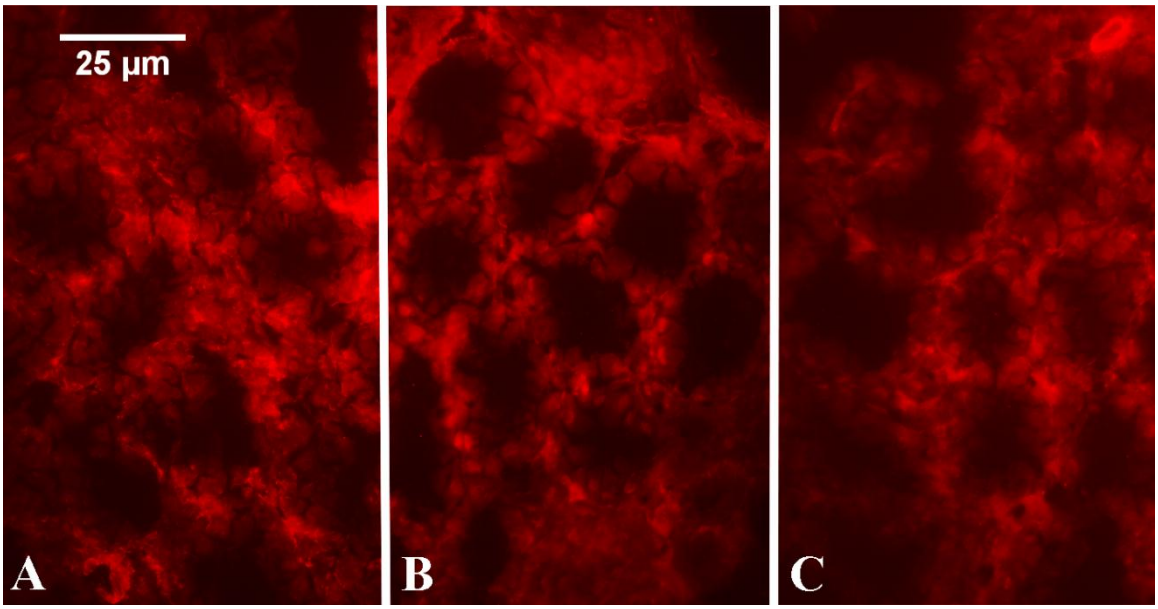

Figure 25. Actin Immunofluorescent Localization. The general actin localization pattern seen in each experimental group of rats. Each image in the figure was acquired with the 40x objective and a 10 second exposure time. A.) Sedentary female WKY rat. B.) Exercised female SHR rat. C.) Exercised male WKY rat.

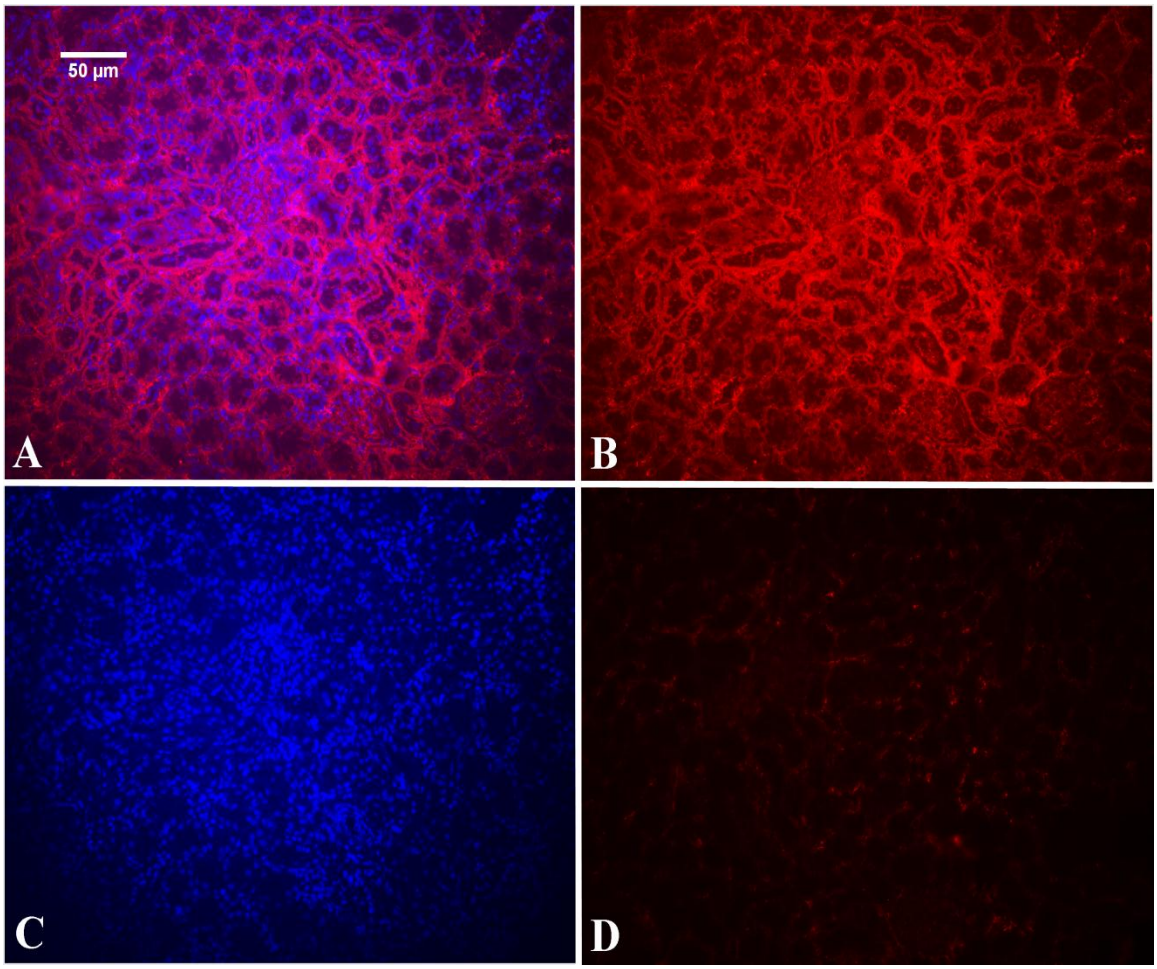

Figure 26. Immunofluorescent Localization of ET-A Receptors in F-SHR-E (20x).
Immunohistochemical analysis of ET-A receptors in an exercised female SHR rat. Each image in the figure was acquired with the 20x objective and a 4 second exposure time. A.) Kidney section probed with Endothelin-A and DAPI antibodies. B.) Kidney section probed with Endothelin-A antibody. C.) Kidney section probed with DAPI antibody. D.) Kidney section probed with secondary antibody.

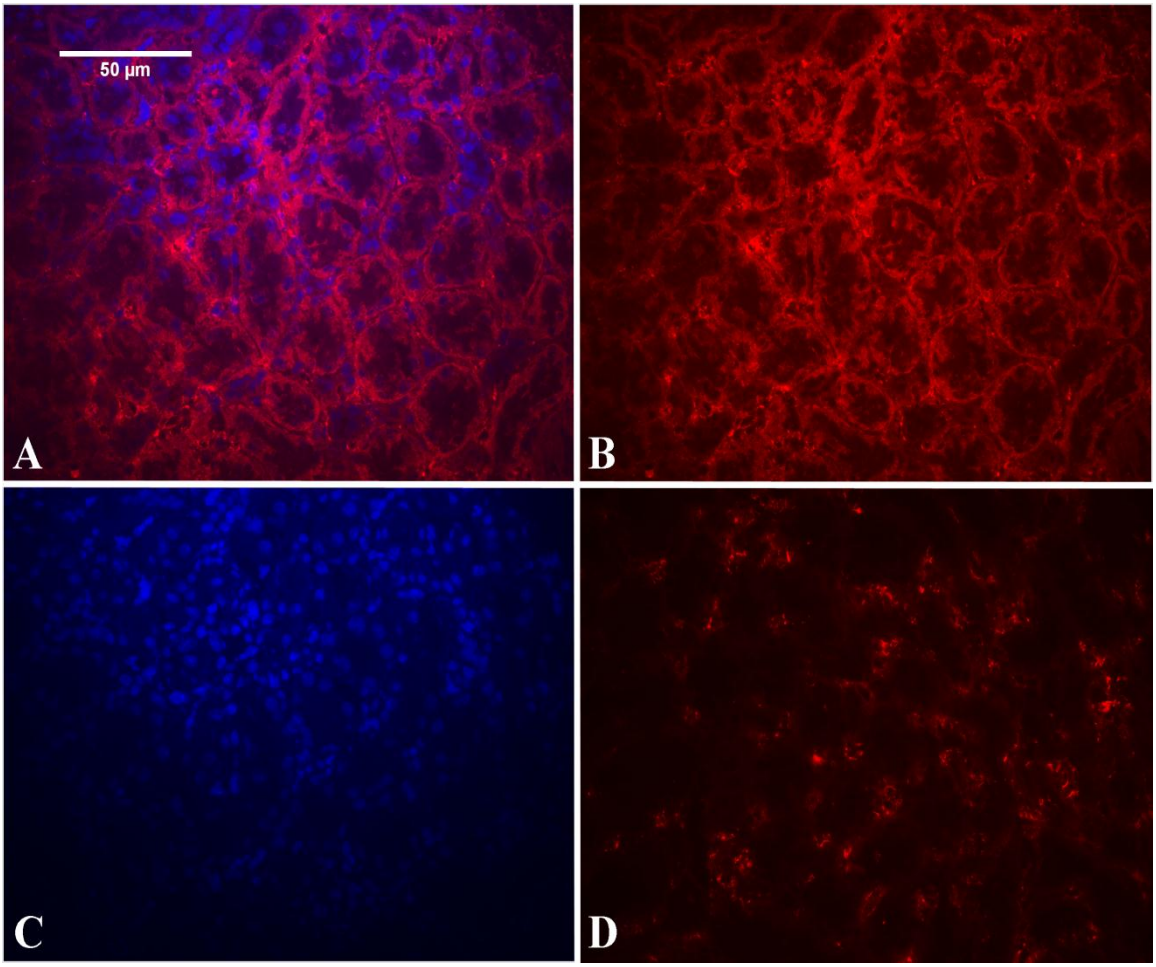

Figure 27. Immunofluorescent Localization of ET-A Receptors in F-SHR-E (40x).
Immunohistochemical analysis of ET-A receptors in an exercised female SHR rat. Each image in the figure was acquired with the 40x objective and a 5 second exposure time. A.) Kidney section probed with Endothelin-A and DAPI antibodies. B.) Kidney section probed with Endothelin-A antibody. C.) Kidney section probed with DAPI antibody. D.) Kidney section probed with secondary antibody.

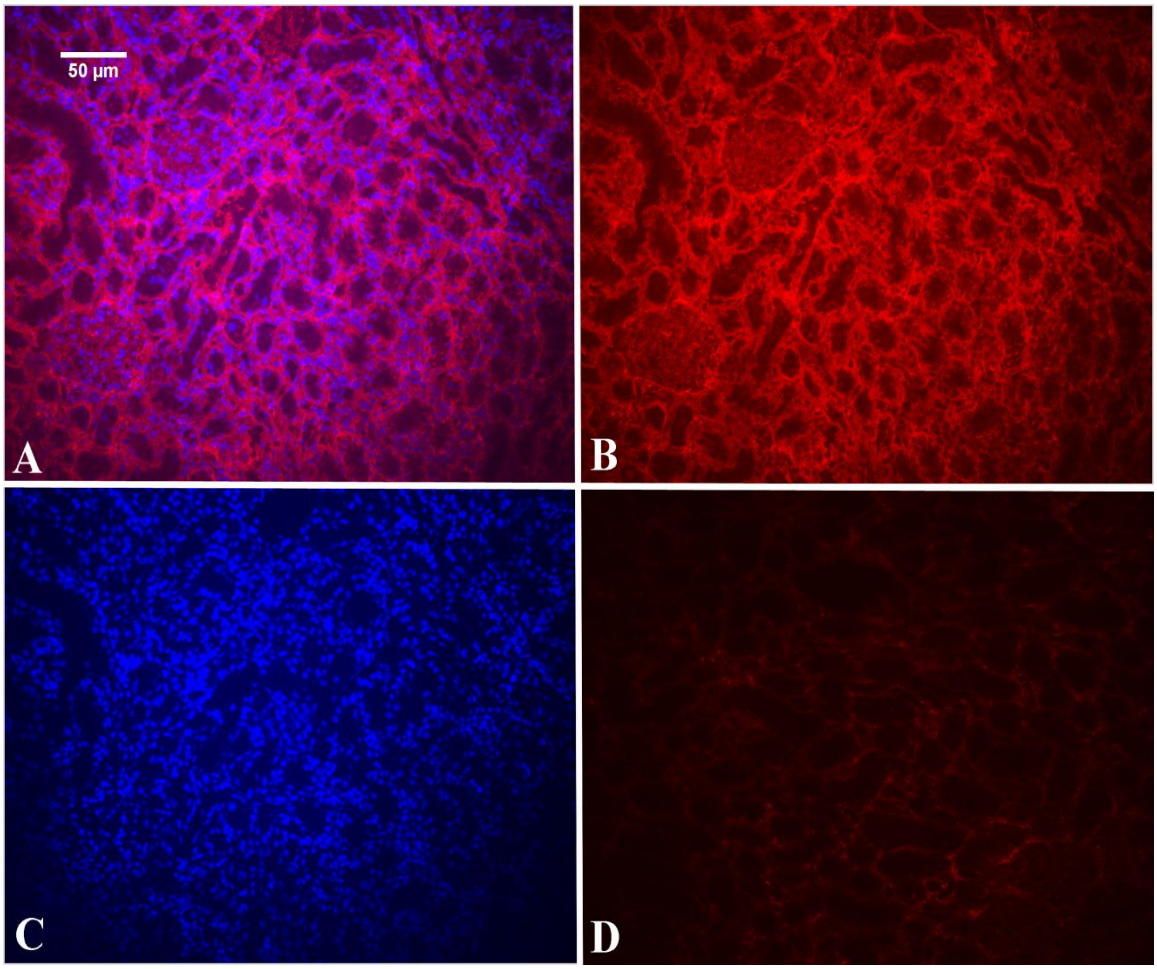

Figure 28. Immunofluorescent Localization of ET-A Receptors in F-SHR-S (20x).
Immunohistochemical analysis of ET-A receptors in a sedentary female SHR rat. Each image in the figure was acquired with the 20x objective and a 4 second exposure time. A.) Kidney section probed with Endothelin-A and DAPI antibodies. B.) Kidney section probed with Endothelin-A antibody. C.) Kidney section probed with DAPI antibody. D.) Kidney section probed with secondary antibody.

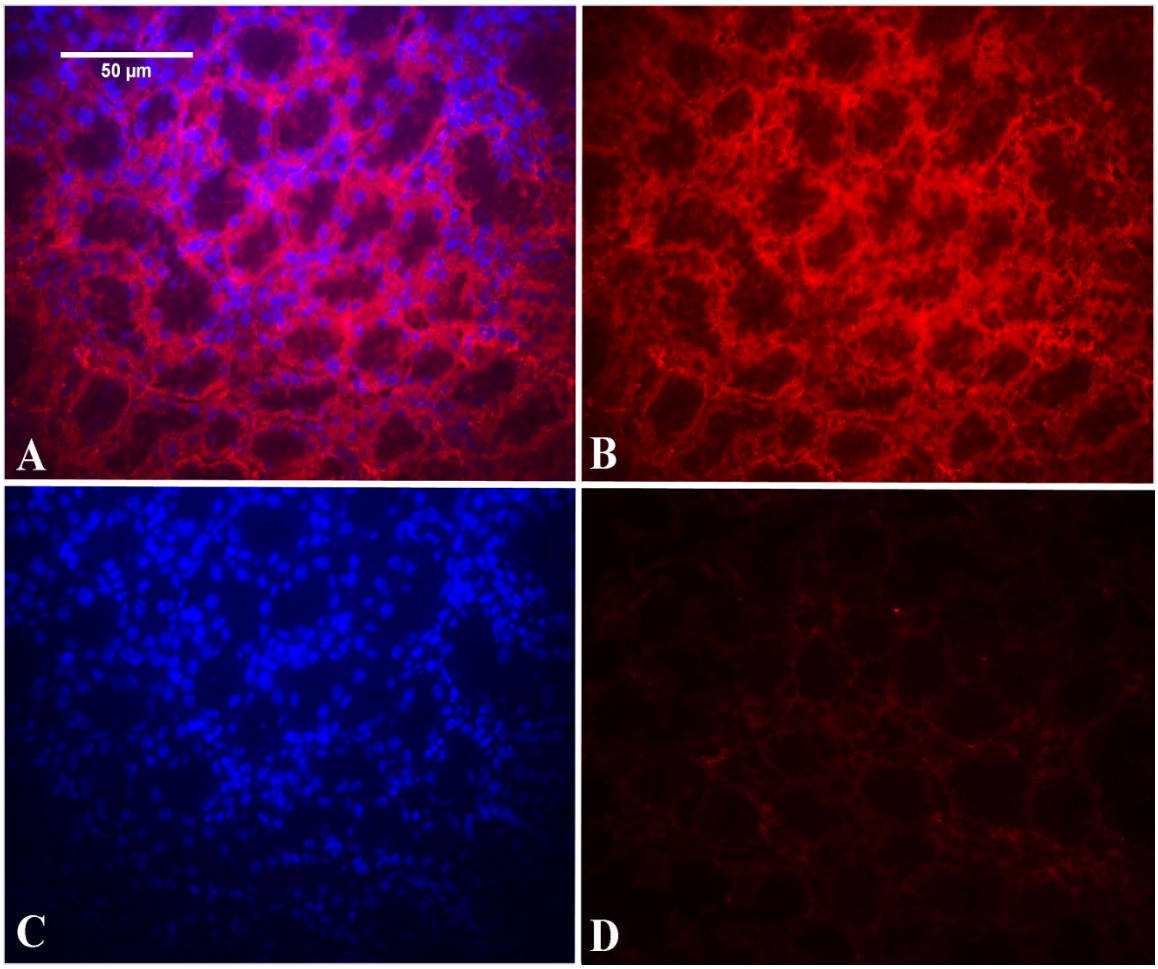

Figure 29. Immunofluorescent Localization of ET-A Receptors in F-SHR-S (40x).
Immunohistochemical analysis of ET-A receptors in a sedentary female SHR rat. Each image in the figure was acquired with the 40x objective and a 5 second exposure time. A.) Kidney section probed with Endothelin-A and DAPI antibodies. B.) Kidney section probed with Endothelin-A antibody. C.) Kidney section probed with DAPI antibody. D.) Kidney section probed with secondary antibody.

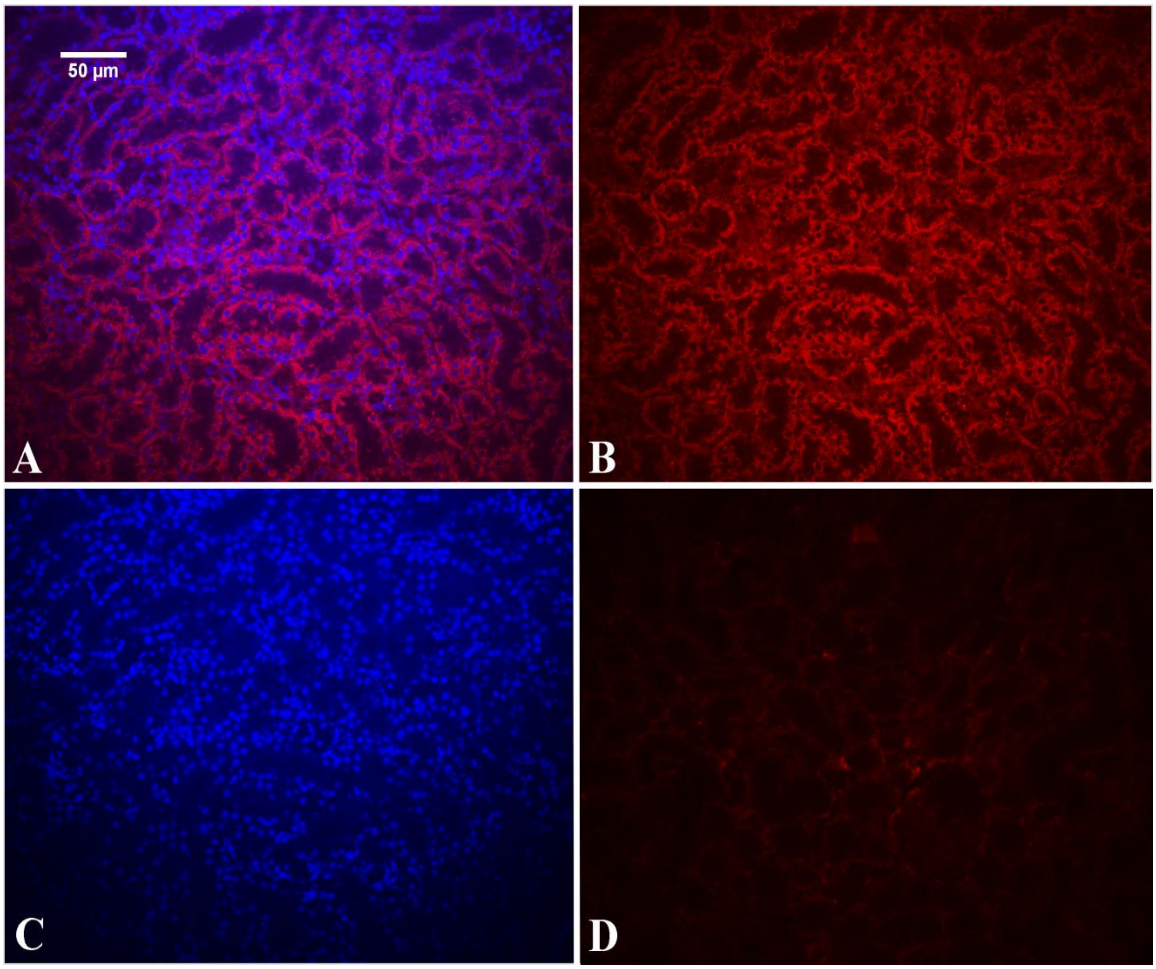

Figure 30. Immunofluorescent Localization of ET-A Receptors in F-WKY-E (20x).
Immunohistochemical analysis of ET-A receptors in an exercised female WKY rat. Each image in the figure was acquired with the 20x objective and a 7 second exposure time. A.) Kidney section probed with Endothelin-A and DAPI antibodies. B.) Kidney section probed with Endothelin-A antibody. C.) Kidney section probed with DAPI antibody. D.) Kidney section probed with secondary antibody.

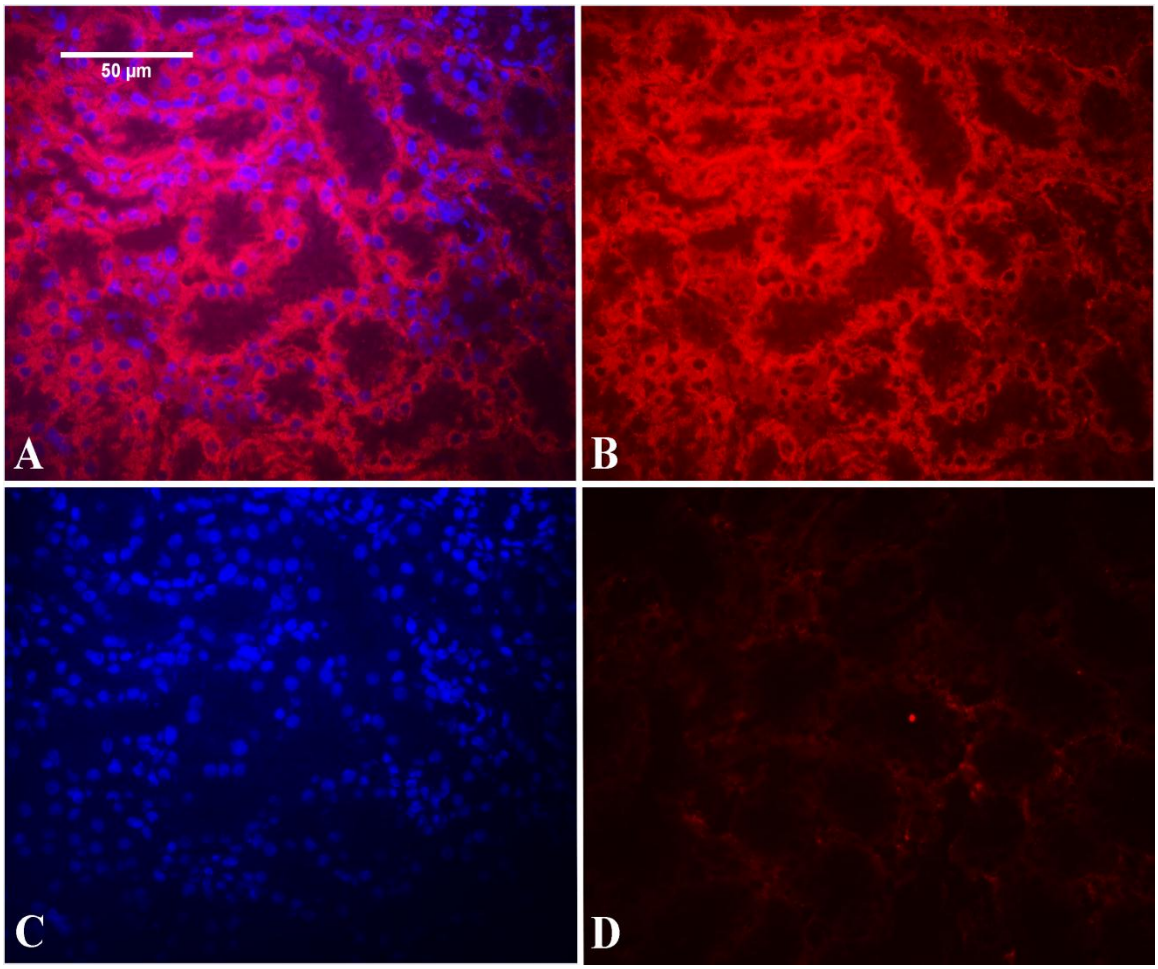

Figure 31. Immunofluorescent Localization of ET-A Receptors in F-WKY-E (40x).
Immunohistochemical analysis of ET-A receptors in an exercised female WKY rat. Each image in the figure was acquired with the 40x objective and a 4 second exposure time. A.) Kidney section probed with Endothelin-A and DAPI antibodies. B.) Kidney section probed with Endothelin-A antibody. C.) Kidney section probed with DAPI antibody. D.) Kidney section probed with secondary antibody.

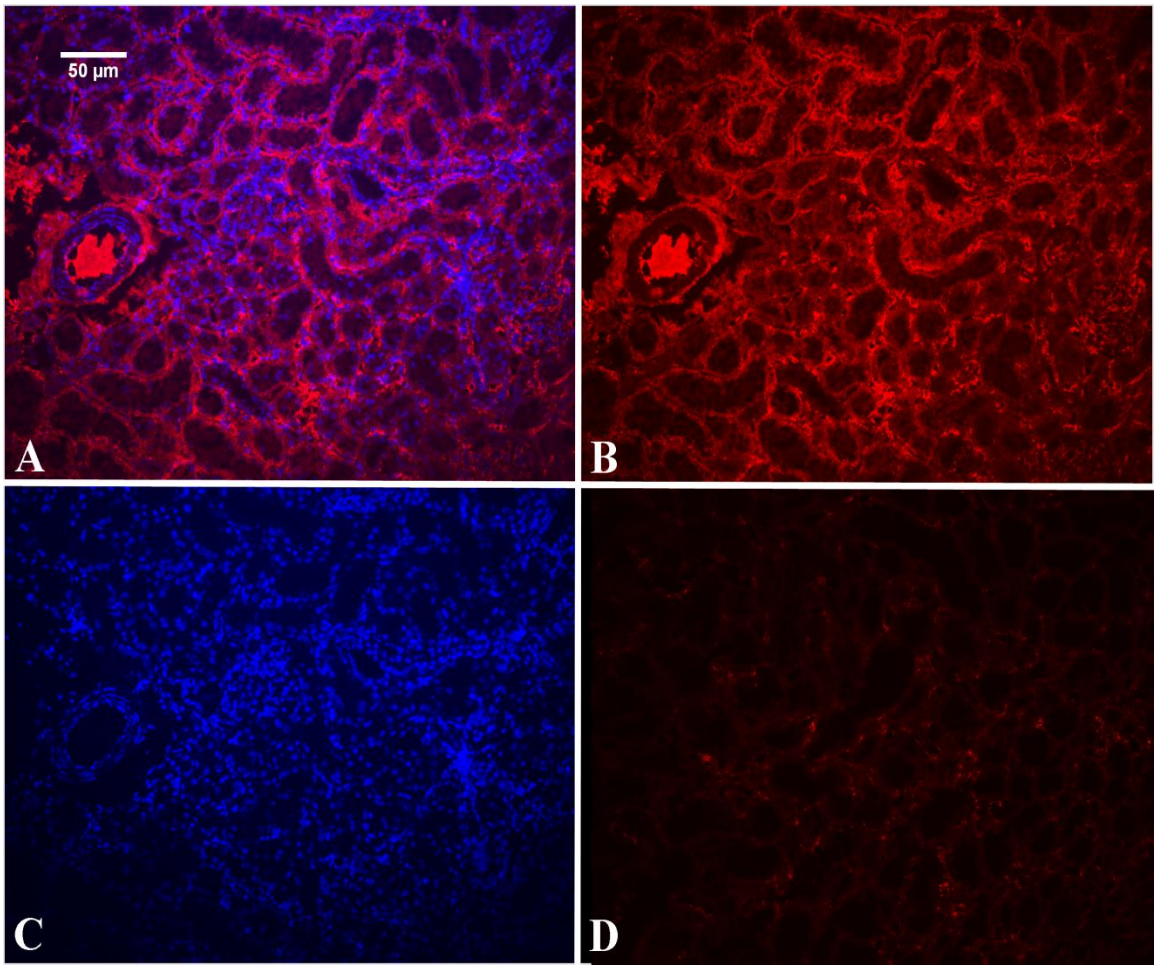

Figure 32. Immunofluorescent Localization of ET-A Receptors in F-WKY-S (20x).
Immunohistochemical analysis of ET-A receptors in a sedentary female WKY rat. Each image in the figure was acquired with the 20x objective and a 7 second exposure time. A.) Kidney section probed with Endothelin-A and DAPI antibodies. B.) Kidney section probed with Endothelin-A antibody. C.) Kidney section probed with DAPI antibody. D.) Kidney section probed with secondary antibody.

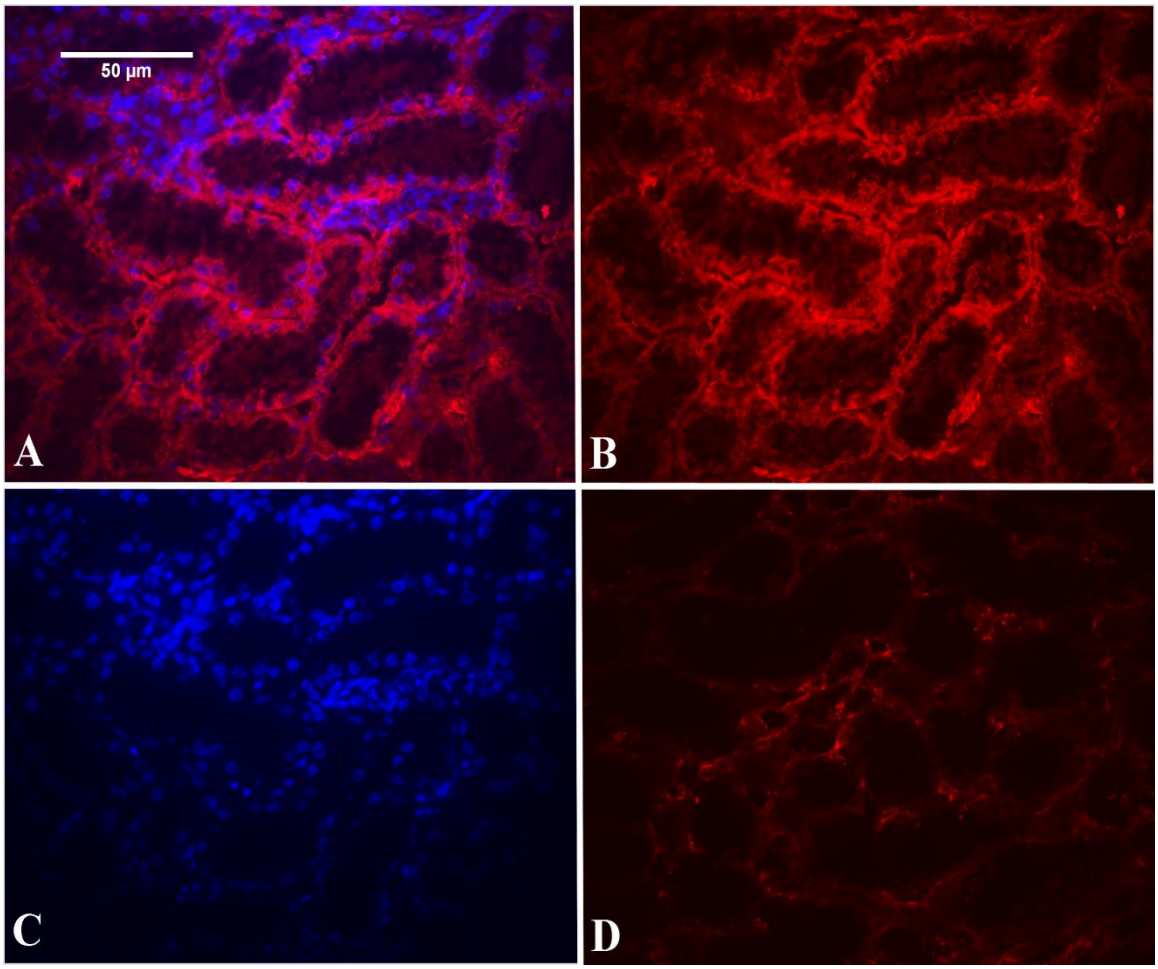

Figure 33. Immunofluorescent Localization of ET-A Receptors in F-WKY-S (40x).
Immunohistochemical analysis of ET-A receptors in a sedentary female WKY rat. Each image in the figure was acquired with the 40x objective and a 4 second exposure time. A.) Kidney section probed with Endothelin-A and DAPI antibodies. B.) Kidney section probed with Endothelin-A antibody. C.) Kidney section probed with DAPI antibody. D.) Kidney section probed with secondary antibody.

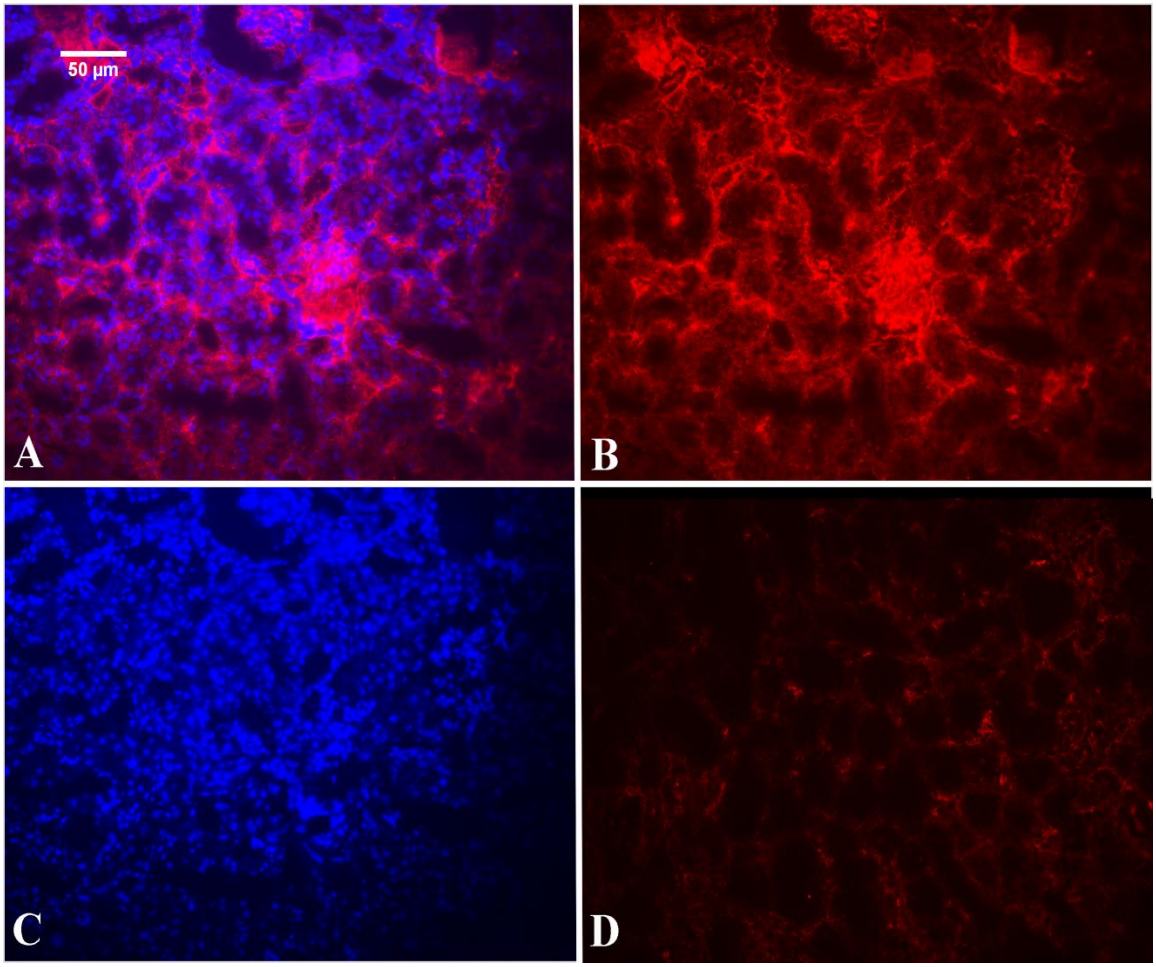

Figure 34. Immunofluorescent Localization of ET-A Receptors in M-SHR-E (20x).
Immunohistochemical analysis of ET-A receptors in an exercised male SHR rat. Each image in the figure was acquired with the 20x objective and a 5 second exposure time. A.) Kidney section probed with Endothelin-A and DAPI antibodies. B.) Kidney section probed with Endothelin-A antibody. C.) Kidney section probed with DAPI antibody. D.) Kidney section probed with secondary antibody.

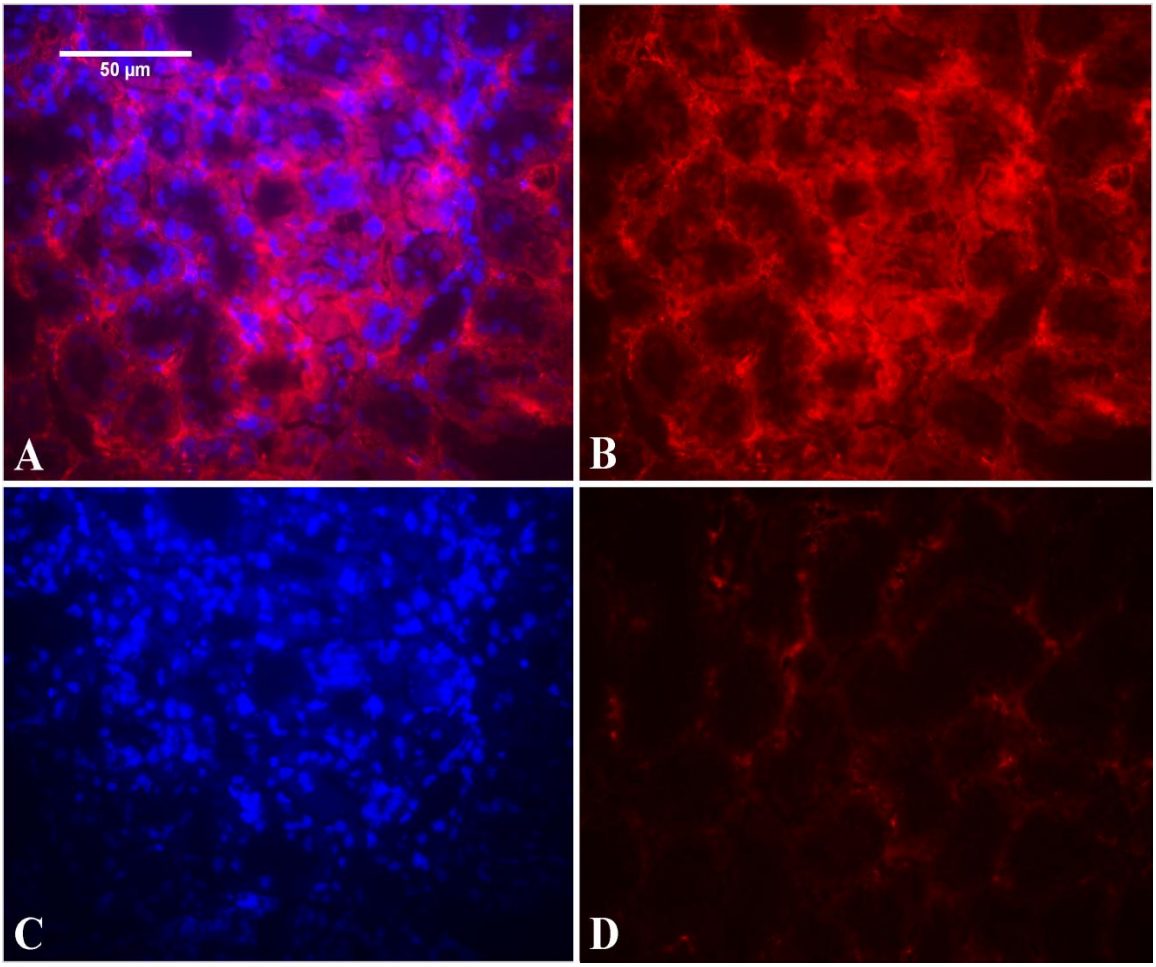

Figure 35. Immunofluorescent Localization of ET-A Receptors in M-SHR-E (40x).
Immunohistochemical analysis of ET-A receptors in an exercised male SHR rat. Each image in the figure was acquired with the 40x objective and a 5 second exposure time. A.) Kidney section probed with Endothelin-A and DAPI antibodies. B.) Kidney section probed with Endothelin-A antibody. C.) Kidney section probed with DAPI antibody. D.) Kidney section probed with secondary antibody.

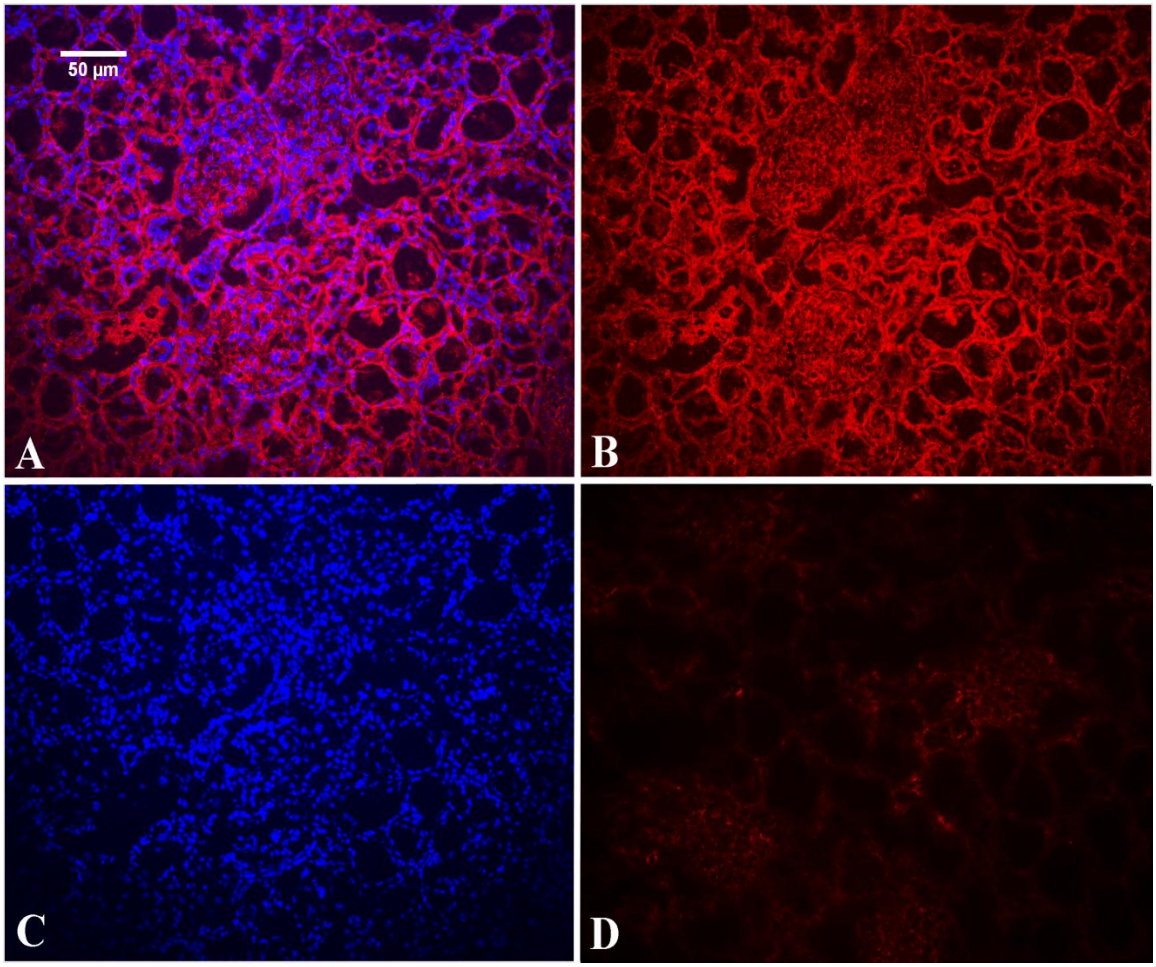

Figure 36. Immunofluorescent Localization of ET-A Receptors in M-SHR-S (20x).
Immunohistochemical analysis of ET-A receptors in a sedentary male SHR rat. Each image in the figure was acquired with the 20x objective and a 6 second exposure time. A.) Kidney section probed with Endothelin-A and DAPI antibodies. B.) Kidney section probed with Endothelin-A antibody. C.) Kidney section probed with DAPI antibody. D.) Kidney section probed with secondary antibody.

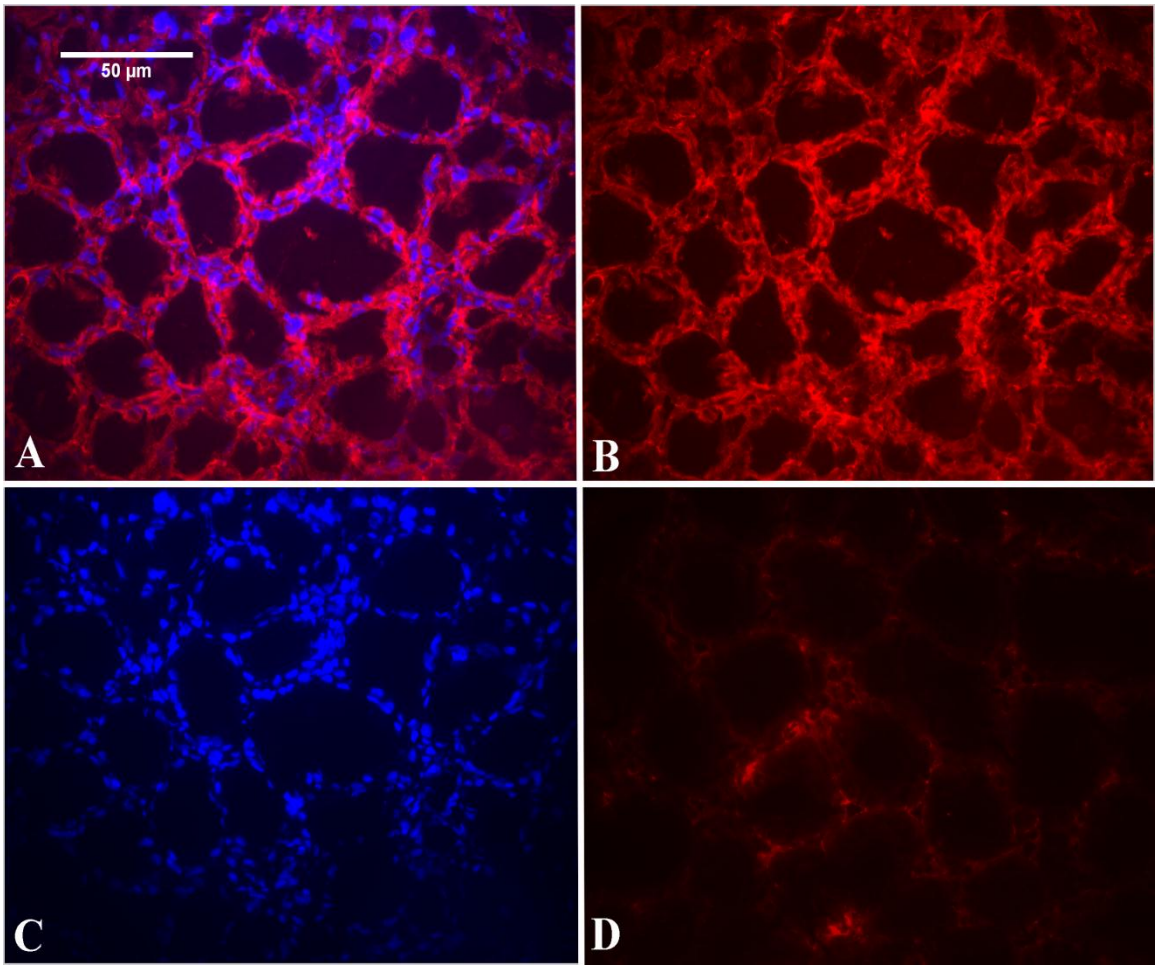

Figure 37. Immunofluorescent Localization of ET-A Receptors in M-SHR-S (40x).
Immunohistochemical analysis of ET-A receptors in a sedentary male SHR rat. Each image in the figure was acquired with the 40x objective and a 5 second exposure time. A.) Kidney section probed with Endothelin-A and DAPI antibodies. B.) Kidney section probed with Endothelin-A antibody. C.) Kidney section probed with DAPI antibody. D.) Kidney section probed with secondary antibody.

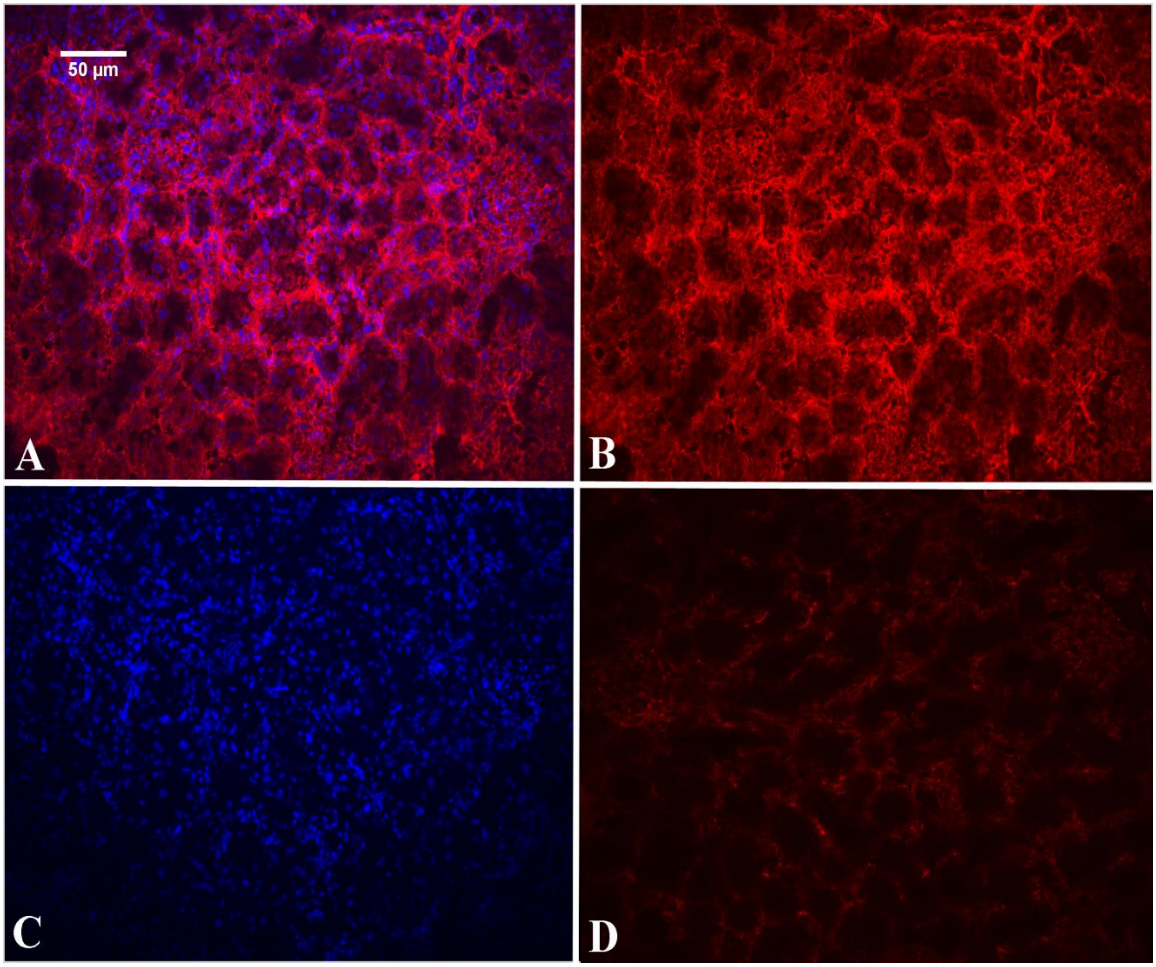

Figure 38. Immunofluorescent Localization of ET-A Receptors in M-WKY-E (20x). Immunohistochemical analysis of ET-A receptors in an exercised male WKY rat. Each image in the figure was acquired with the 20x objective and a 5 second exposure time. A.) Kidney section probed with Endothelin-A and DAPI antibodies. B.) Kidney section probed with Endothelin-A antibody. C.) Kidney section probed with DAPI antibody. D.) Kidney section probed with secondary antibody.

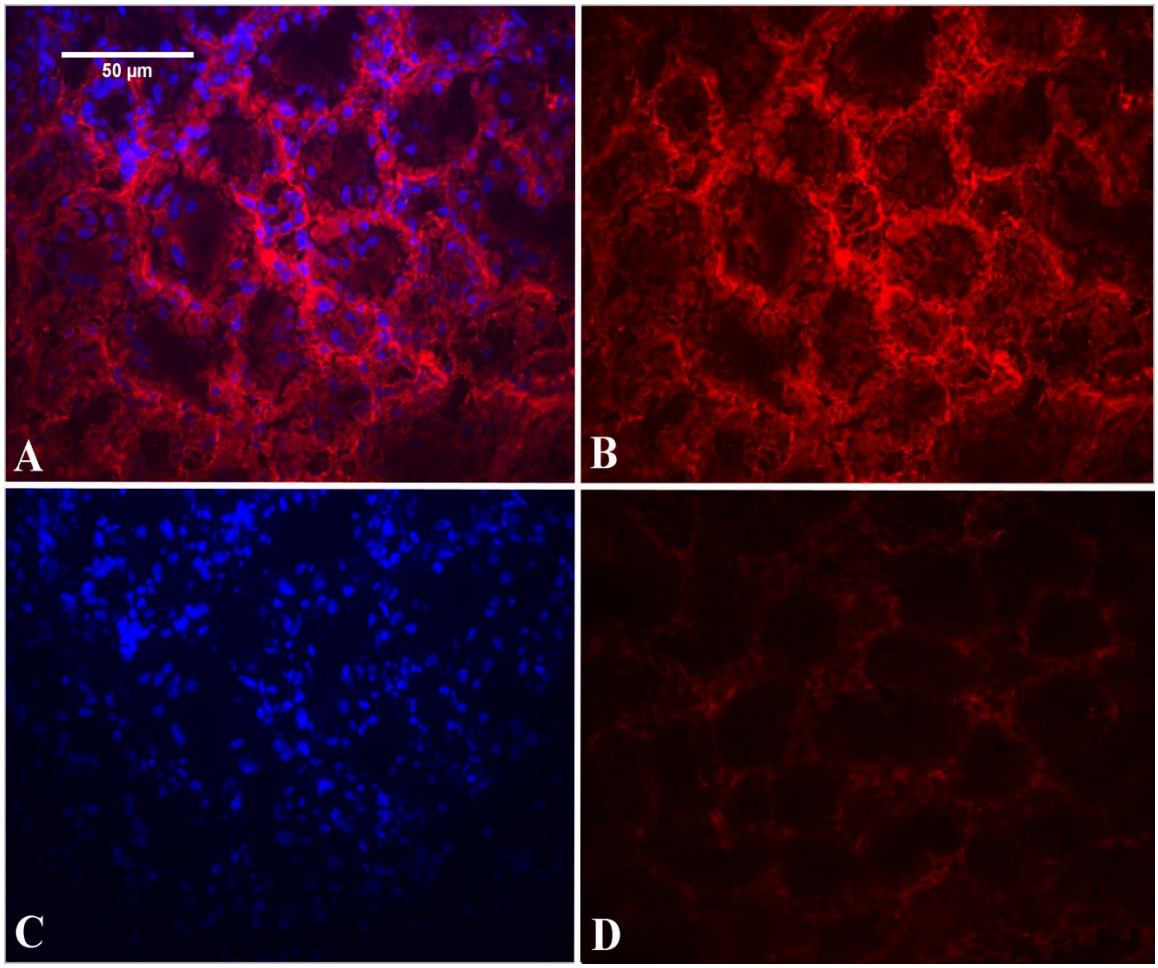

Figure 39. Immunofluorescent Localization of ET-A Receptors in M-WKY-E (40x).
Immunohistochemical analysis of ET-A receptors in an exercised male WKY rat. Each image in the figure was acquired with the 40x objective and a 3.5 second exposure time. A.) Kidney section probed with Endothelin-A and DAPI antibodies. B.) Kidney section probed with Endothelin-A antibody. C.) Kidney section probed with DAPI antibody. D.) Kidney section probed with secondary antibody.

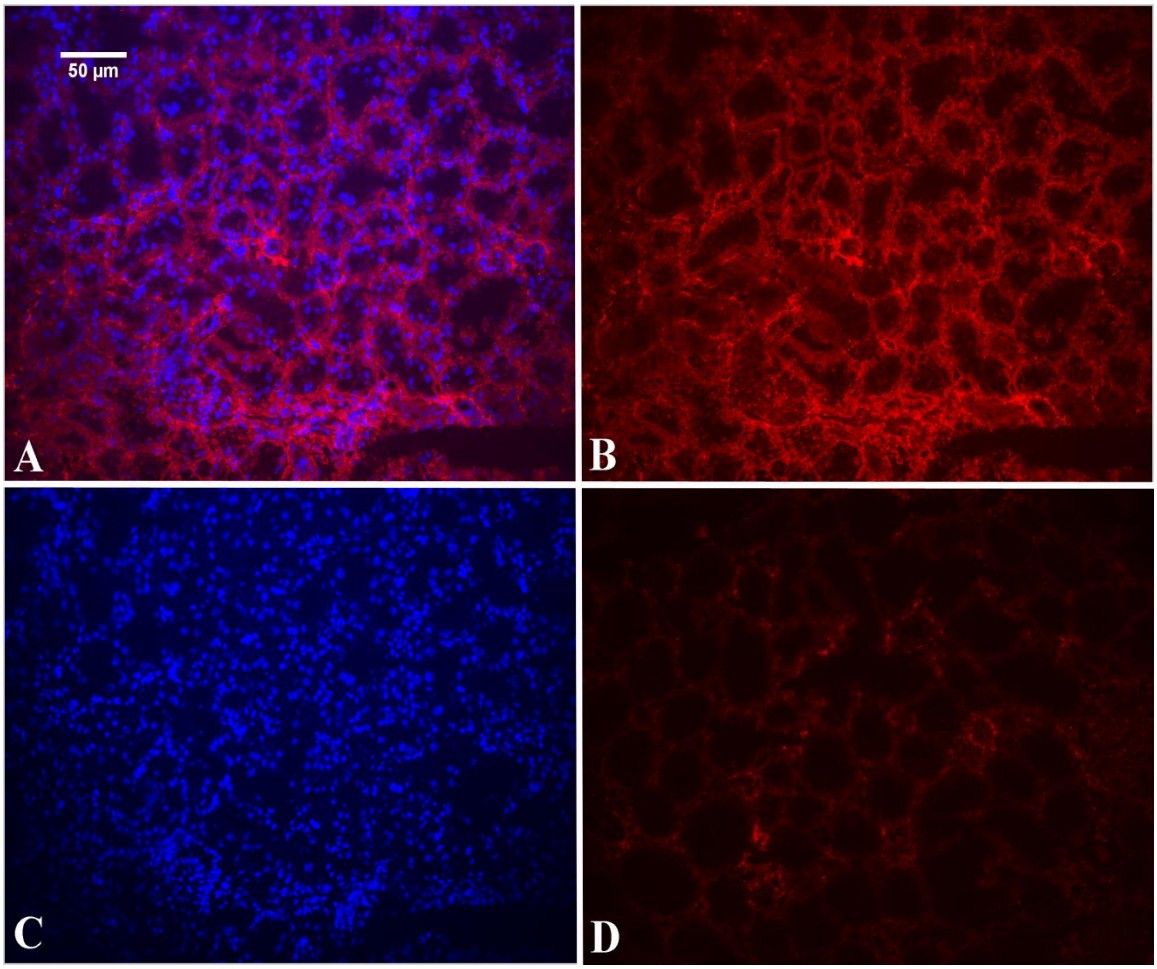

Figure 40. Immunofluorescent Localization of ET-A Receptors in M-WKY-S (20x). Immunohistochemical analysis of ET-A receptors in a sedentary male WKY rat. Each image in the figure was acquired with the 20x objective and a 8 second exposure time. A.) Kidney section probed with Endothelin-A and DAPI antibodies. B.) Kidney section probed with Endothelin-A antibody. C.) Kidney section probed with DAPI antibody. D.) Kidney section probed with secondary antibody.

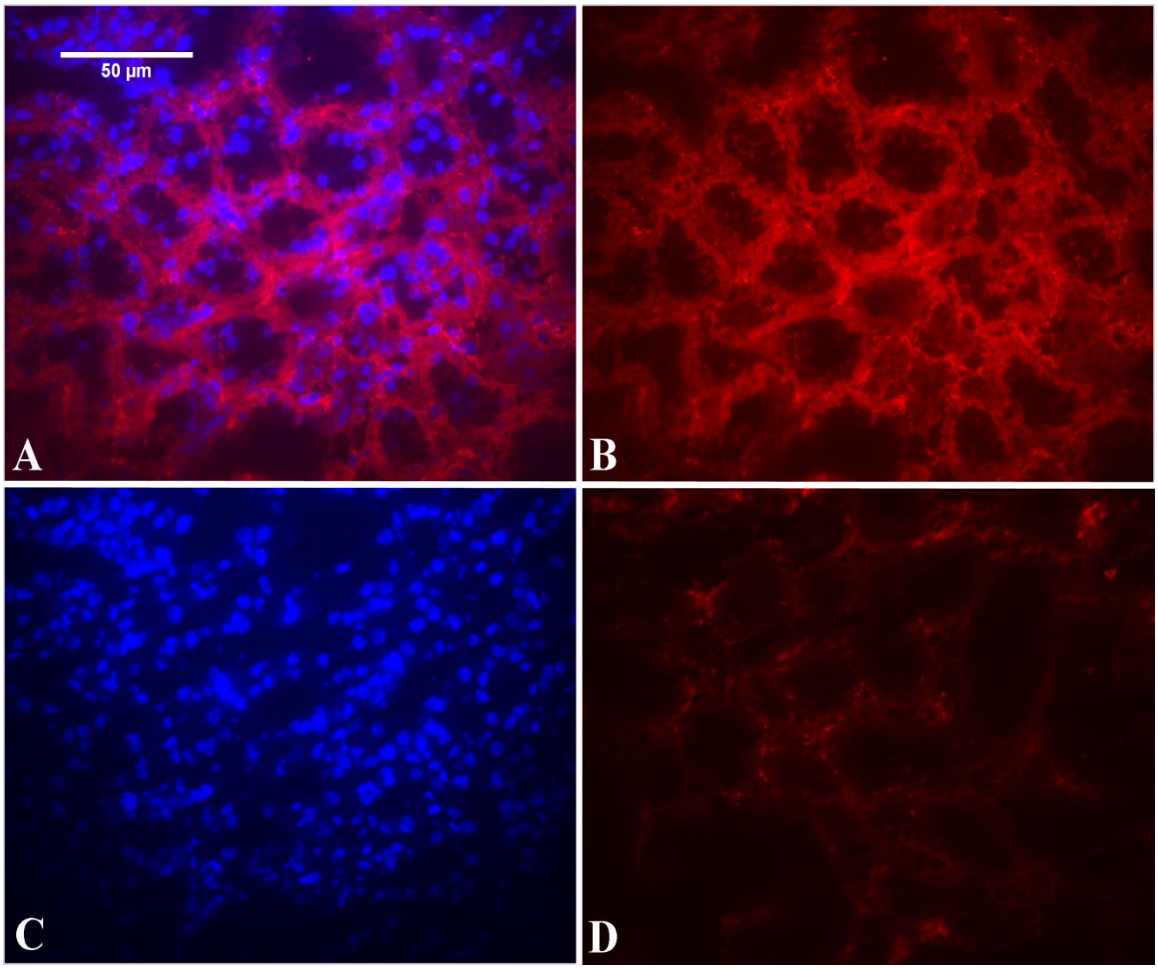

Figure 41. Immunofluorescent Localization of ET-A Receptors in M-WKY-S (40x). Immunohistochemical analysis of ET-A receptors in a sedentary male WKY rat. Each image in the figure was acquired with the 40x objective and a 7 second exposure time. A.) Kidney section probed with Endothelin-A and DAPI antibodies. B.) Kidney section probed with Endothelin-A antibody. C.) Kidney section probed with DAPI antibody. D.) Kidney section probed with secondary antibody.

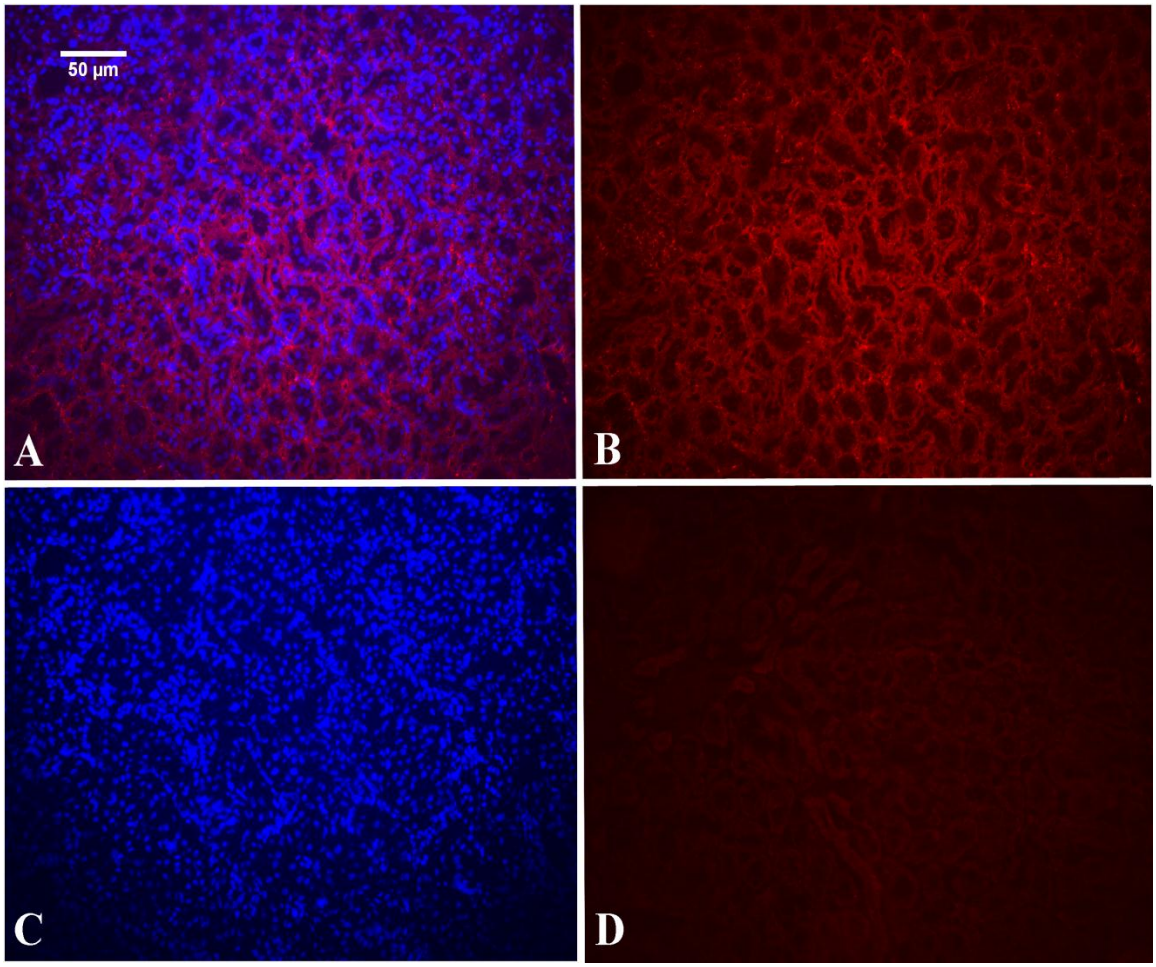

Figure 42. Immunofluorescent Localization of ET-B Receptors in F-SHR-E (20x).
Immunohistochemical analysis of ET-B receptors in an exercised female SHR rat. Each image in the figure was acquired with the 20x objective and a 10 second exposure time. A.) Kidney section probed with Endothelin-B and DAPI antibodies. B.) Kidney section probed with Endothelin-B antibody. C.) Kidney section probed with DAPI antibody. D.) Kidney section probed with secondary antibody.

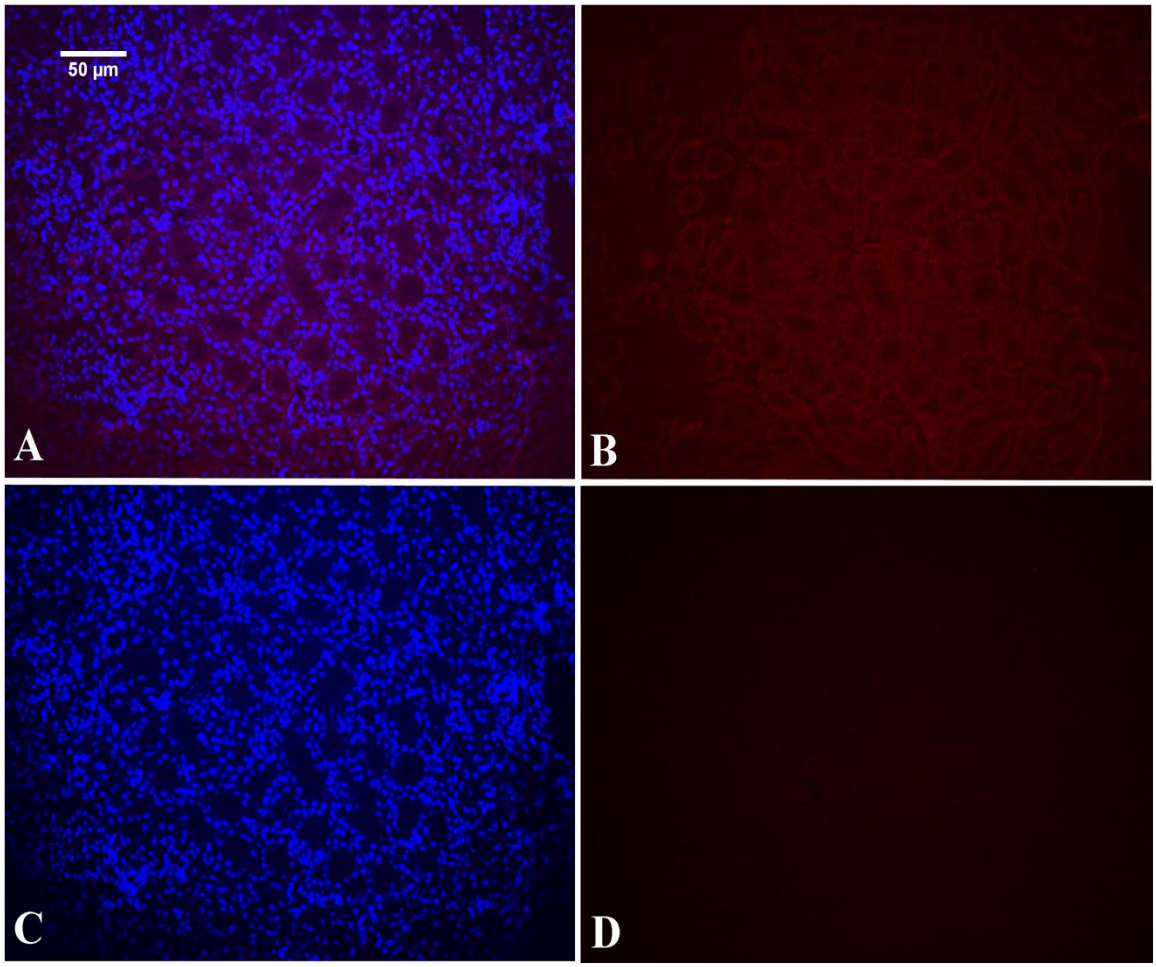

Figure 43. Immunofluorescent Localization of ET-B Receptors (20x). The general ET-B receptor localization pattern and intensity seen in every experimental group of rats other than exercised female SHR rats. Each image in the figure was acquired with the 20x objective and a 10 second exposure time. A.) Kidney section probed with Endothelin-B and DAPI antibodies. B.) Kidney section probed with Endothelin-B antibody. C.) Kidney section probed with DAPI antibody. D.) Kidney section probed with secondary antibody.

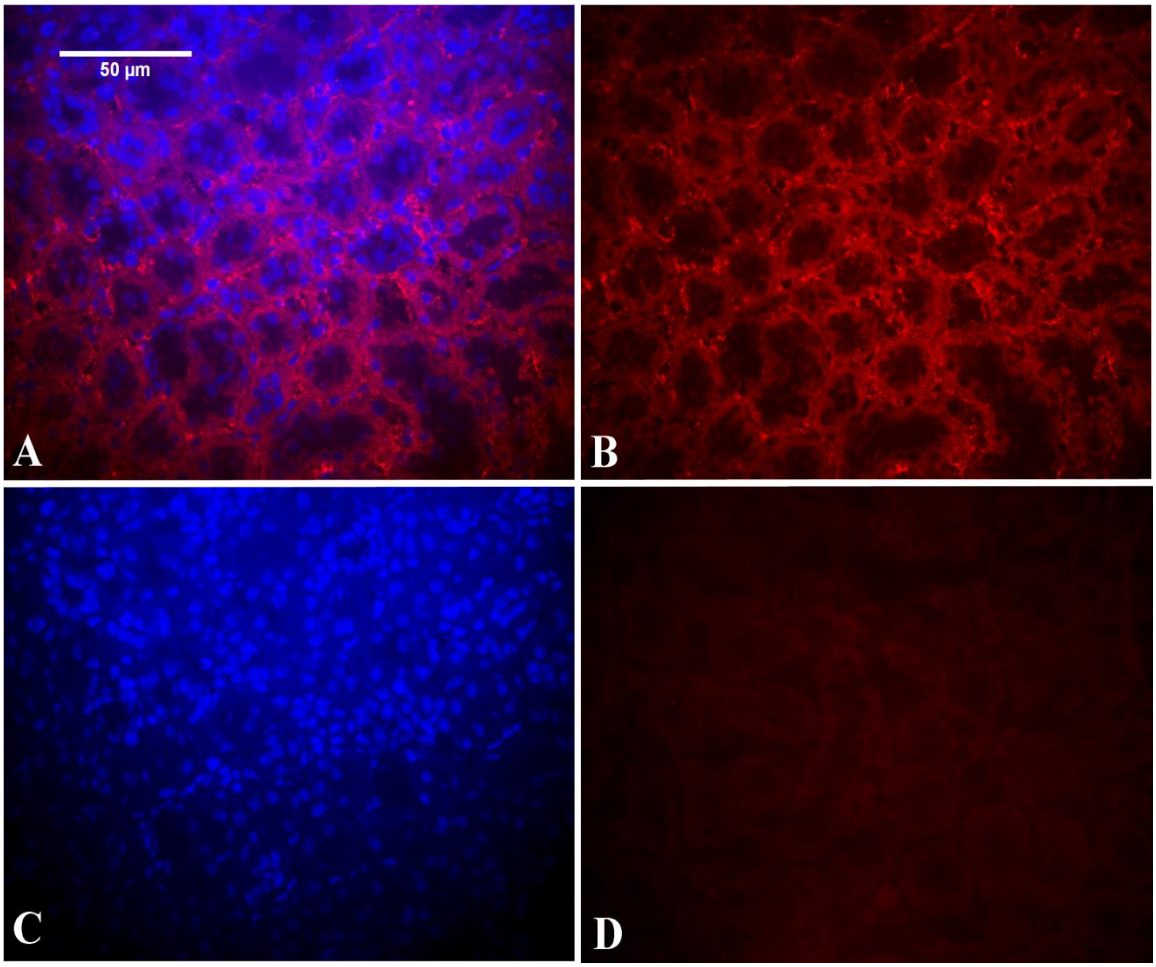

Figure 44. Immunofluorescent Localization of ET-B Receptors in F-SHR-E (40x).
Immunohistochemical analysis of ET-B receptors in an exercised female SHR rat. Each image in the figure was acquired with the 40x objective and a 10 second exposure time. A.) Kidney section probed with Endothelin-B and DAPI antibodies. B.) Kidney section probed with Endothelin-B antibody. C.) Kidney section probed with DAPI antibody. D.) Kidney section probed with secondary antibody.

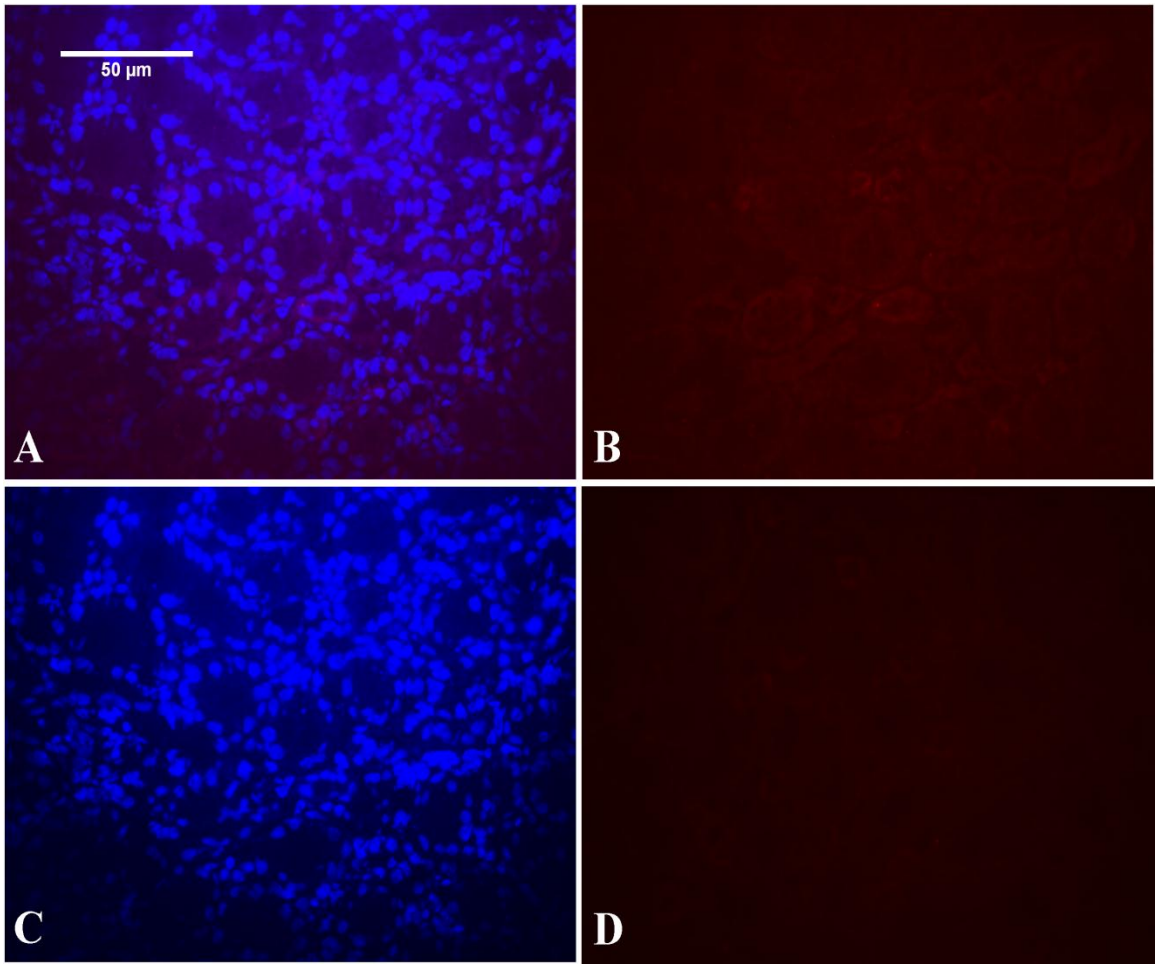

Figure 45. Immunofluorescent Localization of ET-B Receptors (40x). The general ET-B receptor localization pattern and intensity seen in every experimental group of rats other than exercised female SHR rats. Each image in the figure was acquired with the 40x objective and a 10 second exposure time. A.) Kidney section probed with Endothelin-B and DAPI antibodies. B.) Kidney section probed with Endothelin-B antibody. C.) Kidney section probed with DAPI antibody. D.) Kidney section probed with secondary antibody.

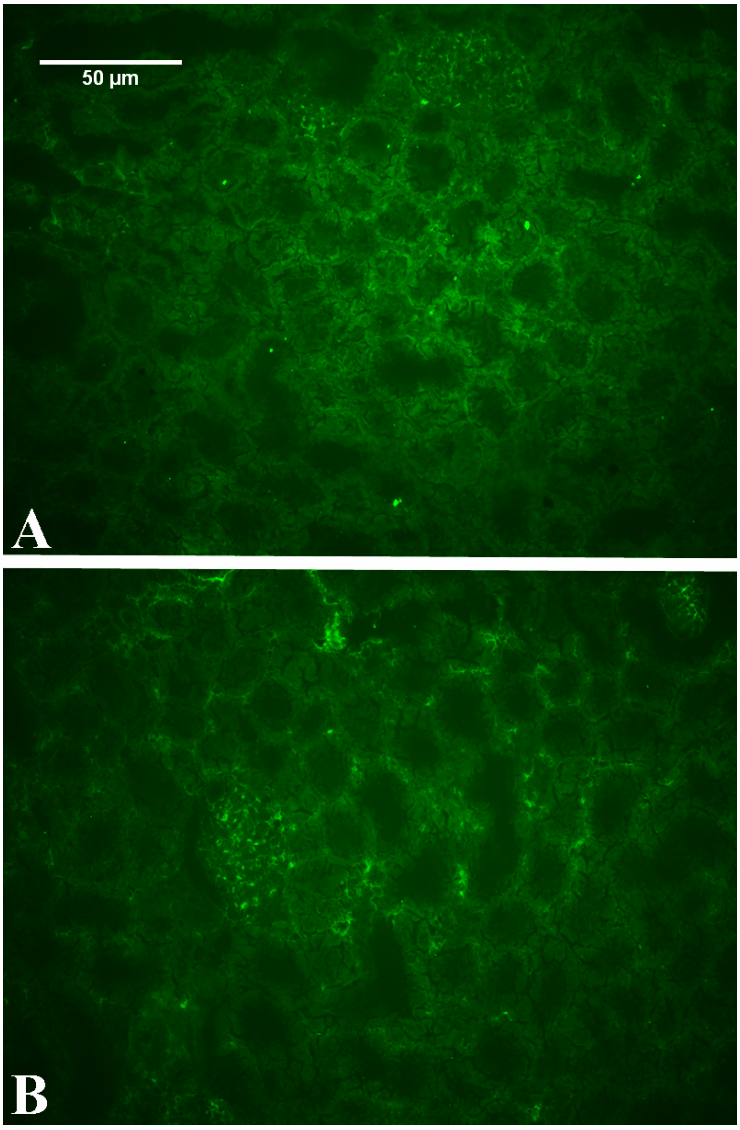

Figure 46. Immunofluorescent Localization of ET-1. The general ET-1 localization pattern and intensity seen in each experimental group of rats. Each image in the figure was acquired with the 20x objective and a 6 second exposure time. A.) Kidney section probed with ET-1 primary antibody and secondary antibody. B.) Kidney section probed with secondary antibody.

DISCUSSION

Previous studies in the laboratory of Dr. Penny Knoblich have shown that exercise increases the amount of sodium excreted in the urine of female WKY and SHR rats. The purpose of this study is to determine if the endothelin system, composed of ET-1 and ET-A and ET-B receptors, contributes to this effect. The effect of exercise on the renal endothelin system of male and female WKY and SHR rats was evaluated by SDS-PAGE and Western Blot analysis, enzyme-linked immunosorbent assay, and immunofluorescence microscopy. The body and kidney mass of each rat was also recorded to analyze the effect exercise has on kidney and overall bodily growth.

Exercise Behavior

To determine the effect of exercise and sex on the endothelin system of WKY and SHR rats, male and female rats of each strain voluntarily exercised on a wire wheel for eleven weeks. Consistent with previous studies, female rats ran a greater distance overall compared to male rats (77; 78). Female SHR rats exercised significantly more throughout the entire experiment and during weeks 2, 3, 4, and 6 relative to male SHR rats. Female WKY rats also exercised more than their male counterpart; however the difference was not statistically significant. According to Wang and associates, female rats have a higher general level of spontaneous activity due to a stimulus arising from the internal secretion of the ovaries (79). Unlike caged male rats, females exercise in excess every four days and this periodic fluctuation in activity has been correlated with their ovulation cycle (79). Female rats with their ovaries removed tend to be less active

than normal females (79). Similarly, the transplantation of ovaries to castrated male rats results in an activity curve similar to that observed in females (79).

In addition to an observed correlation between sex and exercise behavior, it was noted that rats of the WKY strain ran a greater total distance relative to SHR rats. The amount of total work, as determined by multiplying the mean body weight by the mean weekly running distance of each group of exercised rats, was greater in male and female WKY rats relative to male and female SHR rats. This finding is consistent with previous studies (73; 76). According to Kingwell, WKY rats run a greater distance relative to SHR rats due to an exercise induced increase in aortic elasticity or compliance, which allows the aorta to more easily accommodate a rise in arterial blood volume associated with exercise (73). In contrast with WKY rats, Kingwell suggests that SHR rats run a lesser distance due an increased blood pressure and lack of ability to alter their aortic compliance (80).

Kidney and Body Mass

It is well documented that male rats have an increased kidney and body mass relative to female rats (81) and that rats of the WKY strain have an increased kidney and body mass relative to rats of the SHR strain (67). Our data are consistent with this trend. The mean kidney and body mass of female rats was significantly decreased relative to male rats and the mean kidney and body mass of SHR rats was significantly decreased relative to WKY rats.

Limited information is available of the effect of exercise on the kidney and body mass of male and female SHR and WKY rats. However, this study revealed that exercised female WKY and SHR rats had a significantly increased kidney mass and female WKY rats had a significantly increased body mass compared to sedentary female WKY and SHR rats. This result is not consistent with prior studies in which exercised female rats have been reported to maintain a body weight similar to sedentary rats (82). One possible explanation for the anomaly is that exercise may promote alterations in the body composition of female rats, such as an increase in muscle mass and or a depression in body fat.

It was observed that exercised male WKY rats had a significantly decreased body mass and an elevated ratio of mean kidney mass to mean body mass relative to sedentary rats of the same sex and strain. Exercise has been reported in a similar study to contribute to a decrease in the body mass of male rats compared to sedentary male rats due to an increase in energy expenditure (82). The reduced body weight of exercised males caused the increase in mean kidney mass to mean body mass observed in exercised male WKY rats.

Levels of Renal Endothelin-A Receptor

In Western blot analysis, ET-A receptor levels were elevated in SHR rats relative to WKY rats, suggesting that protein expression was upregulated in the kidneys of SHR rats. These results are consistent with previous studies in which an overexpression of ET-A receptor in the glomeruli and smooth muscle cells of intrarenal arteries of SHR rats

compared to age-matched WKY rats was detected (55). Hocher also determined that SHR rats injected with bosentan, an ET-A/ET-B antagonist, experience a decrease in blood pressure and increase in renal blood flow of the same magnitude as SHR rats injected with BQ-123, an ET-A antagonist (55). These results suggest that vascular ET-A overexpression regulates renal blood flow and contributes to high blood pressure in SHR rats and may explain the upregulation of ET-A receptor levels in the renal tissue of SHR rats relative to WKY rats observed in this study.

The results of the experiment also suggest that high ET-A expression in SHR rats might be a compensatory mechanism for low levels of ET-1 excreted in the urine of SHR rats relative to WKY rats. Receptors commonly increase their number or decrease their degradation with a reduction in circulating ligand (14).

Exercise had a variable effect on renal ET-A receptor expression. Western blot analysis of exercised female SHR and exercised male WKY rats revealed an increased level of ET-A receptors relative to their sedentary counterparts. Exercised female WKY and exercised male SHR rats had a decreased level of ET-A receptors relative to their sedentary counterparts. The variable effect of exercise on ET-A receptor expression suggests that ET-A receptors are not responsible for inducing the natriuretic response of exercised female SHR and WKY rats previously described in the laboratory of Dr. Penny Knoblich (76).

ET-A expression was determined by Western blot analysis to be increased in the kidney tissue of male rats relative to female rats of the same strain and activity level,

with male SHR exercised rats being the only exception. Other studies have reported a similar ET-A receptor increase in males compared to females. Human males have been reported to have an increased ratio of ET-A to ET-B receptors relative to age-matched women. According to Ergul and colleagues, the saphenous veins from men contain a greater number of ET-A receptors than women and the ratio of ET-A to ET-B receptors is 3:1 in men compared to 1:1 in women (83). Ergul has also reported two-fold greater ET-1-induced contractions in males relative to females and believes that the overabundance of ET-A receptors in men is responsible for this contractile response (83).

Because ET-A receptors are involved in the vasoconstrictive response to ET-1 and male experimental models of hypertension tend to have a more severe form of hypertension compared to females, the increase in renal ET-A expression was anticipated. However, elevated male expression was not absolute as exercised female SHR rats exhibited slightly higher renal levels of ET-A receptors relative to exercised male SHR rats. Although this result was not predicted, it is consistent with a recent study that found that both ET-B and ET-A receptors contribute to ET-1 dependent natriuresis in female rats (84). Intramedullary infusion of ET-1 produced greater diuretic and natriuretic responses in female rats relative to male rats primarily because of an ET-A receptor-dependent mechanism (84). The natriuretic properties of ET-A receptors in female rats may explain the upregulation of renal ET-A observed in exercised female SHR rats compared to exercised male SHR rats in this study.

Levels of Renal Endothelin-B Receptor

Western blot analysis determined that renal tissue extracted from exercised female SHR rats exhibited a high level of ET-B receptor expression but ET-B receptors were undetectable in the renal tissue of all other experimental groups of rats.

Studies over the past decade have clearly established that ET-B receptor activation by ET-1 is an important mechanism that serves to regulate and maintain the pressure-natriuresis relationship (28). The selective deletion of ET-B receptor expression in collecting duct cells induces sodium retention and mean arterial pressure elevation in mice (85). Studies from the laboratory of Dr. Penny Knoblich indicate that exercised female SHR and WKY rats excrete significantly more sodium in their urine than sedentary female SHR and WKY rats and exercised and sedentary male SHR and WKY rats in response to a rise in blood pressure (76). These observations suggest that the increased level of natriuresis in the renal system of exercised female SHR and WKY rats corresponds with increased renal ET-B receptor expression. Our results support this hypothesis in the case of exercised female SHR rats but not exercised female WKY rats.

However, a similar upregulation of ET-B receptor expression in SHR rats relative to WKY rats has been observed in other studies. ET-B receptor mediated vasodilation is greater in SHR rats than normotensive control rats (47). Previous research in the laboratory of Dr. Penny Knoblich has reported higher sodium excretion levels in exercised female SHR rats in response to angiotensin II infusion relative to exercised female WKY rats (76). According to Hocher and associates, an increased level of

vasodilation and natriuresis in SHR rats is caused by an overexpression of ET-B receptors in the glomeruli of SHR rats compared to age-matched WKY rats (55). An increase in ET-B receptor expression in response to high levels of blood pressure has also been reported by Lauth and associates (86). According to Lauth, isolated segments of the rabbit jugular vein upregulate the expression of ET-B mRNA and functional ET-B protein in response to an increase in intraluminal perfusion pressure (86). Given this information, it is possible to conclude that although an increase in renal ET-B receptor expression is believed to be responsible for higher levels of natriuresis in exercised female SHR rats, another unknown mechanism may be responsible for the previously observed increase in sodium excreted in the urine of exercised female WKY rats.

An increase in ET-B receptors in the renal tissue of exercised female SHR rats may be caused by the effect of exercise on ET-B receptor expression. It is widely accepted that physical activity increases the level of vascular shear stress. According to Taylor and associates, the amount of vascular wall shear stress is significantly increased in the human abdominal aorta following physical activity (87). Studies have also reported a link between an increase in shear stress and an ET-B receptor upregulation. According to Morawietz and colleagues, human umbilical vein endothelial cells that are exposed to increasing degrees of long-term laminar shear stress upregulate ET-B receptor mRNA (49). Similar studies have reported the overexpression of ET-B receptors in primary cultures of bovine aortic endothelial cells isolated from vessels previously

exposed to arterial shear stress in vivo (88) and canine arterial smooth muscle cells in response to chronic increases in blood flow (89).

An upregulation of renal ET-B receptors in exercised female SHR rats relative to male experimental groups of rats is believed to be caused by the effect of endothelial function on ET-B receptor expression. Males are known to have more endothelial dysfunction, be less responsive to NO-mediated arteriolar dilations, and experience a reduced natriuretic response to ET-1 relative to females (90). Recent studies have also determined that the pressure-natriuresis relationship in SHR females is shifted toward lower blood pressures for a given level of sodium intake compared to SHR males (28). According to Kittikulsuth and associates, the lower level of natriuresis in angiotensin II hypertensive male rats is caused by their impaired renal ET-B receptor function and reduced number of ET-B receptor binding sites (91).

Renal Localization of Endothelin-A and Endothelin-B Receptors

Staining with ET-A and ET-B receptor primary antibodies resulted in very broad immunofluorescence localization patterns that included staining of most of the nephron components, such as around the perimeter of proximal and distal convoluted tubules and within glomeruli of the renal corpuscles. The localization of ET-A and ET-B receptors is consistent with a previous study conducted to determine the distribution of endothelin receptors within the rat kidney (57). According to Wendel and associates, both ET-A and ET-B receptor immunoreactivity can be detected within the glomerular matrix of the renal corpuscle; however the receptors are present on distinct cell

types (57). Only ET-B receptors are found on endothelial glomerulus cells, whereas both types of receptors are present on mesangial cells (57). Wendel also reported that endothelin receptors are located among the renal tubule system, with ET-A receptors predominating within cortical collecting ducts and distal tubules and ET-B receptors mainly restricted to proximal tubules (57). Although endothelin receptors are widely distributed throughout the nephron, Wendel has postulated that their precise cellular location exerts differential effects on renal function (57). The detailed cellular localization of endothelin receptor subtypes were not determined using this experimental design; however, future immunofluorescence studies should emphasize their distribution.

While ET-A receptor immunofluorescence staining was observed in each experimental group of rats, sedentary male SHR rats had the most intense tubular extracellular membrane staining. This result is consistent with Western blot analysis that reported kidney homogenate extracted from sedentary male SHR rats expressed the highest level of ET-A receptor expression. An increase in ET-A receptor staining in the renal tissue of sedentary male SHR rats is expected. As previously noted, ET-A receptor expression has been reported to be upregulated in the kidneys of SHR rats relative to WKY rats and male rats relative to female rats (55; 83).

Consistent with Western blot analysis results, ET-B receptor immunofluorescence staining was only observed in renal tissue extracted from exercised female SHR rats. This result supports the hypothesis that an upregulation of

renal ET-B receptors may be responsible for an increase in sodium excreted in the urine of exercised female SHR rats as previously reported by the laboratory of Dr. Penny Knoblich (76).

Levels of Renal and Urinary Endothelin-1

The presence of ET-1 in the renal tissue of each group of rats was undetectable using Western blot analysis and immunofluorescence microscopy. These results suggest that ET-1 is expressed at a level which was not detectable using this experimental design and primary antibody. However, it has been reported in previous studies that ET-1 is expressed in relatively high amounts in the kidneys of WKY and SHR rats (92) . The lack of renal ET-1 expression in both Western blot analysis and immunofluorescence microscopy may have been due to an ineffective primary antibody, as both experiments utilized the same antibody. In future studies, Western blot analysis and immunofluorescence microscopy could be repeated using antibodies from additional sources including the one utilized in the laboratory of Wong.

ELISA analysis of urinary excretion of ET-1, which is believed to reflect renal ET-1 synthesis, revealed that the amount of ET-1 was greater in the pooled urine of exercised and sedentary male and female WKY rats relative to exercised and sedentary male and female SHR rats. This is consistent with previous studies in which a reduction in ET-1 excretion in hypertensive patients was noted (93). Patients with essential hypertension excrete significantly less ET-1 in their urine compared with normotensive patients (93). Due to the natriuretic properties of ET-1, Hoffman has postulated that the reduction in

renal ET-1 excretion may be responsible for the development and sustainability of high blood pressure in these patients (93). In similar studies, ET-1 synthesis was reduced in the inner medullary collecting duct (IMCD), an area of the kidney in which ET-1 is believed to be produced in amounts greater than other tubule segments, of hypertensive rats (75; 94). The renal medulla of SHR rats contains approximately 20% of the ET-1 found in the renal medulla of normotensive WKY control rats (94). Hughes and associates have also reported that ET-1 production is reduced in IMCD cells of SHR rats relative to age-matched WKY control rats (75). According to Hughes, ET-1 is responsible for preventing sodium and water reabsorption pathways in the IMCD and a reduction in renal medullary ET-1 synthesis in SHR rats may contribute to their hypertensive state (75), which may explain why a decrease in ET-1 urinary excretion was observed in SHR rats relative to WKY rats.

According to results derived from ELISA analysis, the effect of exercise on urinary ET-1 excretion was variable in hypertensive and normotensive rats. In this study, exercised WKY rats excreted more ET-1 relative to sedentary WKY rats and exercised SHR rats excreted less ET-1 relative to sedentary SHR rats. The effect of exercise on ET-1 excreted in the urine of hypertensive urinary ET-1 excretion was unexpected. In a similar study, an increased expression of the ET-1 precursor, preproET-1 mRNA, was detected in the kidneys of exercised rats compared to sedentary control rats (64). An exercise-induced increase in ET-1 expression is responsible for renal vasoconstriction and the

redistribution of tissue blood flow from the kidney to working muscles during endurance exercise (64).

One possible explanation for this anomaly in rats of the SHR strain is the presence and effect of increased vascular shear stress. Recent studies have reported that an increase in shear stress is associated with hypertension and that endothelial dysfunction is increased and shear stress-induced vascular dilation is decreased in SHR relative to WKY rats (74; 95). The long-term application of shear stress to cultures of human umbilical vein endothelial cells results in a down regulation of preproET-1 mRNA, ECE-1 mRNA, and ET-1 release (49). Exercise has also been reported to increase vascular shear stress (87). The exercise-induced shear stress added to the inherent shear stress of SHR rats is postulated to be the mechanism behind the reduction of urinary ET-1 excretion observed in exercised hypertensive rats in this study. A similar effect may not be observed in WKY rats because due to their improved endothelial function and lower level of vascular shear stress relative to SHR rats.

The effect of shear stress predominates in animal models of hypertension. This may explain why sex was not a determining factor in the amount of ET-1 excreted in the urine of SHR rats. However, in this study female WKY rats were found to excrete significantly more ET-1 than their male counterparts. Males are known to develop earlier and a more severe form of hypertension relative to females (96). Coinciding with higher mean arterial pressures, males have also been reported to be inflicted with lower levels of endothelial function compared to females (96; 97). In age-matched healthy

adults, females have significantly greater flow-mediated dilation than males due to the smaller vessel size of females (97). Increased endothelial function in females may be responsible for the higher amount of ET-1 excreted in the urine of female WKY rats relative to male WKY rats in this study.

In ELISA analysis, the amount of ET-1 excreted in the urine of exercised female SHR rats was much lower than that of other experimental groups. Exercised female SHR rats had a significantly increased renal concentration of ET-B receptors relative to other rat groups. According to recent studies, ET-B receptors are responsible for the clearance of ET-1 from circulation (47). For example, it has been reported that BQ-788, an ET-B receptor antagonist, inhibits the accumulation of intravenously administered ET-1 in the lungs and kidneys, thereby slowing its clearance from the circulation (47). Treatment with BQ-123, an ET-A receptor antagonist, has been reported to have no such effect (47). Therefore, it is believed that exercised female SHR rats excreted very little ET-1 in their urine at least in part due to the upregulation of ET-1 clearance resulting from an increased number of renal ET-B receptors.

Conclusion

The purpose of this study was to determine if an exercise induced change in the endothelin system is responsible for the increase in sodium excretion in exercised female SHR and WKY rats as previously reported by the laboratory of Dr. Penny Knoblich. Because ET-A receptors function in vasoconstriction and sodium retention, it was hypothesized that ET-A receptor expression would be decreased in the renal tissue

of exercised female SHR and WKY rats relative to sedentary female SHR and WKY rats and that exercise will have no effect on ET-A receptor expression in male SHR and WKY rats. Consistent with this hypothesis, Western blot analysis determined that the kidneys of exercised female WKY rats had lower ET-A receptor levels compared to sedentary female WKY rats. However, exercised female SHR rats were found to have an increased renal ET-A receptor expression relative to their sedentary counterpart and ET-A receptor expression was affected by exercise in the case of male SHR and WKY rats. It was also noted that ET-A receptor expression was increased in SHR rats relative to WKY rats and male rats relative to female rats, with exercised female SHR rats being the only exception.

ET-B receptors are responsible for vasodilation and sodium excretion, which is why it was initially hypothesized that exercise leads to an upregulation of ET-B receptor levels in female SHR and WKY rats and that exercise will have no effect of ET-B receptor expression in male SHR and WKY rats. An increased level of ET-B receptor expression was observed in exercised female SHR rats according to Western blot analysis; however, this result was not seen in exercised female WKY rats. In accordance with the hypothesis, it was determined that ET-B receptor expression was not mediated by physical activity in male SHR and WKY rats.

ET-1 mediates vascular changes by activating both ET-A and ET-B receptors; therefore, it was hypothesized that ET-1 expression would not vary in the renal tissue of male and female rats regardless of physical activity level or strain. This hypothesis can

neither be accepted nor rejected with data derived from Western blot analysis or immunofluorescence microscopy because both assays were unable to detect ET-1 expression. However, ELISA analysis reported varying urinary ET-1 excretion levels in each experimental group of rats. ET-1 excretion was increased in WKY rats relative to SHR rats and in females relative to males, with female SHR exercised rats being the exception. The greatest amount of ET-1 was excreted in the urine of exercised female WKY rats. Exercise was found to have a variable effect on the amount of ET-1 excreted in the urine.

In conclusion, exercise induced changes in the endothelin system may be responsible for increased sodium excretion levels in exercised female hypertensive and normotensive rats as described by the laboratory of Dr. Penny Knoblich. According to Western blot analysis, ET-A receptors are upregulated in the kidneys of exercised female SHR rats. Although ET-A receptors are predominately involved in mediating vasoconstriction, a recent study has determined that ET-A receptors also contribute to ET-1 dependent natriuresis in female rats (84). As determined by Western blot analysis and immunofluorescence microscopy, ET-B receptors were also upregulated in exercised female SHR rats relative to other experimental groups of rats. ET-1 activated ET-B receptors mediate vasodilation and the clearance of ET-1 from systemic circulation, which may explain why urinary ET-1 excretion levels were reduced in comparison to the other rat groups. These exercise induced changes in the endothelin system of female

SHR rats might be the mechanism behind their previously reported increase in sodium excretion levels in response to an artificial rise in mean arterial blood pressure.

Contradictory to expectations, ET-B expression levels were not increased in the renal system of exercised female WKY rats. However, ET-1 excretion levels were determined by ELISA analysis to be the greatest in the urine collected from exercised female WKY rats. Therefore, an increase in ET-1 synthesis in response to exercise may explain the increase in sodium excreted in the urine of exercised female WKY rats as previously described by the laboratory of Dr. Penny Knoblich.

Further Studies

Additional studies are necessary to fully elucidate the effect of exercise on the endothelin system of male and female SHR and WKY rats. To confirm and extend the ELISA analysis of ET-1 urinary excretion, urine should be collected and analyzed throughout the entire eleven weeks of physical activity instead of the time of euthanasia only. Western blot expression of ET-1 and ET-A and ET-B receptors could be expanded and confirmed by characterizing mRNA expression using Northern blot analysis and or Reverse Transcriptase-PCR analysis. Several additional ET-1 primary antibodies should be tested using Western blot analysis and immunofluorescence microscopy to evaluate ET-1 expression. Immunofluorescence localization analysis could be correlated with differential staining such as hematoxylin and eosin staining to determining the specific cellular location of ET-1 and ET-A and ET-B receptors in the vascular and tubular renal system of the experimental rats. Double immunofluorescence staining depicting the

colocalization patterns of ET-A receptors and ET-B receptors may be beneficial. Quantitative immunofluorescence and a quantitative acquisition software program could be also utilized to further immunofluorescence analysis and determine the approximate amount of renal ET-1 and ET-A and ET-B receptor expression.

LITERATURE CITED

1. Fields, L. E., Burt, V. L., Cutler, J. A., Hughes, J., Roccella, E. J. & Sorlie, P. (2004). The burden of adult hypertension in the United States 1999 to 2000: a rising tide. *Hypertension* **44**, 398-404.
2. Guyton, A. C. (1990). Long-term arterial pressure control: an analysis from animal experiments and computer and graphic models. *Am J Physiol* **259**, R865-77.
3. Franjic, B. & Marwick, T. H. (2009). The diabetic, hypertensive heart: epidemiology and mechanisms of a very high-risk situation. *J Hum Hypertens* **23**, 709-17.
4. Mohrman & Heller. (2006). *Cardiovascular Physiology*. 6th edit, Lange Medical Books/McGraw-Hill, New York, NY.
5. Ackermann, U. (2004). Regulation of arterial blood pressure. *Surgery (Oxford)* **22**, 120a-120f.
6. Standfield, C. L. (2011). *Principles of Human Physiology* 4th edit, Benjamin Cummings Pearson Education, Boston, MA.
7. Martini, T., Tallitsch. (2006). *Human Anatomy*. 5th edit, Pearson Benjamin Cummings, San Francisco, CA.
8. Kronenberg, H. M. (2008). *Williams Textbook of Endocrinology*. 11th edit, Elsevier Saunders, Philadelphia, PA.
9. Doohan, J. (2000). Summary of Factors that Effect Mean Arterial Pressure. McGraw-Hill Companies, Inc.
10. Clarkson, P., Prasad, N. & MacDonald, T. M. (1994). Left ventricular hypertrophy in hypertension--general and local trends in diagnosis and therapy. *Scott Med J* **39**, 35-7.
11. Go, A. S., Hylek, E. M., Phillips, K. A., Chang, Y., Henault, L. E., Selby, J. V. & Singer, D. E. (2001). Prevalence of diagnosed atrial fibrillation in adults: national implications for rhythm management and stroke prevention: the AnTicoagulation and Risk Factors in Atrial Fibrillation (ATRIA) Study. *JAMA* **285**, 2370-5.
12. Peacock, F., Amin, A., Granger, C. B., Pollack, C. V., Jr., Levy, P., Nowak, R., Kleinschmidt, K., Varon, J., Wyman, A., Gore, J. M. & Stat, I. (2011). Hypertensive heart failure: patient characteristics, treatment, and outcomes. *Am J Emerg Med* **29**, 855-62.
13. Kannel, W. B. & Cobb, J. (1992). Left ventricular hypertrophy and mortality--results from the Framingham Study. *Cardiology* **81**, 291-8.
14. Starr, T., Evers, and Starr. (2009). *Biology: The Unity and Diversity of Life*. 12th edit.
15. Brenner, B. (2007). *Brenner and Rector's The Kidney*. 8th edit, Elsevier Saunders, Philadelphia, PA.
16. Evans, R. G., Majid, D. S. & Eppel, G. A. (2005). Mechanisms mediating pressure natriuresis: what we know and what we need to find out. *Clin Exp Pharmacol Physiol* **32**, 400-9.
17. Granger, J. P., Alexander, B. T. & Llinas, M. (2002). Mechanisms of pressure natriuresis. *Curr Hypertens Rep* **4**, 152-9.
18. Cowley, A. W., Jr. (1997). Role of the renal medulla in volume and arterial pressure regulation. *Am J Physiol* **273**, R1-15.
19. Farrugia, E., Lockhart, J. C. & Larson, T. S. (1992). Relation between vasa recta blood flow and renal interstitial hydrostatic pressure during pressure natriuresis. *Circ Res* **71**, 1153-8.

20. Knox, F. G., Mertz, J. I., Burnett, J. C., Jr. & Haramati, A. (1983). Role of hydrostatic and oncotic pressures in renal sodium reabsorption. *Circ Res* **52**, 491-500.
21. Roman, R. J., Cowley, A. W., Jr., Garcia-Estan, J. & Lombard, J. H. (1988). Pressure-diuresis in volume-expanded rats. Cortical and medullary hemodynamics. *Hypertension* **12**, 168-76.
22. Roman, R. J. (1988). Pressure-diuresis in volume-expanded rats. Tubular reabsorption in superficial and deep nephrons. *Hypertension* **12**, 177-83.
23. Evans, R. G., Szenasi, G. & Anderson, W. P. (1995). Effects of NG-nitro-L-arginine on pressure natriuresis in anaesthetized rabbits. *Clin Exp Pharmacol Physiol* **22**, 94-101.
24. Pollock, J. S. & Pollock, D. M. (2008). Endothelin and NOS1/nitric oxide signaling and regulation of sodium homeostasis. *Curr Opin Nephrol Hypertens* **17**, 70-5.
25. Salom, M. G., Lahera, V., Miranda-Guardiola, F. & Romero, J. C. (1992). Blockade of pressure natriuresis induced by inhibition of renal synthesis of nitric oxide in dogs. *Am J Physiol* **262**, F718-22.
26. Ikenaga, H., Suzuki, H., Ishii, N., Itoh, H. & Saruta, T. (1993). Role of NO on pressure-natriuresis in Wistar-Kyoto and spontaneously hypertensive rats. *Kidney Int* **43**, 205-11.
27. Navar, L. G. (2005). The role of the kidneys in hypertension. *J Clin Hypertens (Greenwich)* **7**, 542-9.
28. Nakano, D., Pollock, J. S. & Pollock, D. M. (2008). Renal medullary ETB receptors produce diuresis and natriuresis via NOS1. *Am J Physiol Renal Physiol* **294**, F1205-11.
29. Atlas, S. A. (2007). The renin-angiotensin aldosterone system: pathophysiological role and pharmacologic inhibition. *J Manag Care Pharm* **13**, 9-20.
30. Paul, M., Poyan Mehr, A. & Kreutz, R. (2006). Physiology of local renin-angiotensin systems. *Physiol Rev* **86**, 747-803.
31. Carretero, O. A. & Oparil, S. (2000). Essential hypertension. Part I: definition and etiology. *Circulation* **101**, 329-35.
32. Onusko, E. (2003). Diagnosing secondary hypertension. *Am Fam Physician* **67**, 67-74.
33. August, P. (2004). Overview: mechanisms of hypertension: cells, hormones, and the kidney. *J Am Soc Nephrol* **15**, 1971-3.
34. Franco, V., Oparil, S. & Carretero, O. A. (2004). Hypertensive therapy: Part II. *Circulation* **109**, 3081-8.
35. Karppanen, H. & Mervaala, E. (2006). Sodium intake and hypertension. *Prog Cardiovasc Dis* **49**, 59-75.
36. Rettig, R. & Grisk, O. (2005). The kidney as a determinant of genetic hypertension: evidence from renal transplantation studies. *Hypertension* **46**, 463-8.
37. Coffman, T. M. (2011). Under pressure: the search for the essential mechanisms of hypertension. *Nat Med* **17**, 1402-9.
38. Brenner, B. M., Garcia, D. L. & Anderson, S. (1988). Glomeruli and blood pressure. Less of one, more the other? *Am J Hypertens* **1**, 335-47.
39. Intengan, H. D. & Schiffrin, E. L. (2001). Vascular remodeling in hypertension: roles of apoptosis, inflammation, and fibrosis. *Hypertension* **38**, 581-7.
40. Gibbons, G. H. & Dzau, V. J. (1994). The emerging concept of vascular remodeling. *N Engl J Med* **330**, 1431-8.
41. Hall, J. E., Mizelle, H. L., Hildebrandt, D. A. & Brands, M. W. (1990). Abnormal pressure natriuresis. A cause or a consequence of hypertension? *Hypertension* **15**, 547-59.

42. Konishi, Y., Okada, N., Okamura, M., Morikawa, T., Okumura, M., Yoshioka, K. & Imanishi, M. (2001). Sodium sensitivity of blood pressure appearing before hypertension and related to histological damage in immunoglobulin a nephropathy. *Hypertension* **38**, 81-5.
43. Duarte, D., Santos-Araujo, C. & Leite-Moreira, A. F. (2011). Hypertension and angiogenesis in the aging kidney: a review. *Arch Gerontol Geriatr* **52**, e93-102.
44. Coffman, T. M. & Crowley, S. D. (2008). Kidney in hypertension: guyton redux. *Hypertension* **51**, 811-6.
45. Ritz, E., Adamczak, M. & Zeier, M. (2003). Kidney and hypertension-causes. Update 2003. *Herz* **28**, 663-7.
46. DiBona, G. F. (2004). The sympathetic nervous system and hypertension: recent developments. *Hypertension* **43**, 147-50.
47. Hynynen, M. M. & Khalil, R. A. (2006). The vascular endothelin system in hypertension--recent patents and discoveries. *Recent Pat Cardiovasc Drug Discov* **1**, 95-108.
48. Cecioni, I., Modesti, P. A., Poggesi, L., Rocchi, F., Rega, L. & Neri Serneri, G. G. (1999). Endothelin-1 urinary excretion, but not endothelin-1 plasma concentration, is increased in renovascular hypertension. *J Lab Clin Med* **134**, 386-91.
49. Morawietz, H., Talanow, R., Szibor, M., Rueckschloss, U., Schubert, A., Bartling, B., Darmer, D. & Holtz, J. (2000). Regulation of the endothelin system by shear stress in human endothelial cells. *J Physiol* **525 Pt 3**, 761-70.
50. Shao, R., Yan, W. & Rockey, D. C. (1999). Regulation of endothelin-1 synthesis by endothelin-converting enzyme-1 during wound healing. *J Biol Chem* **274**, 3228-34.
51. Miyauchi, T. & Masaki, T. (1999). Pathophysiology of endothelin in the cardiovascular system. *Annu Rev Physiol* **61**, 391-415.
52. Luscher, T. F. & Barton, M. (2000). Endothelins and endothelin receptor antagonists: therapeutic considerations for a novel class of cardiovascular drugs. *Circulation* **102**, 2434-40.
53. Yanagisawa, M., Kurihara, H., Kimura, S., Tomobe, Y., Kobayashi, M., Mitsui, Y., Yazaki, Y., Goto, K. & Masaki, T. (1988). A novel potent vasoconstrictor peptide produced by vascular endothelial cells. *Nature* **332**, 411-5.
54. Frishman, W. H., Tamirisa, P. & Kumar, A. (1997). Endothelins and their role in hypertension. *Baillière's Clinical Anaesthesiology* **11**, 561-580.
55. Hocher, B., Rohmeiss, P., Zart, R., Diekmann, F., Vogt, V., Metz, D., Fakhury, M., Gretz, N., Bauer, C., Koppenhagen, K., Neumayer, H. H. & Distler, A. (1996). Function and expression of endothelin receptor subtypes in the kidneys of spontaneously hypertensive rats. *Cardiovasc Res* **31**, 499-510.
56. Goraca, A. (2002). New views on the role of endothelin (minireview). *Endocr Regul* **36**, 161-7.
57. Wendel, M., Knels, L., Kummer, W. & Koch, T. (2006). Distribution of endothelin receptor subtypes ETA and ETB in the rat kidney. *J Histochem Cytochem* **54**, 1193-203.
58. Abassi, Z. A., Ellahham, S., Winaver, J. & Hoffman, A. (2001). The intrarenal endothelin system and hypertension. *News Physiol Sci* **16**, 152-6.
59. Boniface, S. & Reynaud-Gaubert, M. (2011). Endothelin receptor antagonists -- their role in pulmonary medicine. *Rev Mal Respir* **28**, e94-e107.

60. Ciolac, E. G., Guimaraes, G. V., VM, D. A., Bortolotto, L. A., Doria, E. L. & Bocchi, E. A. (2009). Acute effects of continuous and interval aerobic exercise on 24-h ambulatory blood pressure in long-term treated hypertensive patients. *Int J Cardiol* **133**, 381-7.
61. Casillas, J. M., Gremeaux, V., Damak, S., Feki, A. & Perennou, D. (2007). Exercise training for patients with cardiovascular disease. *Ann Readapt Med Phys* **50**, 403-18, 386-402.
62. Higashi, Y. & Yoshizumi, M. (2004). Exercise and endothelial function: role of endothelium-derived nitric oxide and oxidative stress in healthy subjects and hypertensive patients. *Pharmacol Ther* **102**, 87-96.
63. Sessa, W. C., Pritchard, K., Seyedi, N., Wang, J. & Hintze, T. H. (1994). Chronic exercise in dogs increases coronary vascular nitric oxide production and endothelial cell nitric oxide synthase gene expression. *Circ Res* **74**, 349-53.
64. Maeda, S., Miyauchi, T., Kobayashi, T., Goto, K. & Matsuda, M. (1998). Exercise causes tissue-specific enhancement of endothelin-1 mRNA expression in internal organs. *J Appl Physiol* **85**, 425-31.
65. Maeda, S., Miyauchi, T., Iemitsu, M., Tanabe, T., Goto, K., Yamaguchi, I. & Matsuda, M. (2004). Endothelin receptor antagonist reverses decreased NO system in the kidney in vivo during exercise. *Am J Physiol Endocrinol Metab* **286**, E609-14.
66. Merkus, D., Houweling, B., Mirza, A., Boomsma, F., van den Meiracker, A. H. & Duncker, D. J. (2003). Contribution of endothelin and its receptors to the regulation of vascular tone during exercise is different in the systemic, coronary and pulmonary circulation. *Cardiovasc Res* **59**, 745-54.
67. Dickhout, J. G. & Lee, R. M. (1998). Blood pressure and heart rate development in young spontaneously hypertensive rats. *Am J Physiol* **274**, H794-800.
68. Okamoto, K. & Aoki, K. (1963). Development of a strain of spontaneously hypertensive rats. *Jpn Circ J* **27**, 282-93.
69. Hojna, S., Kunes, J. & Zicha, J. (2010). Alterations of NO synthase isoforms in brain and kidney of rats with genetic and salt hypertension. *Physiol Res* **59**, 997-1009.
70. Overton, J. M., Tipton, C. M., Matthes, R. D. & Leininger, J. R. (1986). Voluntary exercise and its effects on young SHR and stroke-prone hypertensive rats. *J Appl Physiol* **61**, 318-24.
71. Edwards, M. T. & Diana, J. N. (1978). Effect of exercise on pre- and postcapillary resistance in the spontaneously hypertensive rat. *Am J Physiol* **234**, H439-46.
72. Kohno, H., Furukawa, S., Naito, H., Minamitani, K., Ohmori, D. & Yamakura, F. (2002). Contribution of nitric oxide, angiotensin II and superoxide dismutase to exercise-induced attenuation of blood pressure elevation in spontaneously hypertensive rats. *Jpn Heart J* **43**, 25-34.
73. Kingwell, B. A., Arnold, P. J., Jennings, G. L. & Dart, A. M. (1998). The effects of voluntary running on cardiac mass and aortic compliance in Wistar-Kyoto and spontaneously hypertensive rats. *J Hypertens* **16**, 181-5.
74. Qiu, H. Y., Henrion, D., Benessiano, J., Heymes, C., Tournier, B. & Levy, B. I. (1998). Decreased flow-induced dilation and increased production of cGMP in spontaneously hypertensive rats. *Hypertension* **32**, 1098-103.
75. Hughes, A. K., Cline, R. C. & Kohan, D. E. (1992). Alterations in renal endothelin-1 production in the spontaneously hypertensive rat. *Hypertension* **20**, 666-73.

76. Janssen, K. (2009). The Increase in Renal Sodium Excretion in Response to Angiotensin II Infusion in Exercised Female Rats is Dependent on a Rise in Renal Perfusion Pressure, Minnesota State University, Mankato.
77. Cortright, R. N., Chandler, M. P., Lemon, P. W. & DiCarlo, S. E. (1997). Daily exercise reduces fat, protein and body mass in male but not female rats. *Physiol Behav* **62**, 105-11.
78. Eikelboom, R. & Mills, R. (1988). A microanalysis of wheel running in male and female rats. *Physiol Behav* **43**, 625-30.
79. Wang, G. F., Richter, C. P. & Guttmacher, A. F. (1925). Activity Studies on Male Rats with Ovarian Transplants and Correlation of the Activity with the Histology of the Grafts. *American Journal of Physiology* **73**, 581-599.
80. Kingwell, B. A., Arnold, P. J., Jennings, G. L. & Dart, A. M. (1997). Spontaneous running increases aortic compliance in Wistar-Kyoto rats. *Cardiovasc Res* **35**, 132-7.
81. Berg, B. N. (1960). Nutrition and longevity in the rat. I. Food intake in relation to size, health and fertility. *J Nutr* **71**, 242-54.
82. Applegate, E. A., Upton, D. E. & Stern, J. S. (1982). Food intake, body composition and blood lipids following treadmill exercise in male and female rats. *Physiol Behav* **28**, 917-20.
83. Ergul, A., Shoemaker, K., Puett, D. & Tackett, R. L. (1998). Gender differences in the expression of endothelin receptors in human saphenous veins in vitro. *J Pharmacol Exp Ther* **285**, 511-7.
84. Nakano, D. & Pollock, D. M. (2009). Contribution of endothelin A receptors in endothelin 1-dependent natriuresis in female rats. *Hypertension* **53**, 324-30.
85. Ge, Y., Bagnall, A., Stricklett, P. K., Strait, K., Webb, D. J., Kotelevtsev, Y. & Kohan, D. E. (2006). Collecting duct-specific knockout of the endothelin B receptor causes hypertension and sodium retention. *Am J Physiol Renal Physiol* **291**, F1274-80.
86. Lauth, M., Berger, M. M., Cattaruzza, M. & Hecker, M. (2000). Pressure-induced upregulation of preproendothelin-1 and endothelin B receptor expression in rabbit jugular vein in situ : implications for vein graft failure? *Arterioscler Thromb Vasc Biol* **20**, 96-103.
87. Taylor, C. A., Cheng, C. P., Espinosa, L. A., Tang, B. T., Parker, D. & Herfkens, R. J. (2002). In vivo quantification of blood flow and wall shear stress in the human abdominal aorta during lower limb exercise. *Ann Biomed Eng* **30**, 402-8.
88. Ogawa, Y., Nakao, K., Arai, H., Nakagawa, O., Hosoda, K., Suga, S., Nakanishi, S. & Imura, H. (1991). Molecular cloning of a non-isopeptide-selective human endothelin receptor. *Biochem Biophys Res Commun* **178**, 248-55.
89. Barber, D. A., Michener, S. R., Ziesmer, S. C. & Miller, V. M. (1996). Chronic increases in blood flow upregulate endothelin-B receptors in arterial smooth muscle. *Am J Physiol* **270**, H65-71.
90. Huang, A., Sun, D., Koller, A. & Kaley, G. (1998). Gender difference in flow-induced dilation and regulation of shear stress: role of estrogen and nitric oxide. *Am J Physiol* **275**, R1571-7.
91. Kittikulsuth, W., Pollock, J. S. & Pollock, D. M. (2011). Sex differences in renal medullary endothelin receptor function in angiotensin II hypertensive rats. *Hypertension* **58**, 212-8.

92. Wong, M. & Jeng, A. Y. (1995). Determination of tissue endothelin levels. *Biochem Mol Biol Int* **35**, 1359-64.
93. Hoffman, A., Grossman, E., Goldstein, D. S., Gill, J. R., Jr. & Keiser, H. R. (1994). Urinary excretion rate of endothelin-1 in patients with essential hypertension and salt sensitivity. *Kidney Int* **45**, 556-60.
94. Kitamura, K., Tanaka, T., Kato, J., Ogawa, T., Eto, T. & Tanaka, K. (1989). Immunoreactive endothelin in rat kidney inner medulla: marked decrease in spontaneously hypertensive rats. *Biochem Biophys Res Commun* **162**, 38-44.
95. Fisher, A. B., Chien, S., Barakat, A. I. & Nerem, R. M. (2001). Endothelial cellular response to altered shear stress. *Am J Physiol Lung Cell Mol Physiol* **281**, L529-33.
96. Tostes, R. C., Fortes, Z. B., Callera, G. E., Montezano, A. C., Touyz, R. M., Webb, R. C. & Carvalho, M. H. (2008). Endothelin, sex and hypertension. *Clin Sci (Lond)* **114**, 85-97.
97. Sader, M. A. & Celermajer, D. S. (2002). Endothelial function, vascular reactivity and gender differences in the cardiovascular system. *Cardiovasc Res* **53**, 597-604.